FINAL TECHNICAL REPORT

PROJECT NO. A-661

# CHEMICAL REACTIVITY OF HYDROGEN, NITROGEN, AND OXYGEN ATOMS AT TEMPERATURES BELOW 100° K

By Henry A. McGee, Jr.

Prepared for
National Aeronautics and Space Administration
Washington, D. C.

NASA Grant NsG-337 July 1966

Engineering Experiment Station
GEORGIA INSTITUTE OF TECHNOLOGY
Atlanta, Georgia

GEORGIA INSTITUTE OF TECHNOLOGY
Engineering Experiment Station
and
School of Chemical Engineering
Atlanta, Georgia

FINAL TECHNICAL REPORT

PROJECT A-661

# CHEMICAL REACTIVITY OF HYDROGEN, NITROGEN, AND OXYGEN ATOMS AT TEMPERATURES BELOW 100° K

By

Henry A. McGee, Jr.

NASA GRANT NsG-337

Performed for
National Aeronautics and Space Administration
Washington, D. C.

July 1966

TABLE OF CONTENTS

TABLE OF CONTENTS

# LIST OF FIGURES

# LIST OF FIGURES

# LIST OF TABLES

# PREFACE

This report covers work performed from December 1, 1962, to December 31, 1965 under NASA grant NsG-337. The research was very largely conducted as a series of Ph.D. thesis problems in chemical engineering with the several facets receiving varying support from this grant and from other institutional sources. This Summary Technical Report presents a reasonable overview of the research and serves as a guide to the more detailed theses and journal articles that have been forwarded and which will continue to be forwarded to NASA as they are developed. Predoctoral and postdoctoral students who have participated in this work are W. J. Martin, T. J. Malone, D. B. Bivens, J. H. Wilson, R. H. Holt, and E. Kirschner. Similar studies are continuing in this laboratory under NASA grant NsG-337, Supplement No. 1.

## SUMMARY

This project has been concerned with the development of chemistry at cryogenic temperatures with a particular emphasis on systems that appear to be of significance in cometary phenomena and in the atmospheric and surface chemistry of the Jovian planets. Specifically, reactions of H, N, and O atoms with low molecular weight compounds of these same elements and carbon were of interest. The current lack of developed manipulative apparatus and technique, particularly as relates to chemical analysis, suggested that a significant effort also be expended in these more pragmatic problem areas.

Cryogenic inlet systems to a time-of-flight mass spectrometer have been developed which permit positive identification of species regardless of their stability at or below room temperature and regardless of whether or not the compound has been previously observed. Temperature control of the present inlet arrangements is limited to the region from $55^{o}$ K to somewhat above room temperature. The design is such that the ionizing electron beam makes grazing tangential incidence with the cold inlet port. The refrigerated inlet arrangements also function as multipurpose reactors in which (1) electric discharge processes may be conducted, (2) the effluent from furnance pyrolyses may be quenched, (3) products from cracking on heated filaments may be quenched, and (4) in which low pressure atomic diffusion flames may be quenched. The adaptability of a much less sophisticated mass spectrometric reactor-inlet arrangement was explored and found to be only marginally useful. This reduced suitability stemmed largely from the inability to make appearance potential measurements with the smaller machine. Energy measurements, together with the temperature and hence the relative volatility control that was obtained were usually sufficient for positive identification of reaction products.

Since almost all low temperature reactions require that at least one of the reactants be a free radical or an energetically excited species, it was necessary to explore the utility of pyrolyses and discharges for the production of such reactant species. Fast inlet systems rather like those highly developed by previous investigators were designed and used for the analysis of the gases from these high energy operations. The several

arrangements that were studied include (1) a molecular beam furnace inlet system, (2) a direct injection (no differential pumping) furnace inlet system, (3) heated filament inlet systems, and (4) a system for the direct injection into the ionization chamber (no differential pumping) of the effluent pumped from an rf discharge. An impedance matching network was developed to insure maximum rf power transfer into the plasma. A furnace and also a heated filament arrangement for studying the pyrolysis of species stable only at cryogenic temperatures was also developed and successfully used to pyrolyze $O_2F_2$ in an experiment in which the "furnace" was heated to $250^{\circ}$ K.

Two instrumental modifications to increase the sensitivity of the spectrometer were accomplished and are of general utility. A high voltage, short risetime pulsing circuitry was developed to pulse out any portion of the spectrum prior to the entrance of the electrons corresponding to that portion of the spectrum into the magnetic electron multiplier. This prevented multiplier saturation, permitted the study of small signals near a large and perhaps partially masking signal, and prolonged the effective life of the multiplier between cleanings. Another modification established new values of the various biases applied to the five grid electron gun which greatly increased the sensitivity of the instrument in determining appearance potentials by the retarding potential difference technique.

Atomic oxygen has been reacted with ethane, ethylene and acetylene in a low pressure, quenched ($90^{\circ}$ K) diffusion flame type experiment. With ethane the only product is ethanol which is likely formed by the direct insertion of an excited $^1D$ oxygen atom into a carbon-hydrogen bond. No unstable hydroperoxides were observed. Both of the currently fashionable theories of the mechanism of hydrocarbon oxidation, the aldehyde and the peroxide theories, involve the initial formation of an alkyl radical, but these low temperature data do not suggest that such a radical was ever present. In the reaction with ethylene, $CO_2$, HCHO, $CH_3CHO$, $CH_2OCH_2$, $CH_3OH$, $H_2O$ and HCOOH are observed, with the most interesting observation being the formation under these unusual experimental conditions of large amounts of ethylene oxide, $CH_2OCH_2$. It was earlier suggested that the high temperature oxidation of $C_2H_4$ proceeded first by the formation of an energy rich molecule

of ethylene oxide which was an intermediate that rapidly decomposed and hence was not observable in the reaction. These new low temperature data lend credance to this proposal for it appears that the energy rich intermediate has been stabilized by the cryogenic quench. The results with both ethane and ethylene illustrate the relevance of cryochemistry to kinetic studies of room and higher temperature processes. With acetylene $CO_2$, $O_2$, $(CHO)_2$, HCOOH, $H_2O$ and a solid polymeric material are formed. The low temperature product mass is red,and it changes to yellow on warming through -135° to -116° C with a simultaneous evolution of $C_2H_2$. This color and gas evolution phenomenon has been tentatively explained in terms of a charge transfer complex between $C_2H_2$ and HCOOH which is stable only at low temperatures. Atomic O and benzene behave similarly. Apparently $^3P$ oxygen atoms react with $C_2H_2$ at low temperatures to produce ketene while $^1D$ atoms are expected to form the unstable acetylene oxide or oxirene.

Depending upon the quenching conditions either of two unusual products, both of which are unknown at room temperature, could be produced from the atomic oxygen-ammonia flame. Diimide, $N_2H_2$, a bright yellow solid, was formed if the reaction was quenched to 90° K, whereas ammonium ozonide, $NH_4O_3$, an orange-red solid, was formed upon quenching to 77° K. This ozonide was also formed by the reaction of $NH_3$ and liquid $O_3$ at 77° K. The several products, NO, $N_2O$, $N_2$, $H_2O$, $N_2H_4$, $NH_2OH$, and $NH_4NO_3$ were also identified in the diimide reaction and suggests that the quenching was not fast enough to completely arrest the reaction. The observation of hydroxyl amine, $NH_2OH$, was significant to current discussions concerning its presence as an intermediate in the oxidation of ammonia.

A study of the reaction of atomic hydrogen with NO in a quenched low pressure diffusion flame configuration was conducted with a view toward the possible preparation of nitroxyl, HNO, as a stable low temperature reagent. Only NO, $N_2O$, and $H_2O$ were observed indicating that HNO probably was present as an intermediate, but the quenching efficiency and/or its inherent instability combined to prevent its stabilization.

A study of the reaction of atomic hydrogen with liquid ozone at 77° K was conducted in an attempt to resolve the controversy concerning the low temperature existence of the superperoxides, $H_2O_3$ and $H_2O_4$. These experiments

were plagued by explosions, but the earlier reports pertaining to these compounds have been verified. The data remain ambiguous, but it appears that $H_2O_4$ does exist.

The reaction of diazomethane with liquid ketene at -145°C was explored in an attempt to produce the much discussed, but never observed cyclopropanone. It appears that the very low temperature is necessary for the stabilization of cyclopropanone, but once produced, it seems reasonably stable at room temperature.

The results obtained from this series of experiments indicate that depending upon the molecular complexity and upon the energetics, a variety of intermediates may be stabilized and studied as "reagents" by low temperature quenching techniques.

An area of important data for the low temperature chemist is that of solubility and miscibility. An annotated partial bibliography on solubility at low temperatures appears as an appendix to this report. The number of solvents for possible use in cryochemistry is not as limited as one might have expected in that a somewhat cursory search revealed about 100 organic and about 25 inorganic substances which have melting points below 150° K.

# CHAPTER I

## INTRODUCTION AND BACKGROUND INFORMATION

A study of the reactivity of hydrogen, nitrogen, and oxygen atoms with several simple molecules of these same elements and carbon would appear to be a rather ordinary or routine sort of a chemical investigation. The present work is concerned with such reactivity studies, but at cryogenic temperatures, and this extreme operating condition makes this study most unordinary and non-routine as we shall see subsequently.

The development of our understanding of the cryochemical behavior of the astronomically dominant elements is essential to the understanding of atmospheric phenomena exhibited by those planets having low surface temperatures (usually the Jovian planets). Cryochemical data are also relevant to our understanding of comets. According to Whipple (I.1) and Donn and Urey (I.2), these strange nomads of space have a nucleus composed of frozen masses of low molecular weight compounds of C, H, N, and O, together with dust or grains of heavier materials. "Dirty snowball" is the rather apt name that has been attached to this conjectural model.

### A. BRIEF HISTORY OF CRYOGENICS

The field of cryogenics, which is now very diversified, is concerned with phenomena at temperatures below about $100^{\circ}$ K. This upper temperature is not clearly defined, but it is appropriate to take as the temperature domain of cryogenics, that region below the usual limits of vapor recompression refrigeration machines. Cryogenic temperatures are obtained by the liquefaction of gases whose critical temperatures are below room temperature, with the liquefaction accomplished by isenthalpic and isentropic expansion of the regeneratively cooled high pressure gas. A chronology of the production of low temperatures may be given as follows:

| Date | Event |
|---|---|
| 1823 | Faraday liquefied chlorine |
| 1835 | Dry-Ice discovered |
| 1844 | All gases liquefied except "permanent" gases |

| Date | Event |
|---|---|
| 1878 | Oxygen and nitrogen liquefied |
| 1884 | Dewar experimenting with liquefied permanent gases held in vacuum jacketed flasks |
| 1884 | Hydrogen liquefied in spray or jet |
| 1898 | Quietly boiling hydrogen obtained |
| 1908 | Helium liquefied |

Until about 1950 the field of cryogenics was almost exclusively concerned with physical phenomena, and primarily with superconductivity and with the superfluidity of liquid helium. The Office of Naval Research did much for the growth and ultimate diversification of cryogenics by its sponsorship of a unified program of research dispersed among a number of universities around the country. This program, which is a model of efficient operation and rapid scientific growth through university research and government agency administration, was presented and discussed in a series of Semiannual ONR Cryogenics Conferences that were held between June 1946 and March 1952 (I.3). The primary forum for the presentation of new data in cryophysics was assumed in 1949 by IUPAP in the First International Congress of the Low Temperature Commission, but within the last decade specialization has grown and with it a diffuseness such that today cryophysicists meet in many conference groups to discuss progress in their now many fields of specialization.

The National Bureau of Standards established a Cryogenic Engineering Laboratory at Boulder, Colorado, in 1950. This laboratory and other industrial sponsors, initiated a Cryogenic Engineering Conference in 1954 to facilitate the interchange of information within this new but rapidly growing field of engineering. These conferences have continued; the proceedings have all been published in book form (I.4) and the volumes are an invaluable source of information for the low temperature experimentalist. Data on insulations, properties of cryogens, temperature measurement, liquid valving, pumping and transport, structural design, materials of construction, etc., are all to be found in these extremely useful volumes. The book, Cryogenic Engineering, by R. B. Scott, the director of the NBS Cryogenic Engineering Laboratory, provides an excellent guide for the low temperature experimentalist as it provides summary information up through 1959 (I.5). The successes of the cryogenic engineers who work for the industrial gas companies have made

available laboratory quantities of liquid nitrogen and liquid oxygen at costs so low that design considerations concerning refrigerant economy are relatively unimportant. Laboratory quantities of liquid hydrogen and even liquid helium are also commercially readily available at only a few dollars per liter. This ready and inexpensive availability of cryogens has been a key in the widespread and still growing diversification of cryogenics since about the mid-fifties.

Cryobiology has opened new possibilities in the life sciences, and has already been applied to the storage of blood and to medical "banks" of human organs of several sorts. The cryogenic storage of bull semen has been an important development in the cattle and diary industry with regard to artificial insimination. The interest in cryogenic implications in the life sciences is sufficiently great to justify a specialist's journal, Cryobiology, which began publication in 1964 (I.6).

Surgical procedures employing cryogenic temperatures constitute an area of special technique that has been appropriately called cryosurgery. In the treatment of Parkinson's disease, a cryogenically cooled probe is used to destroy a localized portion of brain tissue. Cataracts, ulcers, and other ailments have also been successfully treated by techniques utilizing very low temperatures.

Many cryogenic techniques and devices represent useful applications of cryophysics. Superconducting magnets readily yielding kilogauss or even over 100 kilogauss fields are now commonplace in the laboratory. Such magnets are important in controlled thermonuclear fusion studies, and they will likely be required for future space propulsion utilizing thermonuclear techniques. Superconducting levitation for minimum drift gyroscopes for guidance applications as well as for stabilized space platform use are being studied. Magnetometers, bolometers, accelorometers, amplifiers, oscillators, and other instruments are being developed which depend upon superconductivity and hence upon cryogenics. Cryoelectronics is a reasonly descriptive generic term that has been used in discussions of those areas of electronics which involve very low temperatures (I.7).

Finally, the study of chemical phenomena at cryogenic temperatures is, rather peculiarly, both a very old and, at the same time a very new field of inquiry. Like cryophysics, the first experiments were performed shortly

after the first availability of the low temperatures, Sir James Dewar observed in 1885 that neither sodium, potassium, phosphorus, nor several other species would react with liquid oxygen at its normal boiling point of 90° K. But while physicists exploited the new domain of experimentation, chemists did not. This reluctance may sensibly be traced to two causes: (1) cryogenic refrigeration was rare, usually requiring that the investigator build his own liquefier, and (2) the paraphernalia and techniques of chemistry, particularly that of analysis, were not immediately adaptable to operation at very low temperatures, i.e., the techniques and equipment were more foreign to the chemist than they were to the physicist.

A few liters (or even a few $cm^3$) of these liquefied gases were, until rather recently, very precious, and one's experimental arrangement had to be carefully designed with refrigerant economy in mind. The heat of vaporization of hydrogen is 7.6 $cal/cm^3$ and of helium is 0.64 $cal/cm^3$, which should be compared with liquid nitrogen at 38.6 $cal/cm^3$. The Collins helium liquefier that was introduced as a commercial item in 1947 has done much to relieve the scientific investigator (particularly the chemistry oriented investigator) of the "hobby shop" preliminaries of liquefier construction prior to meaningful experimentation. The 300th Collins unit was installed at St. Andrews University (Scotland) in August of 1965. In more recent times large scale liquefaction of hydrogen and helium by commercial vendors has further reduced the cost of these cryogens, such that investment in the Collins machine is often economically unwise. So the refrigerant bottleneck has been broken.

The other bottleneck or deterrent to chemical research at cryogenic temperatures of the lack of suitable analytical equipment and techniques is only now being resolved. Analysis is an imperative and necessary part of any chemical investigation, and suitable tools were not available until the early 1950's. By contrast, the tools of physical research were immediately usable at cryogenic temperatures. It is also necessary that chemical analysis be conducted at the low temperature without prior warm-up of any sort, for in such a warm-up the chemical compound of interest is usually destroyed either by further reaction or by decomposition. Powerful physical techniques of both quantitative and qualitative chemical analyses have been developed for very low temperature operation, and include principally

ultra-violet, visible and infrared spectroscopy, electron spin resonance spectroscopy, and nuclear magnetic resonance spectroscopy. And, as a result of this NASA study, mass spectrometric techniques for low temperature analysis have also been developed. As is discussed in the following chapter, the new mass spectrometric techniques represent the most powerful and generally useful solution to the problem of low temperature analysis.

In the same sense that the refrigerant bottleneck was broken, so now has the analysis bottleneck been overcome. We can then anticipate rapid growth in the field of cryochemistry in the immediately ensuing years.

## B. OBJECTIVES OF THIS RESEARCH

There are several problems within the broad area of chemical reactivity at cryogenic temperatures that were to be examined during the course of this investigation. In the order of their performance in a typical experiment, these include (1) generation of suitable reactants or precursors, (2) low temperature reactions, (3) purification of products, and (4) identification and characterization, by their elementary physical and chemical behavior, of selected product substances. A few sentences on each of these problems will serve to introduce the technical discussions in succeeding chapters of this report.

(1) Very few substances will react upon contact at cryogenic temperatures, (I.8), but rather most will require some manner of activation. An interesting instance of direct reactivity is the $H_2$-$F_2$ system, wherein instantaneous ignition occurs when $H_2$ gas is bubbled beneath the surface of liquid $F_2$ and, more interestingly, solid $F_2$ and liquid $H_2$ will explode on contact at $20^{\circ}$ K. In the present studies, the electrodeless glow discharge was the primary means of activation used for the generation of suitable precursors. From an experimental point of view, design problems are apparent which result from the necessary proximity of the high energy discharge

operation and the low energy reactor operation.

(2) The reactor designs have been such as to quench or trap some species from the above activation process, or to react the effluent from the activation process with a second substance which is already in the cold reactor, or to contact the active species with the second reactant in the vapor phase followed by a rapid quench (i.e., a sort of quenched diffusion flame arrangement).

(3) Purification techniques using continuous fractional sublimation and recondensation which may be called "thermal chromatography" are being developed. Presumably adsorption and absorption schemes are also possibilities. Absolute temperature control both in the reactor and in the subsequent processing is essential since the products are often unstable at some still very low temperature.

(4) Identification of product species is accomplished mass spectrometrically utilizing a cryogenically cooled sample inlet system. The mass spectrometer is also used to follow the chemistry occurring during warm-up as well as to measure the appearance potentials and ionization potentials of species of interest, usually to within an accuracy of $\pm$ 0.1 ev. These data are often sufficient for the development of the molecular energetics of radicals, ions, and molecules that are of interest.

The motivation for the choice of systems to study is based on considerations from space chemistry. For example, it is now generally realized that any real understanding of chemical processes occurring on certain objects of astronomical interest, must be realized in terms of cryochemistry. As immediate examples of this, one may recall the "dirty snowball" model of comets and the atmospheric chemistry of the Jovian planets. It seems reasonable that low temperature chemical phenomena are responsible, in part, for the often striking behavior of comets as observed by astronomers.

The results from cryochemical studies are interesting from several other points of view as well: (1) synthesis of unusual molecules with interesting properties, (2) synthesis of highly endothermic molecules which are interesting as rocket propellants or perhaps as special purpose additives (this is really a sub-case of (1)), (3) highly increased yields of certain industrial chemicals leading to economically attractive processes, and (4) study of simple species in reaction sequences uncomplicated by

"thermal noise" (greatly reduced concurrent and consecutive reactions) which is very attractive in fundamental chemistry. The intent of this NASA program is most concerned with applications and points of relevance to comets and other aspects of space chemistry, and, to a much lesser extent, also with item (2) above. But neither these nor any of the above objectives can materialize until the common operations of bench scale research in chemistry are adapted to operations at cryogenic temperatures. Hence, a major portion of this research was concerned with these more pragmatic problems of technique. Chemical analysis without prior warm-up presents the most difficult challenge in this regard.

# CHAPTER II

## APPARATUS AND EXPERIMENTAL TECHNIQUES

It seemed reasonable that the mass spectrometer could be adapted to cryogenic temperature operation. The cold gaseous sample would have to be ionized, probably either by direct injection of the cold sample into the electron beam or by a molecular beam technique similar to that widely used in Knudsen cell studies, except here the sample cell would be at -200° C rather than at 1500°-2000° C (a sort of inverse or reciprocal Knudsen cell). Also, such an adaptation seemed desirable from a practical point of view, for here the output data are definitive, simple, and relatively easy to understand when compared to epr or nmr or ir. This simplicity and unequivocalness are important if cryochemistry is to lead to more than a series of laboratory curiosities. Although these latter techniques of epr, nmr and ir have been made simple for many routine purposes, the need in cryochemistry is far from routine in that one is particularly interested in detecting molecules that have never been observed before and which will probably exist only so long as the low temperature is maintained.

To achieve reaction at cryogenic temperatures, it is almost always necessary to employ free radicals or excited species as one of the reactants. This means some high energy operation, such as a pyrolysis or electric discharge must be operated in close proximity to the cold reactor. It has been important in this research to determine the composition of the gas that may be pumped from such a high energy operation. These gas analyses were also made by mass spectrometric techniques involving fast inlet systems similar to those that have been developed starting with Eltenton (II.1), but principally by Lossing and his coworkers (II.2). The composition of the effluent from such high energy operations may be either thermodynamically or kinetically controlled, whereas the cold analyses are almost always thermodynamically controlled. That is, although the products from cryogenic reactions may not exist at as high as room temperature, they are, of course, expected to be quite stable, ordinary sorts of species (i.e., chemical reagents) if kept below some critical temperature.

Each of several experimental arrangements for the analysis of both reactive gases and cryogenically stable liquids and solids is discussed in this chapter.

## A. CRYOGENIC INLET SYSTEM FOR TOF MASS SPECTROMETER[a]

The only earlier cryogenic mass spectrometer adaptation that seems reasonably related to the present arrangement was described by Blanchard and LeGoff (II.3). In their apparatus, the walls of the ionization chamber were cooled with liquid nitrogen, whereas in the present arrangement, a refrigerated delivery system injects the sample directly into the ionizing electron beam. In the earlier apparatus, a molecular beam from a nearby furnace could be directed onto the inner walls of the cooled ionization chamber, and the vapor evolved from such deposits during gentle warming could be monitored without subsequent further warming.

Since reactions which proceed at cryogenic temperatures usually involve at least one reactant which is a highly reactive free radical, it is necessary that this species be generated either within or very near the cryogenic reactor by electric discharge, pyrolysis, photolysis, or by chemical reaction (such as a low pressure flame). The experimental arrangement should be versatile enough to reasonably accommodate these several free radical generation operations. Because of this and because of the difficulty of even simple operations or manipulations, it seemed desirable to combine into one device, insofar as it was possible, the features of a versatile chemical reactor, some capability for separative operations, and chemical analysis by mass spectrometric means.

### 1. Design Considerations

Both the synthesis reactions and the subsequent studies of the reactivity and energetics of the species of interest must be conducted in cryogenically cooled apparatus. Experience has shown that simple transfer operations such as pipetting, liquid flow, or vaporization and recondensation become somewhat difficult to perform when the working substance is

---

[a] Much of the material in this section has appeared in a paper by McGee, Malone and Martin, Rev. Sci. Inst. 37, 561 (1966).

thermally unstable at cryogenic temperatures. The important operations of purification that might be applicable to such systems are complicated by the temperature requirement, and hence each will require development prior to its use. Simple or equilibrium distillation that is frequently used at more ordinary temperatures may be adapted for use with these unstable systems provided the vapor conduit between the boiler and the condenser is maintained at a temperature no greater than that of the boiler. Also, if a thermal gradient can be maintained along this flow channel, the constituents of the vapor will, to a degree, condense separately in bands depending upon their respective vapor pressures. The occurrence of this latter phenomenon in cold traps is familiar to investigators having experience with vacuum rack manipulations of condensable gases. These notions, which were employed in the device developed in this work, were first used in a related situation by Sir James Dewar in 1910 in the first successful quenching of a highly reactive species from an electric glow discharge (II.4). He found that solid CS would violently explode upon warming above liquid air temperature only if it was first separated from the undissociated $CS_2$ that had survived the discharge. This he accomplished by condensing the two-component system in a thermal gradient.

Another advantage of mass spectrometric analysis is the very low sample pressure, i.e., the very small amount of sample that is sufficient to permit analysis. In the system to be described below, identification may be obtained provided only that a species exert a vapor pressure of about $3 \times 10^{-6}$ torr, that this vapor, upon electron impact, will give a sufficient intensity and variety of either positive or negative ions, and that these ions have a lifetime of the order of 50 microsec (the ion processing time of the spectrometer).

Positive identification is also aided by the use of an ionizing electron beam of controlled energy, and by the control of the temperature of the inlet system which takes advantage of the relative volatility and hence the separability of the several components that may be present from a particular experiment.

The open structure of the source of the Bendix time-of-flight (TOF) spectrometer, which makes it possible to assemble complex cryogenic hardware adjacent to and even within the source itself, was the deciding factor in

Note: An error in page numbering in which numbers 11-13 were omitted was discovered after this report had been printed. There is no gap or omission in the text.

the selection of that machine. A recent review summarizes many other adaptations of the TOF instrument in situations where this open source structure has been advantageous (II.5). The Bendix instrument also allows continuous observation of any portion of the mass spectrum displayed on an oscilloscope (Tektronix Model 543), as well as simultaneous recording of the spectrum (with a Honeywell Model 906C Visicorder). The disadvantages of the TOF instrument stem from the low duty cycle of 0.005 which results from a control pulse of 0.25 microsec at a frequency of 20 Kc.

Maximum detectability corresponds to the observation of usable spectra at the lowest sample pressures, hence at the lowest temperatures of the condensed samples that are of interest here, and therefore in the region of greatest thermal and chemical stability of these rather labile compounds. It is possible to calculate (II.6) the intensity of molecules effusing into a vacuum from a circular inlet port of area $\pi r^2$ which has some particular ratio of length to radius, L/r. The molecular intensity at any solid angle, $d\omega$, located at some angle, $\theta$, with respect to the center line of the port, may be developed in terms of L/r and $\theta$, in the form of the usual cosine distribution function multiplied by a deviation factor, J, which is a complicated function of L/r and $\theta$

$$N_{t\theta} = [\ (N_t/\pi)(\cos\theta)(d\omega/dA)\ ]J \qquad (1)$$

From the variation of J with L/r and $\theta$, it is evident that both the intensity at any angle and the total flow will be a maximum for a sharp edge orifice for which case J has its maximum value of unity. $N_t$ is the rate at which molecules enter the sample inlet channel and is given by the product of the molecular number density in the sample reservoir, the average molecular speed and the inlet area, i.e., by $pA/(2\pi mkT)^{\frac{1}{2}}$. We are concerned, of course, with the ionization of molecules which have suffered no collisions since leaving the inlet port. The sensitivity, S, is directly proportional to the number of these molecules that are ionized per unit time which is given by the product of the electron flux, $N_e$, the molecular or the target number density, D(x,y,z), and the ionization cross section, $\sigma_i$. The target density, D(x,y,z), is given by Eq. (1) above, but expressed in rectangular coordinates, and divided by the mean molecular speed, $\bar{v}$. Although the electron flux is

uniform, the target density is a function of position within the collision covolume and hence one must integrate over this covolume to determine the total sensitivity, that is,

$$S = K \int_{\text{Covol.}} \sigma_i N_e D(x,y,z) dV \qquad (2)$$

where K is a proportionality constant. It is then possible to analytically examine the relative merits of various configurations of the inlet port relative to the rectangularly collimated electron beam of the TOF mass spectrometer. Since the probability that a given molecule will be ionized during its single pass through the electron beam is very small, it can be assumed that the number density of targets is undiminished as a result of ionization and is therefore correctly given by D(x,y,z). Eq. (2) can then be integrated to give,

$$\begin{aligned} S = \{ 4N_t N_e \sigma_i K/\pi \bar{v} \} \{ & a \ln[\gamma_2(b+\beta_1) / \gamma_1 (b+\beta_2)] \\ & + b \ln [(\alpha_2 + \beta_2 - a)(\alpha_1 + \beta_1 + a)/(\alpha_2 + \beta_2 + a)(\alpha_1 + \beta_1 - a)] \\ & + c_2 \tan^{-1}(a/c_2) - 2c_2 \tan^{-1} [ac_2/(\alpha_2 + b)(\alpha_2 + \beta_2)] \\ & + 2c_1 \tan^{-1} [ac_1/(\alpha_1 + b)(\alpha_1 + \beta_1)] - c_1 \tan^{-1}(a/c_1) \} \end{aligned} \qquad (3)$$

where, $\alpha = (b^2 + c^2)^{\frac{1}{2}}$; $\beta = (a^2 + \alpha^2)^{\frac{1}{2}}$; $\gamma = (a^2 + c^2)^{\frac{1}{2}}$; and where the factor, J, has been taken to be constant and equal to its maximum value of unity, that is, Eq. (3) is applicable to a sharp edge orifice. The geometry of the inlet port and beam configuration is specified by 2a and 2b which are the cross sectional dimensions of the rectangularly collimated electron beam as viewed from the port, and by $c_1$ and $c_2$ which are the perpendicular distances from the port to the near and far faces of the beam respectively.

The relative merits of the various inlet channels having finite lengths may also be explored, but the integration of Eq. (2) is now much more complicated. A similar analytical study of the much greater sensitivity obtainable with a slit shaped inlet port may also be developed.

Two alternative configurations of the inlet port relative to the electron beam of cross section 0.076 x 0.50 cm and effective length of 0.64 cm are possible with the Bendix instrument. The axis of the inlet port may be perpendicular to the ion flight path, or the drift tube, and facing the 0.076 x 0.64 cm side of the electron beam. Or the inlet port may be coaxial with the ion flight path and facing the 0.50 x 0.64 cm side of the electron beam. An indication of the calculated behavior of the two configurations for several values of the distance between the inlet port and the near face of the electron beam, $c_1$, is given in Table II.1.

TABLE II.1

VARIATION OF SENSITIVITY WITH RELATIVE CONFIGURATION OF ELECTRON BEAM AND INLET PORT

| Configuration | Geometrical Parameters (cm) | | | | $\bar{v}\,F^a$ (from Eq. (3)) |
|---|---|---|---|---|---|
| | a | b | $c_1$ | $c_2$ | |
| Perpendicular Arrangement | 0.038 | 0.32 | 0.0 | 0.5 | 0.156 |
| | 0.038 | 0.32 | 0.2 | 0.7 | 0.0387 |
| | 0.038 | 0.32 | 0.8 | 1.3 | 0.0070 |
| | 0.038 | 0.32 | 1.4 | 1.9 | 0.0028 |
| | 0.038 | 0.32 | 2.0 | 2.5 | 0.0015 |
| Coaxial Arrangement | 0.250 | 0.32 | 0.0 | 0.076 | 0.134 |
| | 0.250 | 0.32 | 0.2 | 0.276 | 0.0594 |
| | 0.250 | 0.32 | 0.8 | 0.876 | 0.0087 |
| | 0.250 | 0.32 | 1.4 | 1.476 | 0.0036 |
| | 0.250 | 0.32 | 2.0 | 2.076 | 0.0018 |

[a] F is the fraction of molecules entering the inlet channel that appear in the collision covolume and is equivalent to $S/\sigma_i N_t N_e K$. Maximum detectability with respect to the relative configuration of the electron beam and the inlet port corresponds to a maximum value of F.

Evidently both the perpendicular and the coaxial configurations provide about the same sensitivity at equal displacements from the near face of the electron beam. The paramount importance of minimizing the distance

between the inlet port and the electron beam is clear, for if the inlet port is only 2 mm away from the beam, the sensitivity is down about a factor of four for the perpendicular case. This behavior as well as the other trends that may be inferred from Table II.1 have been experimentally verified. Eq. (3) is equally applicable to the furnace, discharge, and other collision-free inlet arrangements that are discussed below.

Largely as a consequence of the realizable mechanical conveniences, the perpendicular arrangement was selected for these investigations.

This system is, in some sense, rather similar to a heated filament inlet system for use with the Bendix instrument that was developed by Biemann (II.7) and in which thermally sensitive organic substances contained in a tiny capsule may be positioned inside the source adjacent to the ionizing electron beam of the instrument. Heating the capsule produces vaporization directly into the electron beam, and hence there are few collisions and therefore little reaction or degradation before ionization.

2. Mechanical Description

A schematic of the apparatus appears in Fig. II.1 where the reactor-inlet system itself is shown in heavy black while its associated components are shown either in outline or in cross-hatching. The reactor inlet system is suspended from a single header (23)[b] and consists essentially of two independently thermostated chambers (22), (17) that are centered within a polished stainless steel sleeve (21) which can move laterally through a double O-ring gland (5) into a vacuum lock arrangement (6). A 13.3 cm high vacuum gate valve (9) (Consolidated Vacuum Corporation Model VCS-41A) separates the vacuum lock from the separately pumped source and drift tube of the spectrometer. This design is for convenience and permits the reactor-inlet arrangement to be withdrawn for adjustments or modifications without the necessity of breaking vacuum in the mass spectrometer system itself. The sample spaces within the two refrigerant chambers (4), (18) are connected by a 20 cm long x 0.25 cm wall tube (19), and together they form a coaxial tubular reactor and condensation space. Both chambers and the connecting tube are made of copper for rapid thermal equilibration and are

---

[b] Numbers in parentheses are for identification on the several figures. It is obvious from the text which figure is being referred to.

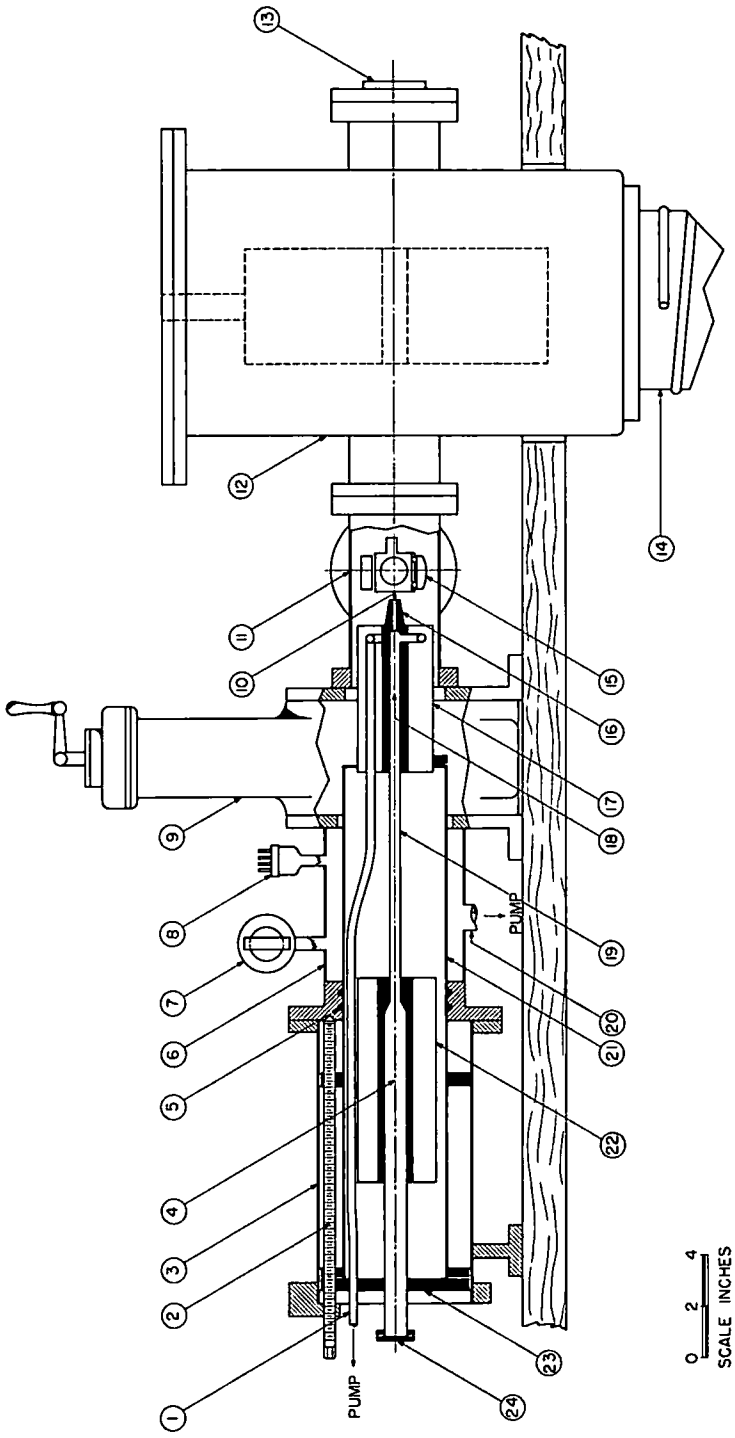


Figure II.1. Schematic of Cryogenic Reactor-inlet System for the Time-of-Flight Mass Spectrometer.

nickel plated on the outside to reduce the emissivity and hence the refrigerant use rate. The entire reactor and condensation tube in which the low temperature species are prepared and manipulated was lined, for chemical inertness, with monel tubing which was sweated in place. At the expense of somewhat poorer heat transfer between the sample and the refrigerant a snug fitting pyrex liner can be inserted into the reactor-condensation tube which effectively allows the sample to be manipulated within an all glass system. Thermostating of each chamber is accomplished by offsetting the natural inward heat leak with a controlled influx of refrigerant which is adjusted to be slightly in excess of that required to just balance the natural heat leak. Fine control is then maintained automatically by two recorder-controllers (Leeds & Northrup Company, Adjustable Zero-Adjustable Range-Speedomax H) which control the power dissipated in 100 ohm constantan heaters wound on the inside of each chamber. Electrical trimming of the heat balance can be much more precisely controlled than is possible with flow control of the liquid refrigerant. Proportional control of these heaters was not required since simple two-position operation resulted in oscillations about the control point which increased to a maximum of only $\pm$ 0.5° K when the apparatus was cooled to near 77° K.

The end of the condensation tube nearest the source is fitted with any one of several flat extension pieces (16) which are positioned to protrude into the ionization chamber of the spectrometer when an analysis is being performed; a channel in this extension piece conducts the sample from the condensation tube into the ion source (15). The inlet port itself (10) may be positioned at any point relative to the electron beam including its being actually submerged in the beam, and hence ionization of the sample occurs prior to wall collisions. A sample molecule must be considered to be background after only one such wall collision. The inlet arrangement properly positioned in the source for analysis is shown schematically in Fig. II.2. Design calculations which were subsequently confirmed by experimental measurements, show that the 0.4 x 1.6 cm cross section of the copper extension piece provides sufficient conductivity along its 2.5 cm length to insure that the sample is not heated significantly above the temperature of the inner refrigerant chamber (17) when it passes through the inlet channel. The lateral positioning of the reactor inlet device is accomplished with a

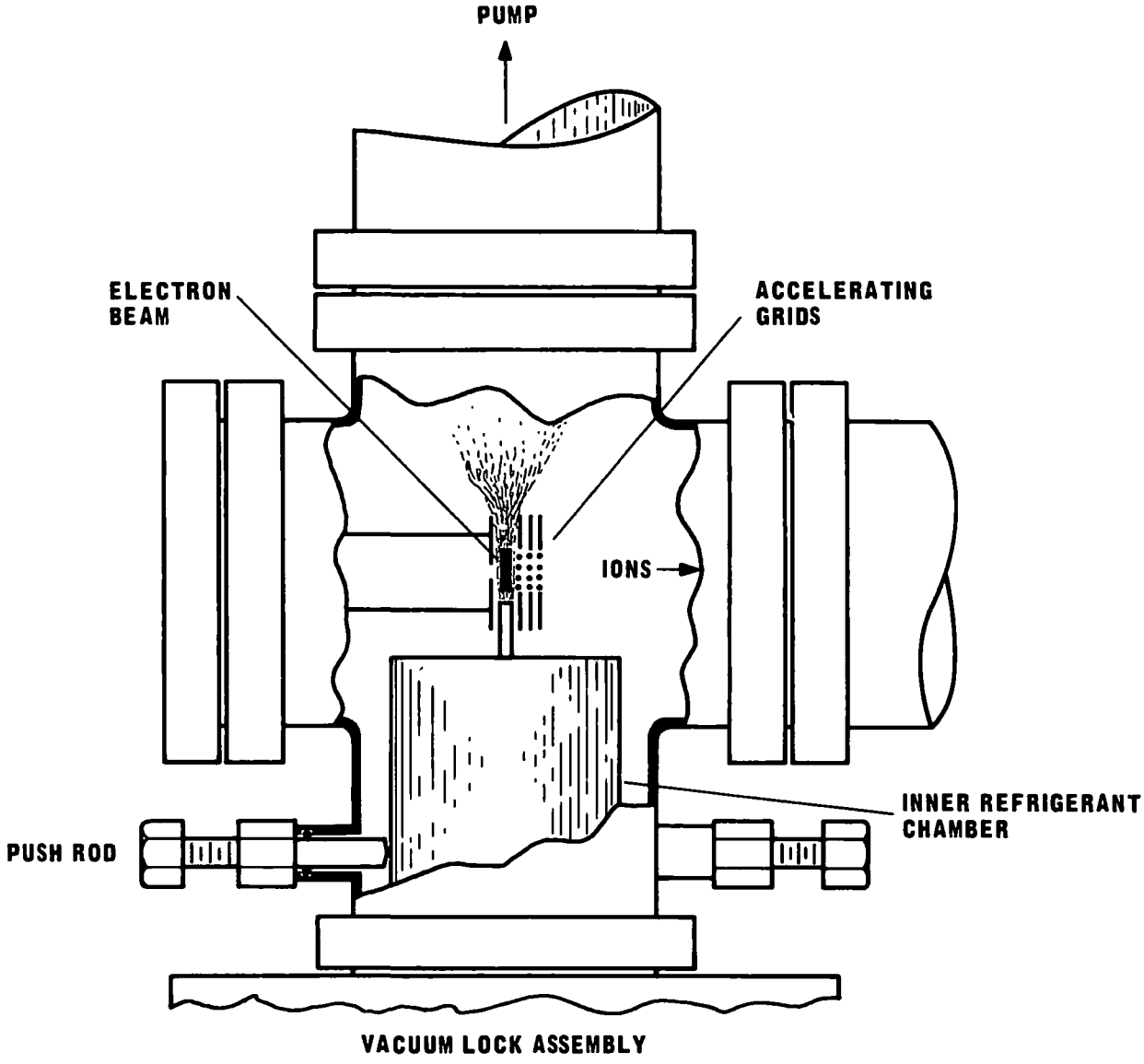


Figure II.2. Schematic of Cryogenic Inlet System in Proper Analytical Position.

screw (2), and an observation port (13) is provided to visually follow the advance of the extension piece into the source structure. Sidewise positioning adjustments in the plane perpendicular to that of Fig. II.1 are made during this advance by a pair of oppositely placed, vacuum sealed push rods which are mounted on the "cross" vacuum chamber (11). This rather delicate alignment situation is apparent in Fig. II.2. When in analytical position, that is, as shown in Fig. II.2, the sample gas from the condensation tube is injected directly into the ionizing electron beam, and a portion of it is ionized before collisions with surfaces at room temperature can occur. Fast pumping in the source region is provided by a nominal 750 l/sec system (14) (National Research Corporation Model HS 4-750).

This two chamber system with a temperature controlled interconnecting vapor conduit (19) may also be used for the physical separation of product mixtures from the reactor (4) by means of either simple distillation or by fractional condensation in a thermal gradient. However, for experiments in which this rough separation is undesirable or unnecessary, a single chamber device has been built which is completely glass lined for chemical inertness, and which is in essence merely the inner refrigerant chamber (17) alone. Either an extension piece similar to that described above or a gold foil leak may be used, but the foil leak cannot be advanced into the source and hence it can be no closer than 1.9 cm to the electron beam. The analysis summarized in Table II.1 indicates that the foil leak results in a loss in sensitivity of about a factor of 100 over that obtained with the extension piece.

The 2.5 cm diameter reactor space (4) of the outer refrigerant chamber (22) was designed to accept a variety of synthesis operations. Glow discharges, furnace pyrolyses and heated filament pyrolyses have been conducted in this reactor. In each instance a labile species from the high energy operation has been either quenched directly from the vapor or it has entered into subsequent heterogeneous reactions on the cold walls of the reactor. Depending upon the experimental requirement, the reactor-condensation tube may be either pumped from the reactor header (24) or from the opposite end (1) which will thus cause a mass flow through the entire system.

If it is not necessary to monitor the reactor off-gases that may be evolved during the synthesis, the reactor-inlet assembly is allowed to rest with atmospheric force on the inlet header (23) of some 102 megadynes pressing the end of the extension piece, which has a cross-section of about 0.15 $cm^2$ at the point of contact, against a teflon block. This acts as a valve to seal the reactor space from the low pressure in the vacuum lock (6) which is required for thermal insulation. Insulation pressures of $10^{-5}$ torr were readily maintained in the vacuum lock while operating with pressures of 30 torr in the reactor. About 4 liters of liquid nitrogen were required to cool and flood each chamber (22), (17). With the chambers flooded, metering of the vented nitrogen gas indicated boil-offs of 1.0 and 0.7 l/hr of liquid nitrogen, respectively, in the outer (22) and inner chambers (17) to offset the natural heat leak. By adjusting the two refrigerant flow rates and the power dissipated in the two heaters, the temperatures of the chambers were stabilized and automatically maintained at any value above the normal boiling point of the refrigerant. Both the voltage applied to the heaters and its percent on-time are variables in the trimming of the heat load on the two refrigerant chambers. In general, a lower voltage and a correspondingly greater percent on-time will result in smaller temperature oscillations about the control point. Typical operating parameters with both chambers near $77^{o}$ K show temperature fluctuations about the control point of $\pm 0.5^{o}$ K, heater voltage of 50, and percent on-time of 40. The temperature fluctuations decrease with increasing temperature.

3. Operations with Typical Systems

Although a variety of cryochemical experiments have been conducted in this apparatus, its operation is best described by considering several typical specific cases. Brief, but hopefully sufficient, data are included to give, if only by inference, the operation of the several permutations of the devices that have been designed and studied.

a) axial electrode reactor

An electric discharge reactor was obtained by mounting a single axially symmetric electrode with a reactant gas inlet on the reactor header (24) as shown in Fig. II.3. A pyrex tube encased the 0.32 cm diameter electrode from just beneath the header to a point some 7.5 cm inside the reactor space

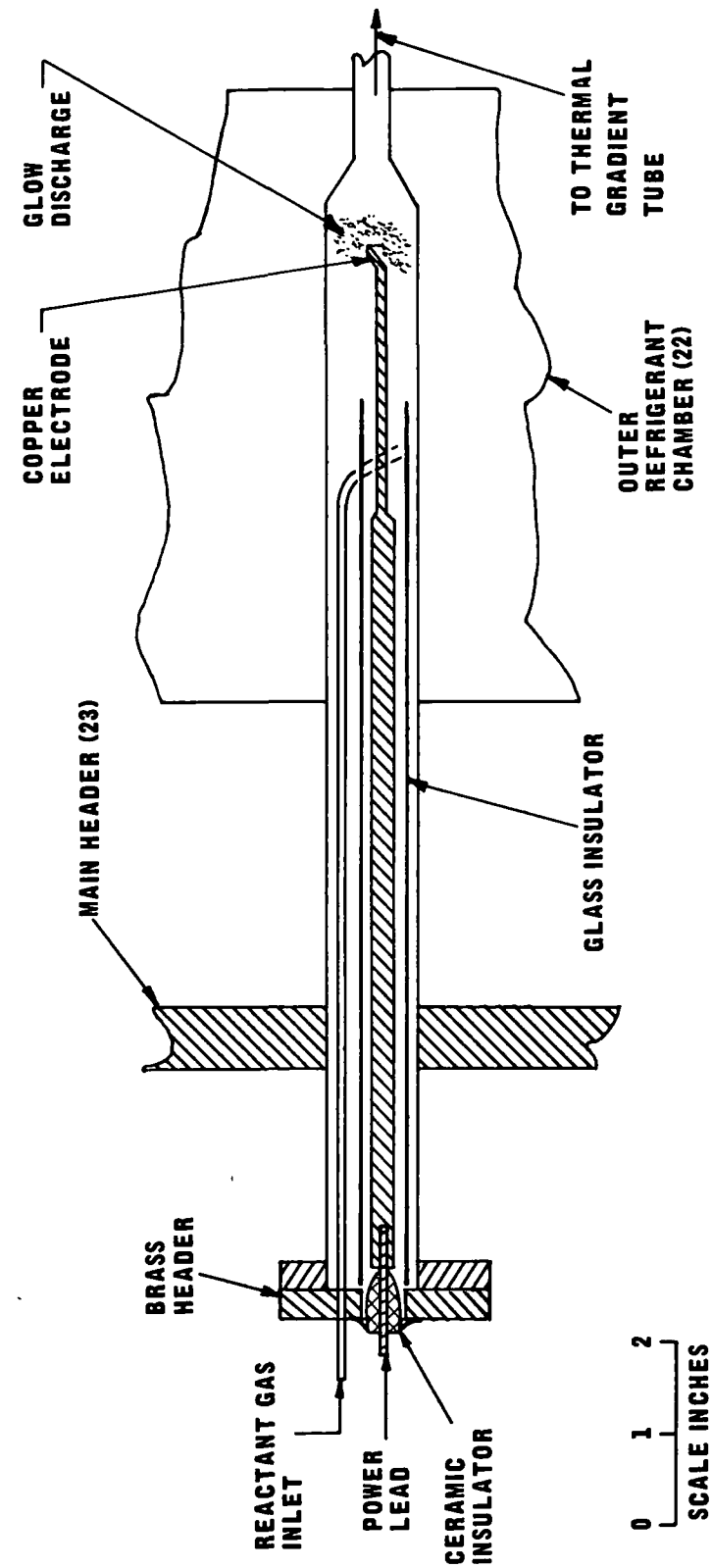


Figure II.3. Schematic Diagram of the Gas Inlet and Single-electrode Arrangement Used for Electric Discharge Syntheses in Situ in the Cryogenic Reactor Inlet System.

(4), which assured that the glow was established only within the refrigerated volume. The reactant gas inlet line was also extended beyond the header to exhaust directly into this discharge region. This system has been used with a potential of 800-1500 volts (60 cycles) to establish a discharge in a mixture of $O_2$ and $F_2$ at 20-40 torr pressure in the annular space between the electrode and the grounded reactor walls which were cooled to below 90° K. The unstable low temperature oxygen fluorides were thereby snythesized (II.8)[c]. When the annular electric discharge is on in the reactor space (4), the liquid nitrogen boil-off rate in the outer chamber is increased from 1 l/hr to 3.7 l/hr. A typical $O_3F_2$ synthesis run required 60 min during which 15 liters (NTP) of premixed $O_2$ and $F_2$ feed gas were pumped through the discharge. Upon completion, the high voltage was turned off, and the reactor space was pumped to remove the excess feed gas. Care is required at this point since excessive pumping could remove product species which have high vapor pressures. From an operational point of view, one may assume that each species present will exert its full vapor pressure since the occurrence of solid solutions, partial miscibility, etc. can only reduce the vapor pressure. Then using the lateral positioning screw (2), the system is backed off of the teflon block valve against which the inlet port had been pressed, the large slide valve (9) is opened, and the system is advanced into the source. This forward advance is followed visually through the observation port (13) and is continued until the inlet port at the end of the extension piece (10) is just touching the electron beam or until the spectrum intensity is maximized.

b) external glass reactor

In similar synthesis experiments, the oxygen fluorides were synthesized externally in a pyrex reactor and electric discharge system that was similar to that used by previous workers (II.9) and shown schematically in Fig. II.4[c]. This external reactor was mounted near the reactor header (24) of the low low temperature inlet system so that a 43 cm long drain line could be used to

---

[c]Results with the $O_2$-$F_2$ system are cited herein due to their being the most successful and interesting accomplishment with this particular, and certainly more generally useful, apparatus development. The $O_2$-$F_2$ work was supported by the Georgia Tech Institutional NASA Grant, NsG-657.

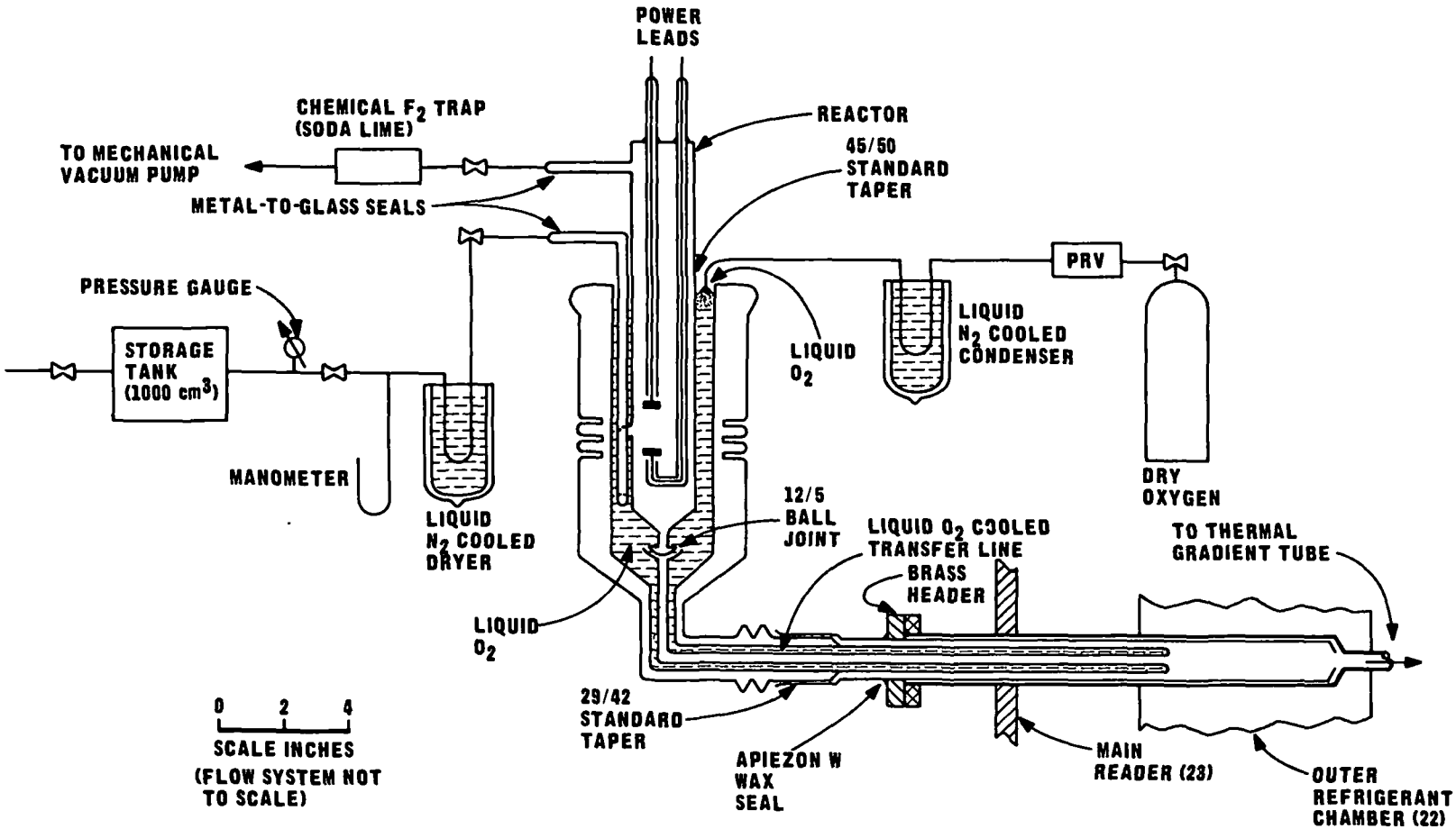


Figure II.4. Schematic Diagram of the Cryogenic Reactor-inlet System Attachment and its Associated Flow Systems for External Syntheses of the Oxygen Fluorides of Other Species Requiring Discharge Type Reactors.

conduct these externally generated liquid products through the reactor header and into the center of the reactor space (4). This drain line was itself immersed over its entire length in the same refrigerant (usually liquid oxygen, 90° K) as was used to cool the reactor.

Mass spectra from an $O_3F_2$ synthesis experiment are presented as a function of temperature between 77° and 150° K in Fig. II.5. Four temperature ranges (80°-90° K, 90°-102° K, 105°-122° K, and 122°-135° K) are evident within which significant changes in the mass spectra occur. These temperature ranges coincide with the melting point of $O_3F_2$ (83°-84°K), the temperature at which ozone has a vapor pressure of one torr (94° K), the decomposition temperature of $O_3F_2$ (110°-120° K), and the temperature region (120°-135° K) in which $O_2F_2$, as a stable entity, exerts a smoothly rising vapor pressure. The vapor pressure of $O_2F_2$ is 1 torr at approximately 130° K. The parent ions of $O_2F_2$, $O_3F_2$ and $O_4F_2$ have not been observed. $A(O_2F^+)$ and $A(OF^+)$ were measured to the 14.0 $\pm$ 0.1 ev and 17.5 $\pm$ 0.2 ev respectively at 130° K, which did, together with other related data, permit the development of the energetics of the $O_2F_2$ molecule, its fragments and its ions (II.8).

c) furnace pyrolysis reactor

The quenching of the effluent from a pyrolysis experiment can be conveniently studied in the basic apparatus of Fig. II.1 by using a furnace arrangement such as appears in Fig. II.6. Several types of furnaces were affixed to the end of a 5/16 in OD monel tube (2), and the assembly was mounted in a brass header (3) provided with power and thermocouple leadthroughs. In cracking experiments with diborane[d], the parameters which optimized the yield of $BH_3$ were determined for a 1/8 in OD stainless steel furnace which was mounted such that the exit port of the furnace was located very close to the ionizing electron beam (this system described in detail in Section II.C.2). This same furnace was then mounted in the cryogenic reactor-inlet arrangement as shown in Fig. II.6 and the pyrolysis conditions were adjusted to coincide with those previously obtained optimum values. The furnace effluent was thereby quenched with the hope of stabilizing $BH_3$. The furnace assembly was connected to the reactor header (4) such

---

[d]Results with this specific system are cited for interest and for illustration.

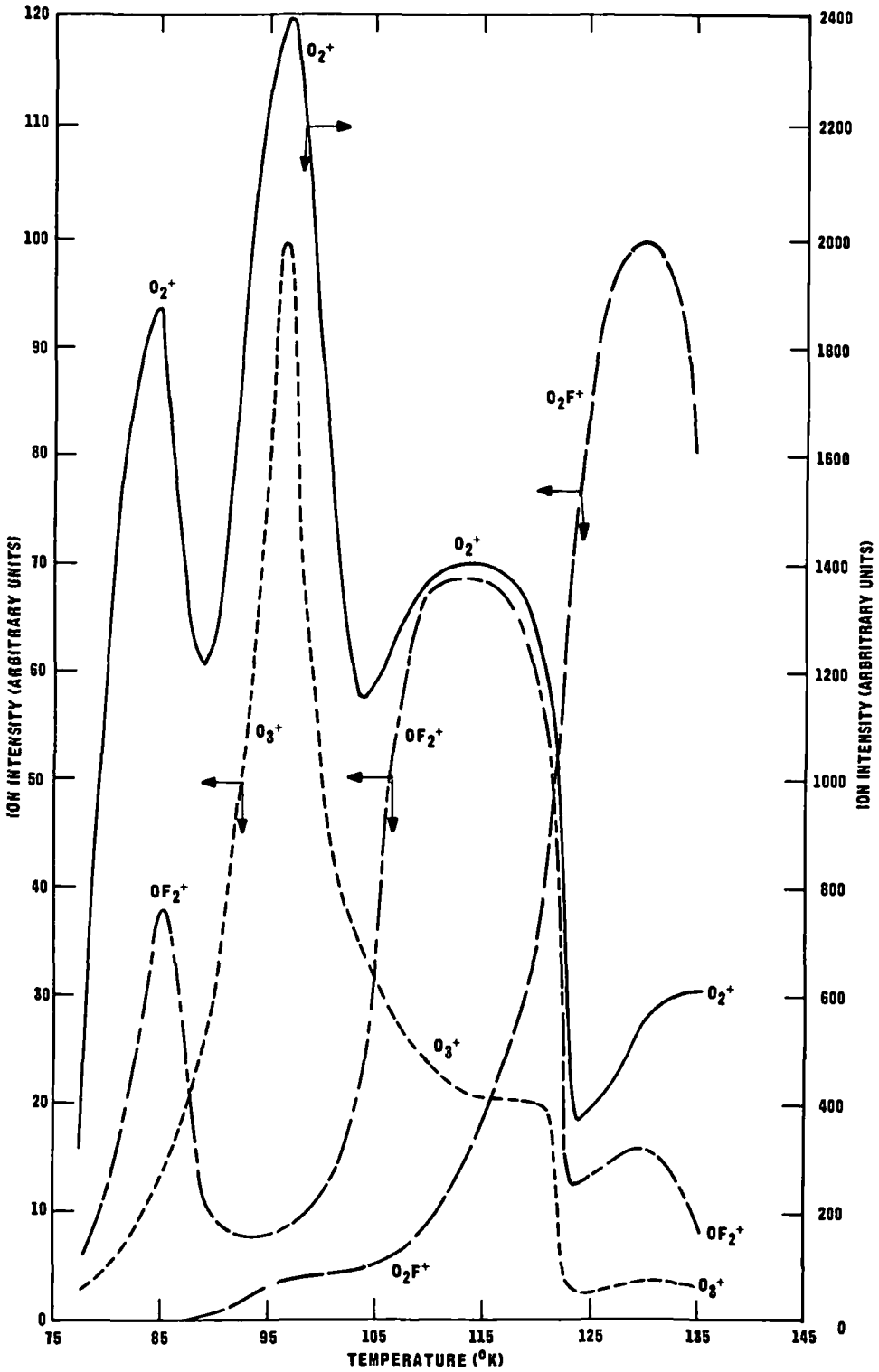


Figure II.5. Variation of Ion Intensity with Temperature for the Principal Ions Observed in Warm-up Studies with an $O_3F_2$ and $O_2F_2$ Product Mixture.

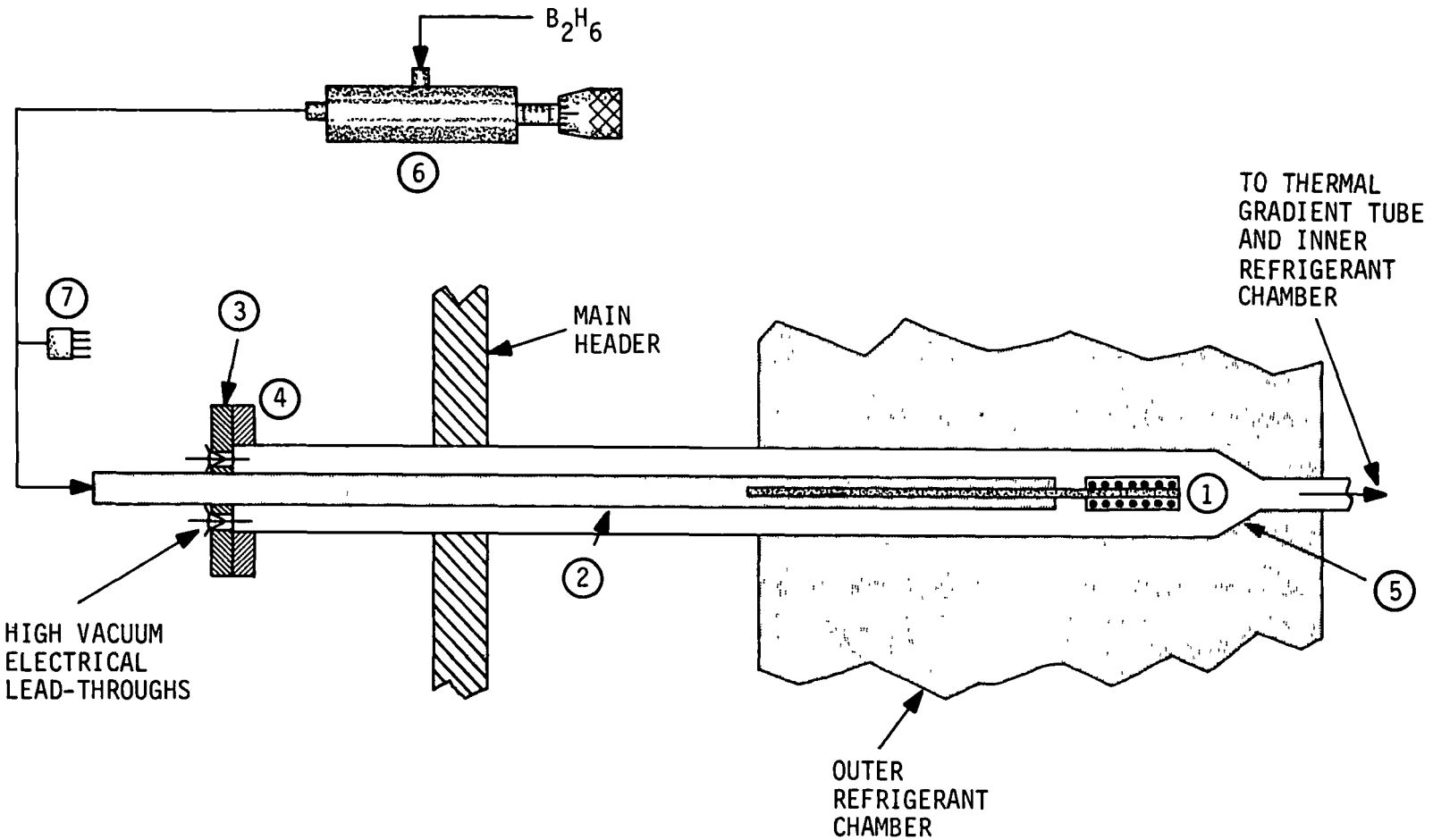


Figure II.6. Schematic Diagram of Apparatus for Pyrolysis and Quench Experiments.

that the furnace exit was positioned within 1/2 inch of the tapered region (5). The parent gas or reactant mixture was usually introduced into the furnace assembly through a high quality leak valve (Vactronic model VV-50)(6) and the pressure was indicated by a thermocouple gauge (7). The pressures in the reactor-inlet system during such a quenched pyrolysis experiment were usually low enough to permit the experiment to take place with the cryogenic inlet system nose-piece advanced into place tangential to the electron beam. Hence, the reactor off-gases could be monitored at quenching temperature. The reactor space itself was continuously evacuated by a separate diffusion pump system.

The lowest temperature at which this system could be conveniently operated was $55^{o}$ K. This temperature was attained by flooding the refrigerant chambers with liquid $O_2$ which was then frozen by pumping on each chamber with a mechanical pump. It was found that the freezing point of $O_2$ could be maintained for approximately one hour before the outer chamber (item 22 of Fig. II.1) began to warm, but the inner chamber (17) could hold the $55^{o}$ K temperature approximately 15 minutes longer. After both chambers had been emptied of $O_2$, no control over warm-up was possible; however, as long as the refrigerant chambers were evacuated, the natural warm-up rate was slow enough to permit a reasonable analysis of evolved products.

Experiments were performed in which pyrolysis products were quenched on the metal walls of the reactor space and also in which the reactor space was glass lined. In addition, conditions corresponding to low deposition rates were usually investigated should a lack of a sufficient rate of heat transfer allow heating of the deposited film of gases.

d) hot filament reactor

In still another pyrolysis type experiment, a heated filament was placed at a point near the center of the reactor space (4). In an experiment typical of this arrangement, $CF_3I$ was efficiently thermally cracked on a platinum filament to yield the stable compound difluorocarbene, $CF_2$, which was immediately quenched on the cold walls of the reactor at $77^{o}$ K. Difluorocarbene, which is known to be more stable than carbene, was explored as a preliminary to studies with the more interesting carbene, $CH_2$, itself. However, a study of the vapor over such composite solids, as it was gently warmed, did not reveal the presence of free $CF_2$ in the cold product mass.

Such a pyrolysis does produce $CF_2$ in good yield, as had been shown by earlier experiments in this laboratory using one of the heated filament arrangements described later in this chapter (Section C.3). Either the $CF_2$ did not survive the quench or the activation energy for its dimerization may not be frozen out at temperatures above 77° K. These observations agreed with those from a concurrent infrared study of $CF_2$ in argon matrices in which it was clear that the species dimerized at 14° K (II.10).

e) rf discharge reactor

An experimental arrangement of the radio frequency discharge coupled to the cryogenic reactor-inlet system is shown in Fig. II.7. The pyrex discharge tube fitted into a 19/22 standard taper joint, which was attached by means of a glass-to-metal seal to the reactor header. The end of the discharge tube extended to the center of the refrigerant chamber, and a 1 mm ID glass capillary was provided for the introduction of a second reactant into the effluent from the discharge. Pressure was indicated by a thermocouple gauge, and experiments could be performed with the reactor space glass lined or not, as desired. Again, operating conditions could be adjusted to permit the reaction and quench to be performed with the cryogenic inlet system advanced into proper analytical configuration and hence continuous monitoring was possible. Either liquid $O_2$ or liquid $N_2$ were used as convenient refrigerants, the lowest temperature that could be conveniently produced being 55° K obtained by pumping on liquid $O_2$. Product analysis was conducted upon warm-up as previously described.

More gentle cracking of some parents was achieved by admitting argon to the discharge to a pressure of about 50 microns to obtain a moderately intense discharge and then admitting the second reactant into the discharged argon through the 1 mm capillary. Condensables were then quenched on the pre-cooled walls of the reactor. The argon stream could clearly be replaced by some direct chemical reactant if desired, such as occurred in the study of the reaction of atomic hydrogen with NO, or atomic oxygen with $NH_3$, etc. The argon functions not as a chemical reactant but merely as an energy transfer medium.

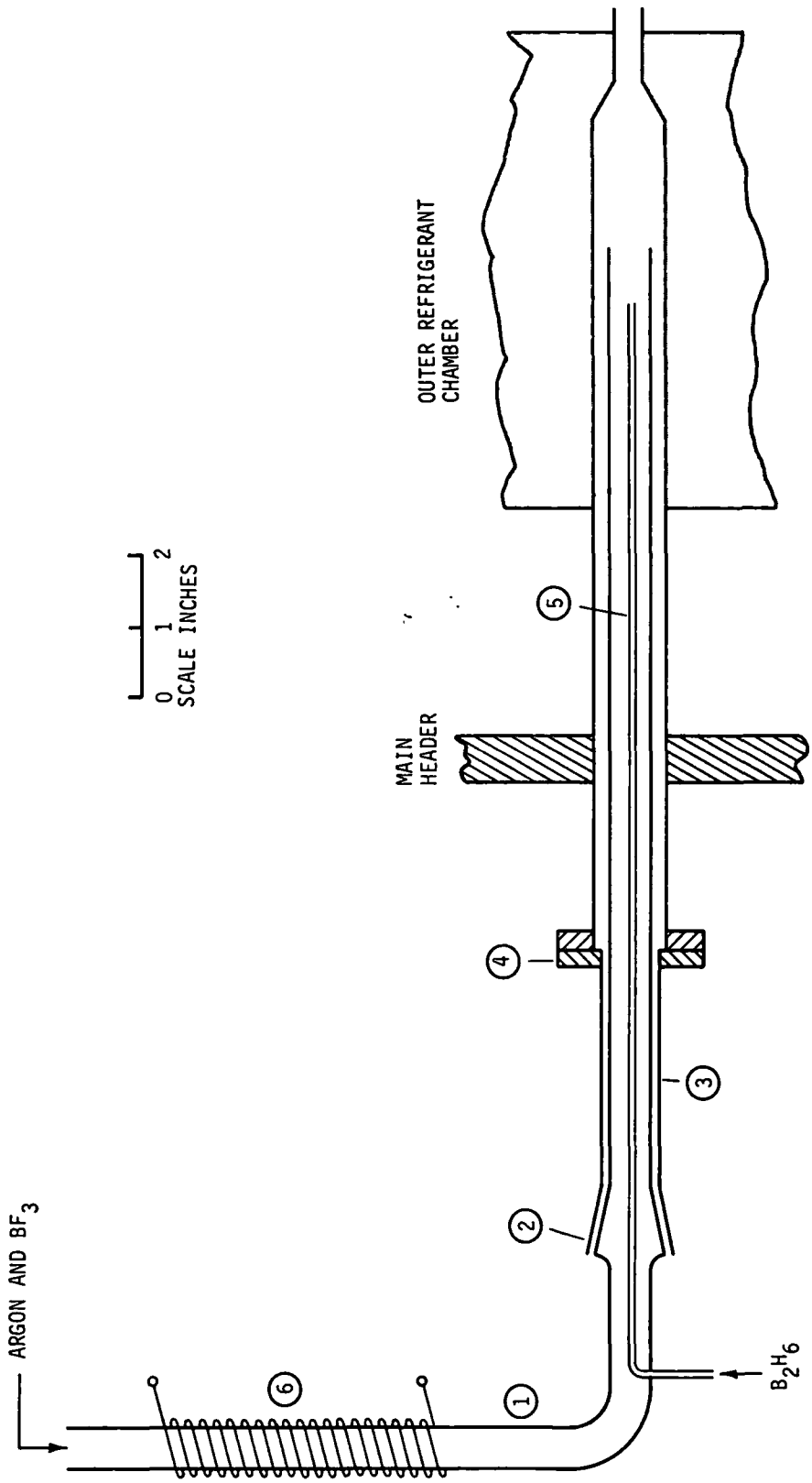


Figure II.7. Reactor Configuration with Precusor Pumped from an RF Discharge.

## B. ALTERNATIVE EXPERIMENTAL ASSEMBLY UTILIZING A SMALL INEXPENSIVE MAGNETIC MASS SPECTROMETER

### 1. Introduction

The possible adaptation of a small and much cheaper (cost approximately $5,500) magnetic deflection mass spectrometer to several low temperature reactors was also explored. The instrument that was used here was the Model MS 10 manufactured by Associated Electrical Industries, Limited of England. This device proved to be only marginally useful and its use has been discontinued. However, it was determined that the rather elaborate system described above is not necessary for many sorts of preliminary or exploratory studies. It appears that one of the quadrupole machines, such as the Series 200 sold by Ultek Corporation, would be the most amenable of the available inexpensive mass spectrometers for adaptation to cryochemical experiments. A successful adaptation of an inexpensive, simple instrument would be an excellent impetus to further the interest of others in participating in cryochemical research.

The same general design criteria were employed here as was the case for the TOF work, i.e., a cold conduit from the reactor to the edge of the electron beam was to be provided. In addition, glass reactors were to be used, to permit correlation of visual phenomena occurring in the quenched reaction product mass with the mass spectrometric analysis of the evolved vapor. A brief description of the complete experimental arrangement is a prerequisite for a proper presentation of the reactor-inlet combination.

### 2. Description of Reactor Configuration

A schematic diagram of a system for reacting atoms with various simple molecules is shown in Fig. II.8. The gas to be dissociated, usually, $H_2$, $O_2$, or $N_2$ entered the system by passing through a rotameter at some known constant pressure. The gas entered the region of an rf discharge coil where partial dissociation and excitation occurred, and then continued around a 90 degree bend to the U-tube reactor. This stream of molecular and atomic species was mixed with a gaseous stream of the second reactant at a point 15 mm above the bottom of the U-tube reactor. Longer lived excited states, such as $^1\Delta$ molecular oxygen[e], may well reach the reactor,

---

[e] Excited $^1\Delta$ molecular $O_2$ from a discharge tube has a half life of the order of hours according to Dr. J. Heicklen of Aerospace Corporation (private communication).

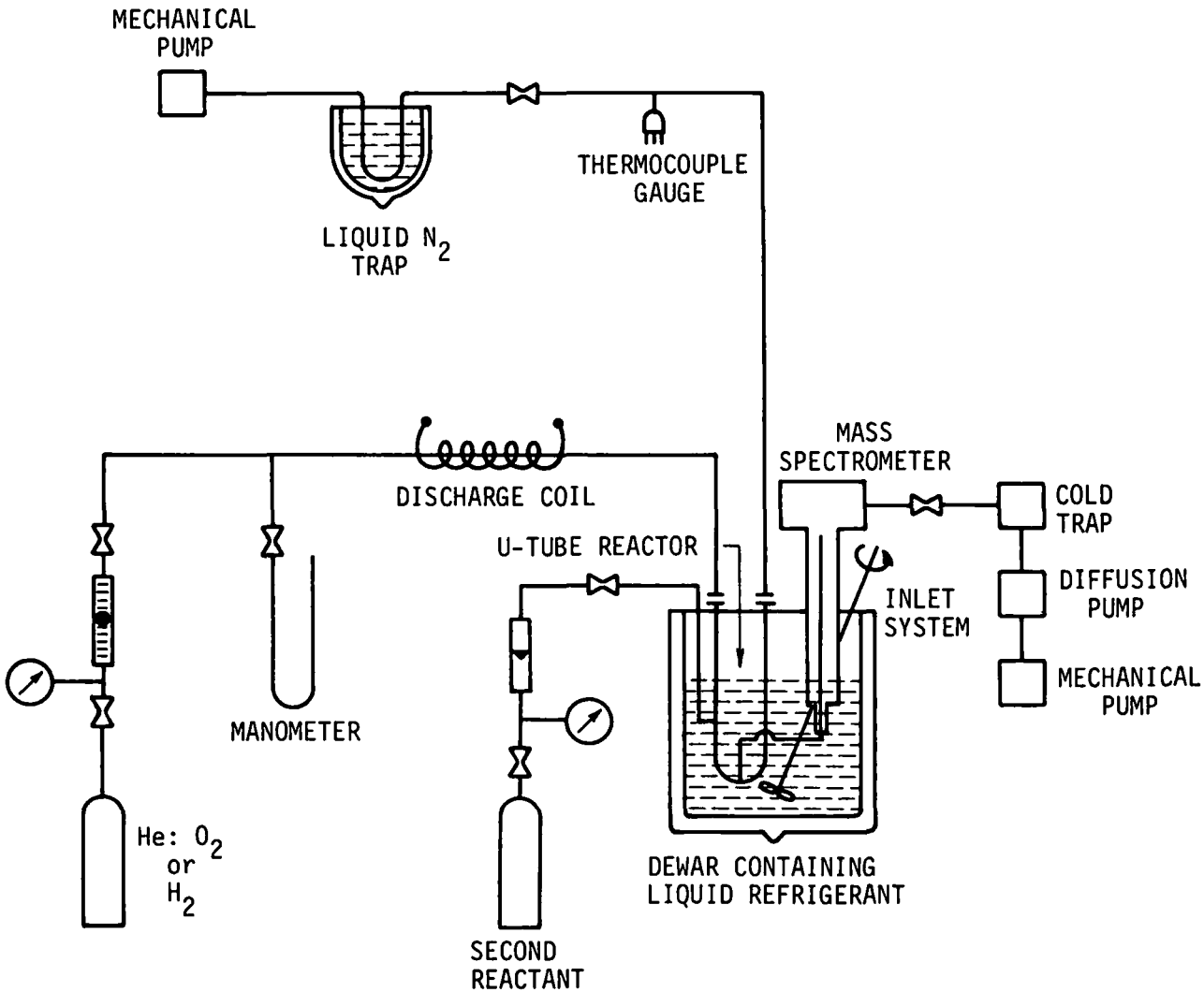


Figure II.8. Schematic of Reaction and Analytical System Utilizing Small Magnetic Mass Spectrometer.

but the ions will have recombined. The second reactant, which in the current research was either ammonia, nitric oxide, acetylene, ethylene, or ethane, also entered the system by passing through a rotameter at a known constant pressure.

This reactor arrangement is, in some sense, a quenched Polanyi diffusion flame, as the low pressure mixture of reaction products and unreacted gases were condensed on the cold walls of the reactor (usually $77^{o}$ to $90^{o}$ K). Noncondensables were continuously removed by a pumping system. The system pressure was indicated in the range $10^{-3}$ to 1 mm Hg with a Vacuum-Electronic Engineering Company thermocouple gauge, type DG2-2T, while higher pressures were measured with a mercury manometer. During reaction, the usual system pressure was in the range 0.5 to 2.5 mm Hg.

a) production of atoms

Atoms were produced by pumping the parent molecular gas through an electrodeless radio frequency discharge coil. The discharge coil was wound on a pyrex tube of 33 mm diameter and was made of fifty turns of 14 gauge copper wire. The discharge was produced in a concentric 12 mm diameter tube, and air was blown into the annular space to provide cooling. The concentric tube arrangement was necessary to prevent high voltage arc-over from the coil to the plasma which would puncture the inner tube, and also the circulating air in the annular space provided efficient cooling, such that pyrex rather than quartz was a completely adequate material for the containment of the plasma.

The discharge coil was powered by a Hallicrafter's radio transmitter model HT-4B having a maximum power output of 320 watts. For maximum power transfer and hence maximum production of atoms, the output impedance of the transmitter had to be matched to the impedance of the plasma. Since the impedance of the plasma is a function of the nature of the gas being excited, the gas pressure, and the flow rate, it was necessary to design an impedance matching network having a wide range of operability. This network is shown in Fig. II.9, where those components enclosed in dashed lines were mounted in a 17 x 13 x 4 in chassis base which was itself mounted within one foot of the discharge tube. The 52 ohm coaxial lead from the transmitter was 10 ft long. The standing wave ratio (SWR) meter was the type P2 sold by Knight Electronics Company, and the two variable air gap capacitors were

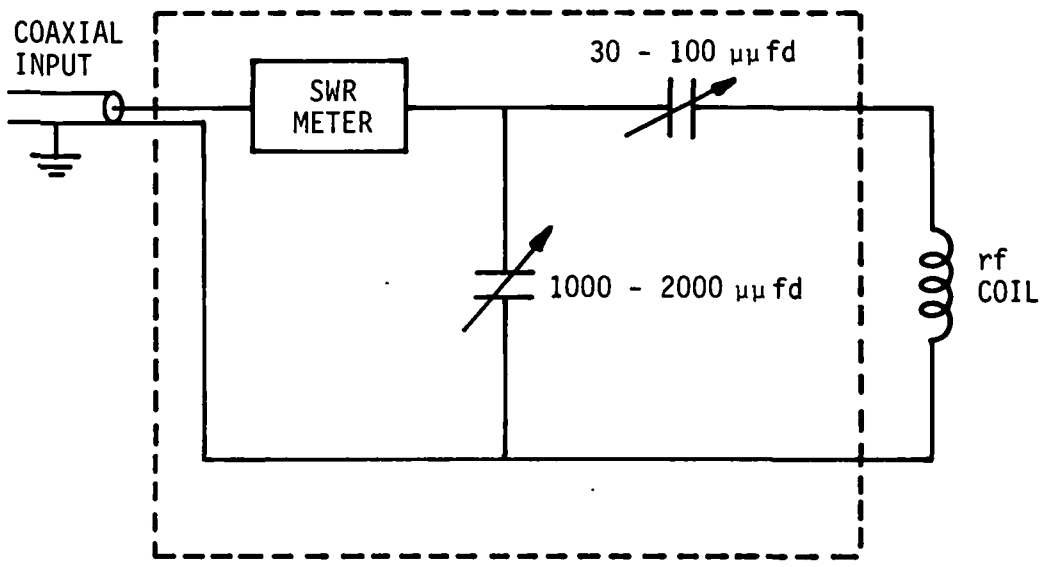


Figure II.9. Impedance Matching Network.

made by Hammarlund Manufacturing Company.

The output impedance of the transmitter was 52 ohms, and it was therefore necessary to adjust the two capacitors until the impedance of the coil system with its plasma core appeared as 52 ohms. The impedance match (or mis-match) was indicated by the SWR meter. It was found that with the series capacitor set at 40 micromicrofarads and the parallel capacitor set at 2000 micromicrofarads, the standing wave ratio was usually less than two at a resonant frequency of approximately 3.5 mcps.

When the discharge coil and matching network were used with the previously described reaction system, an intense discharge could be maintained up to a pressure of about 80 mm Hg when hydrogen was flowing through the system.

Calculations have shown that depending on the particular gas and the flow rate, only 5 to 30 percent of the available power from the transmitter is necessary to dissociate the molecules into atoms in excited states. As an example, at the highest $He:O_2$ flow rate used in these experiments (25 percent $O_2$ and 75 percent He), only 50 watts were actually required to excite the helium to the $2^3S$ state and dissociate the oxygen into atoms in the excited $^1D$ state.

The presence of hydrogen and oxygen atoms at points downstream from the discharge was determined by qualitative tests. Hydrogen atoms will react with yellow molybdic anhydride to form blue-grey molybdenum dioxide according to the equation (II.11),

$$2H + MoO_3 \longrightarrow MoO_2 + H_2O \qquad (4)$$

This test was made periodically during the course of this work and always gave immediate indication of the presence of hydrogen atoms.

The O atom test utilized nitric oxide and was based on the greenish-yellow light emission (II.12) from the reaction

$$O + NO \longrightarrow NO_2 + h\nu \qquad (5)$$

No quantitative tests were made to determine the actual percentage of hydrogen or oxygen atoms at any point in the system.

b) U-tube reactor-inlet system

As can be seen in Fig. II.10, the U-tube reactor was simply a modified cold trap. The upper arms were made of 10 mm ID pyrex tubing which expanded at the U-tube section to 15 mm ID. The upper arms terminated at greaseless, O-ring seal joints, which facilitated the removal of the reactor for cleaning and also eliminated the possibility of contamination from reaction with grease lubricants. The second reactant entered the reactor through a 1 mm ID capillary tubing. The gaseous sample to the mass spectrometer left the reactor through the center section of the U-tube, and was connected to the metal inlet system by means of a 1/4 in Kovar glass-to-metal seal.

Insofar as the mass spectrometer itself is concerned, the objective here was to explore whether or not a small, inexpensive device might be effectively adapted to a cryogenic reactor-inlet system. The only mechanical requirement on a particular commercial machine was that the source be so constructed that a cooled sample delivery tube could be inserted into the ionization chamber such that the electron beam could make grazing contact with the inlet port. The MS-10 was usable to mass 200, required pressures below $10^{-4}$ torr, and the detection limit was claimed to be $10^{-10}$ torr. The ion flight time, which determines the required ion lifetime, is of the order of a microsec. The MS-10 has two main components: (1) the tube unit and magnet assembly which was not much larger than a football and which contained the ion source and collector, and (2) the electronic control unit. The two components were connected by 10 ft of cable, a separation which facilitated the connection of the small tube unit to the cryogenic reaction system.

The vacuum in the mass spectrometer was maintained by a standard diffusion pump system using a Vactronic Laboratory Equipment Company Model HUP-150 diffusion pump having a pumping speed of 140 l/sec. The connecting lines were made of short length, large diameter pipe to keep the pumping speed in the mass spectrometer source as high as possible, but it was estimated that the connecting lines reduced the pumping speed at the source to a value of about 10 l/sec. The pressure in the mass spectrometer was indicated by a Vacuum Electronic Engineering Company Model DG2-2T discharge gauge.

The inlet system itself was maintained at essentially the same temperature as that of the reactor by immersing both the inlet system and the

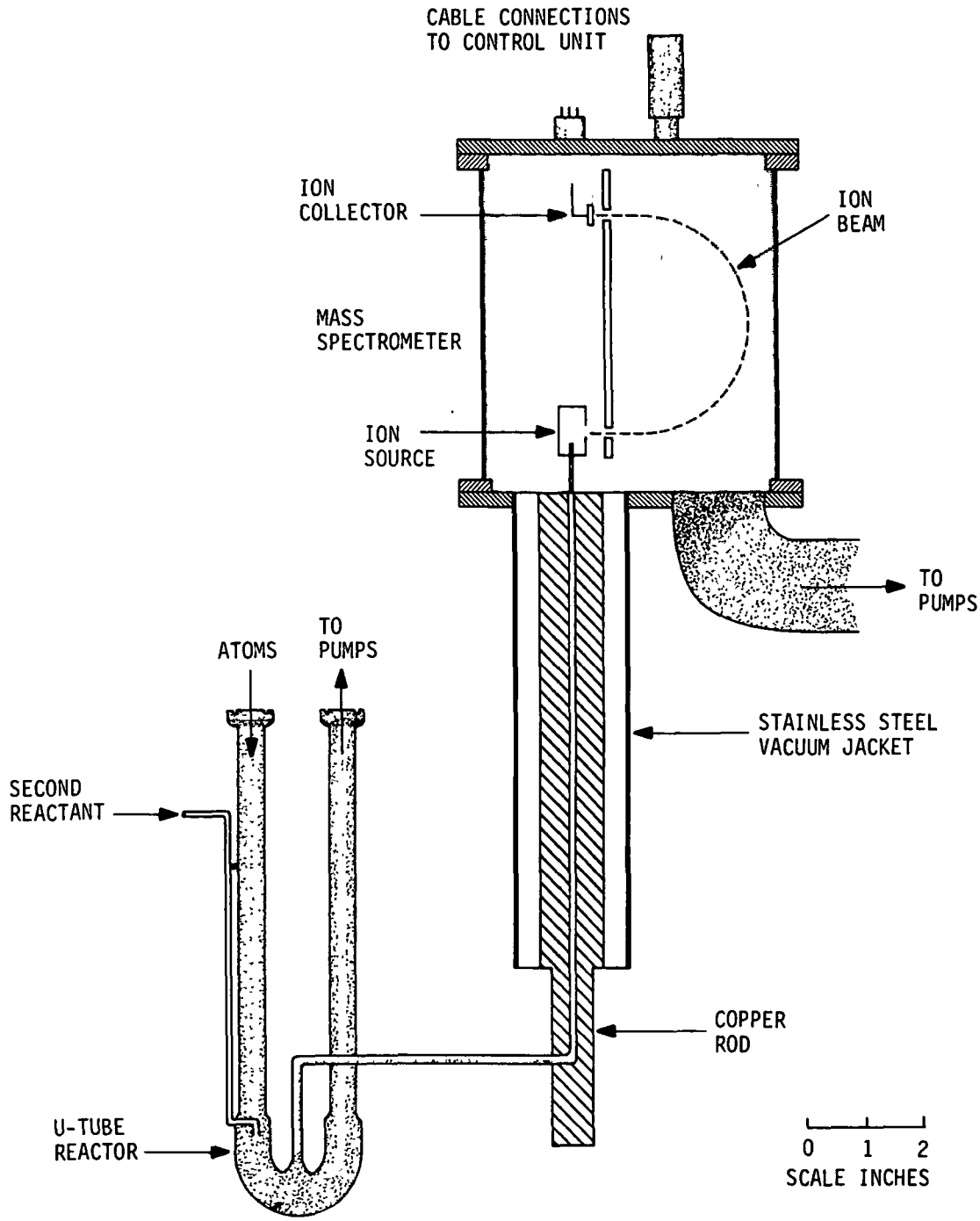


Figure II.10. U-tube Reactor and Inlet System Used with Small Magnetic Mass Spectrometer.

reactor in the same dewar of refrigerant as shown in Fig. II.8. The temperature gradient from the bottom to the top of the inlet system was minimized by three design considerations: (1) the inlet tube was principally contained within a 1¼ in diameter rod of high thermal conductivity copper, (2) the copper rod was nickel plated to reduce the emissivity and hence the heat gain by radiation, and (3) the pressure in the space around the rod (above the refrigerant) was maintained at near $10^{-6}$ torr to minimize heat gain by conduction and convection. Design calculations indicated that a temperature gradient of about $3^{o}$ K might exist over the 9 in length of the 1¼ in diameter copper bar "thermostat" of the inlet tube when its lower end was immersed in liquid nitrogen. This gradient was later verified experimentally. Since the $3^{o}$ K temperature gradient was present when the lower end of the rod was immersed in liquid nitrogen, this was the largest gradient which could have existed.

A final 2 in length of 0.02 in ID monel capillary tubing fitted tightly inside a 2 in length of specially made copper tubing soldered into the upper end of the copper "thermostat". The capillary tubing extended into the ion source region of the mass spectrometer so that the molecules emitted from the capillary were immediately ionized. This is the same notion that was employed in the cryogenic inlet of the TOF machine.

Sensitivity was not as high as might have been supposed. Because this configuration resulted in an inlet passageway of 14 in of 1/4 in tubing, 4 in of 1/16 in tubing and 2 in of 0.02 in tubing, a product partial pressure in the reactor of at least $5 \times 10^{-3}$ mm Hg was necessary for mass spectrometric detection.

c) temperature regulation

Liquid nitrogen and liquid oxygen were the refrigerants used when controlled warm-up was not required. When such warm-ups were required, liquid propane or 2-methyl pentane were used as refrigerants. Propane has a convenient liquid range (melting point to normal boiling point) of $83^{o}$ to $231^{o}$ K, while 2-methyl pentane was a range of $117^{o}$ to $333^{o}$ K. Propane gas from a cylinder of the liquid obtained from a local LPG firm was condensed by passing it through a copper coil immersed in a dry ice-acetone bath. After the dewar (6 in ID x 10 in deep) was filled with about 4 liters of refrigerant, it was cooled to lower temperatures with liquid nitrogen which

was forced into a copper evaporator that was immersed in the continuously stirred refrigerant. With this arrangement the system temperature could be reduced from -60° C to -180° C (using liquid propane) in about 30 minutes.

The temperature was regulated by combined use of an immersion heater (400 watts, quartz, 5/16 in OD x 11 in long) and the liquid nitrogen input to the evaporator. In practice, the temperature was only regulated during the time of reaction. During the warm-up period, the large heat capacity of the refrigerant caused the temperature increase due to the ambient heat leak to be so small that liquid nitrogen cooling was unnecessary. The immersion heater was used when it became necessary to increase the rate of temperature rise. A stirrer was used constantly to reduce temperature gradients in the dewar, and temperatures were measured using a copper-constantan thermocouple and a millivolt potentiometer.

d) safety precautions

Propane and 2-methyl pentane are volatile hydrocarbons and hence several safety precautions were necessitated. The dewar of refrigerant was located within a completely enclosed plexiglass structure. The refrigerant vapors were removed from this "housing" by a centrifugal blower exhausting into a hood. The stirrer motor was located outside the plexiglass structure, and all of the nearby metal was well grounded.

## C. FAST INLET SYSTEMS FOR USE WITH SEVERAL HIGH ENERGY DISSOCIATIVE PROCESSES

It is usually necessary that at least one of the reactants in a cryochemical process be either a free radical or be in an energy rich excited state. This was accomplished experimentally by the utilization of pyrolyses and electric discharges. It is important to know the composition of the effluent that is pumped from such a high energy operation, and therefore several different fast inlet arrangements were developed. The arrangements were similar to inlet systems first used by Eltenton (II.1) and subsequently

highly developed by Lossing (II.2), Dibeler (II.13) and others (II.14).

1. Furnace Beam Inlet System

a) mechanical description

The furnace beam inlet system is shown schematically in Fig. II.11. The main parts are a 3/8 in OD stainless steel furnace tube (1) through which the gas sample is admitted, a 1½ in OD stainless steel exhaust tube (2) which contains the furnace tube and acts as an exhaust tube and cooling tube for the gas from the furnace, and a 4½ in OD stainless steel piston (3) which moves in a double O-ring gland into the same vacuum lock arrangement as used for the cryogenic inlet and which is shown in Fig. II.1. A 3 in OD extension can (4) which is connected to this piston moves to within 3/16 in of the ion grids (or to within 1¼ in of electron beam) of the mass spectrometer. The physical arrangement of the inlet system in place is essentially identical to that of the cryogenic inlet system shown in Fig. II.2. In operation, the gas sample travels down the furnace tube, is heated by a length of nichrome wire wound furnace (5) (whose upper temperature limit is approximately 1000° C), and impinges upon a thin metal foil (6) which is mechanically sealed into the end of the exhaust tube. A cooling coil (7) is provided should it be necessitated by the furnace temperature and gas flow rate. The thin metal foil (about 0.010 in thick) allows a jet of the gas to be admitted into an intermediate differentially pumped space. The foil may be nipple shaped as shown to allow the orifice, in the deepest part of the nipple, to extend into the furnace region and consequently to be at approximately the same temperature as the gas from the furnace. The intermediate pumping space, which is that volume lying within the piston and extension can and outside of the exhaust tube, is evacuated by a separate diffusion pump system. The jet of gas then strikes another thin metal foil (8) which is located within about 2 to 3 cm of the electron beam and which produces a reasonably well collimated molecular beam going into the source. At the pressure of the intermediate space and assuming the gas leaving the first foil is at approximately the same temperature as the furnace, it would be expected that molecular flow is experienced through the final foil and therefore the mass spectrometer would essentially be recording the condition of the reactant gas as it exists in the furnace.

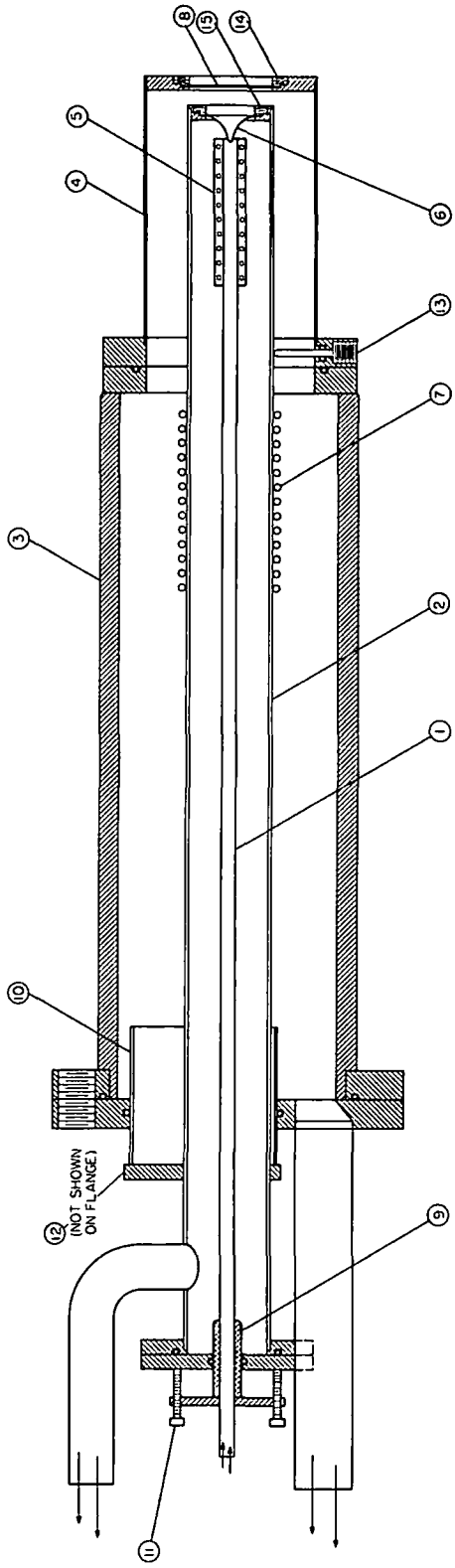


Figure II.11. Schematic Diagram of Furnace Beam Inlet System.

Several features were incorporated into the design of the apparatus to provide for flexibility and convenience in operation and maintenance of the system. For instance, the furnace tube and exhaust tube are mounted through flanges on sleeves (9) and (10) which are free to slide in O-ring seals. By means of adjusting screws on the tubes (11) and (12), the distance between the end of the furnace tube and the first foil may be varied as may the distance between both foils. Adjustment of these two parameters would presumably produce an optimum molecular beam for analysis by the mass spectrometer. Also, for alignment of the holes in the foils, three positioning screws (13) are provided which come in through O-ring seals in the flange on the extension can at right angles to and bearing upon the exhaust tube.

From the point of view of convenient maintance, it was desirable to be able to replace the foils from the end where they are located rather than having to dismantle the whole apparatus. Therefore, the design is such that for removal and replacement or cleaning of the foils, the apparatus may be withdrawn from the mass spectrometer, the compression nut (14) and the foil removed from the outside, and then, through the resulting opening, the remaining compression nut (15) and foil may be removed.

The flanges on the exhaust tube and the piston were provided with terminals for power and thermocouple connections. The temperature of the furnace was measured by a chromel-alumel thermocouple imbedded in the furnace insulation. Thermocouples were also placed at several points, such as near the O-ring seals and wherever it was felt that overheating might occur.

Fig. II.12 shows a simplified flow diagram of the experimental set-up. The flow rate of the input gas from the sample reservoir (1) was measured by a Fischer and Porter flow meter (2). The leak valve (3) and the throttle valve (4) were manipulated to control the flow rate and the furnace pressure, which may be varied from a few microns to several millimeters of mercury. For pressures greater than approximately 1 mm of mercury, an Edwards High Vacuum, Ltd. leak valve (3) model LB2A, was used, whereas a Vactronic model VV-50 leak valve was employed for lower pressures. Vacuum gauges (5) and (6) indicated the pressure drop through the system and also the approximate furnace pressure. Again depending upon the range of pressures involved, a Dubrovin vacuum gauge, a McLeod vacuum gauge, or a Veeco cold cathode

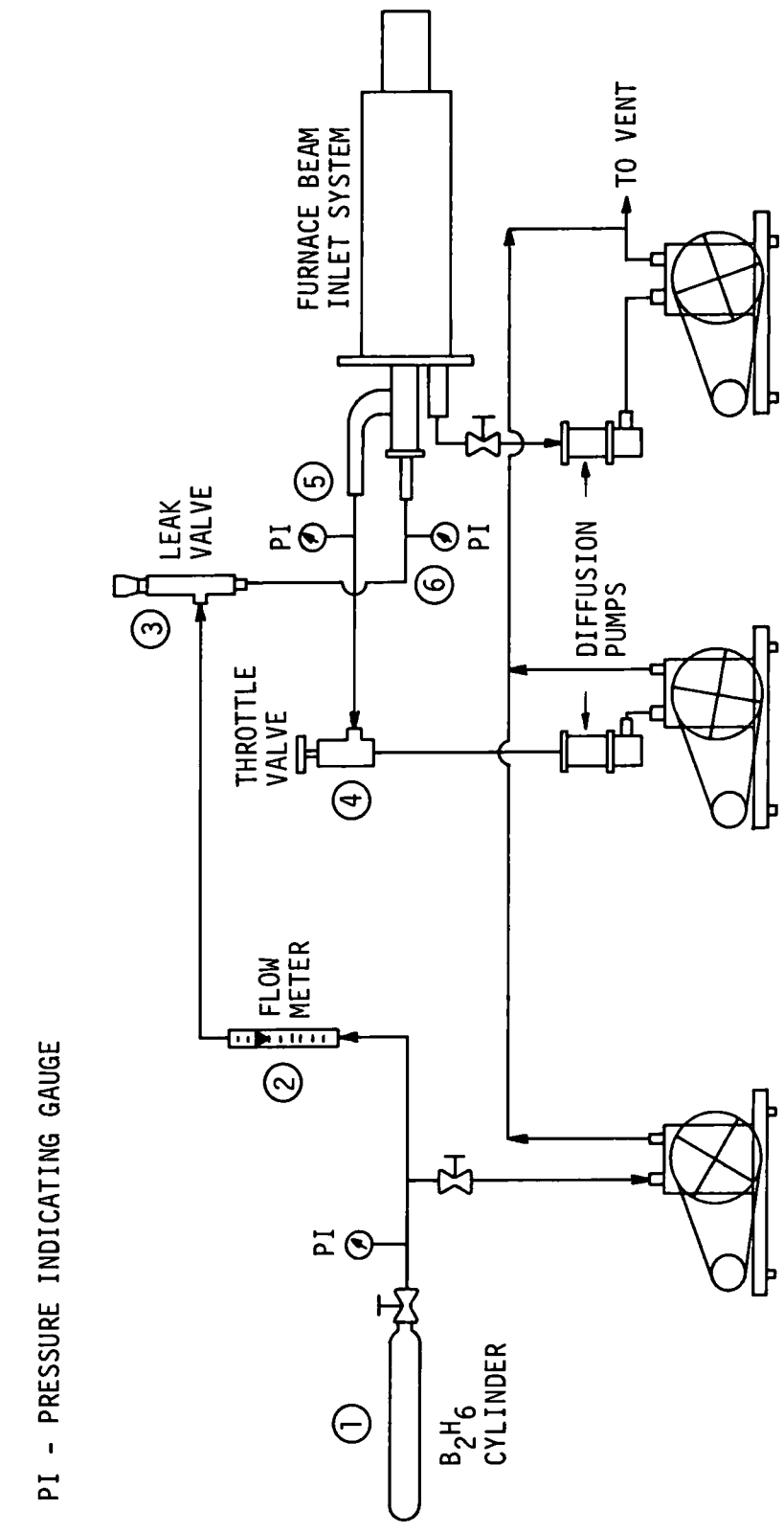


Figure II.12. Flow Arrangement for the Furnace Beam Inlet System.

discharge gauge were utilized. Both the intermediate pumping space and the furnace exhaust tube were evacuated by diffusion pumps, though for pressures above 1 mm Hg only the mechanical pump was used to exhaust the furnace.

b) experimental procedure

Flow rates of parent gases of typically up to about 150 std $cm^3$/min could be studied at pressures of 20 to approximately $10^{-4}$ mm Hg. The flow rates at the lower pressures were too low to permit determination, though the Vactronic leak valve will supposedly allow control down to 0.01 std $cm^3$/sec. Temperatures as high as 900° C could be attained. The pyrolysis furnace was also packed with stainless steel turnings in several experiments.

Although rough calculations were made to determine the amount of gas that would be admitted through the two orifices and into the ionization region of the mass spectrometer, a trial-and-error method was used to determine a satisfactory orifice size for different operating conditions. In all cases, the orifice must allow a quantity of gas to enter the ionization region which is sufficient for appearance potential measurements, yet must not permit a quantity so large to enter that either the multiplier plates of the spectrometer become saturated or the pressure in the mass spectrometer rises above $2 \times 10^{-5}$ mm Hg, a maximum operating pressure if ion-molecule reactions are to be minimized. The orifice sizes varied from 0.010 to 0.063 in in diameter. Additional experiments were conducted in which only one foil was present and in which both foils were removed and the furnace tube advanced so close to the ion source as was possible (about 1¼ in).

2. Coaxial Furnace Inlet System

The tubular furnace shown in Fig. II.13 was constructed for pyrolysis studies at pressures of up to 500 torr and temperatures as high as 500° C. The furnace was mounted coaxially with the drift tube of the mass spectrometer inside the fast reaction chamber of the model S-14-107 ion source. The most desirable feature of this system was that it allowed the furnace exit to be positioned anywhere from being completely immersed in the electron beam to about 2 in away. In comparison, the furnace exit of the furnace beam inlet system could be advanced no closer to the electron beam than 1¼ in.

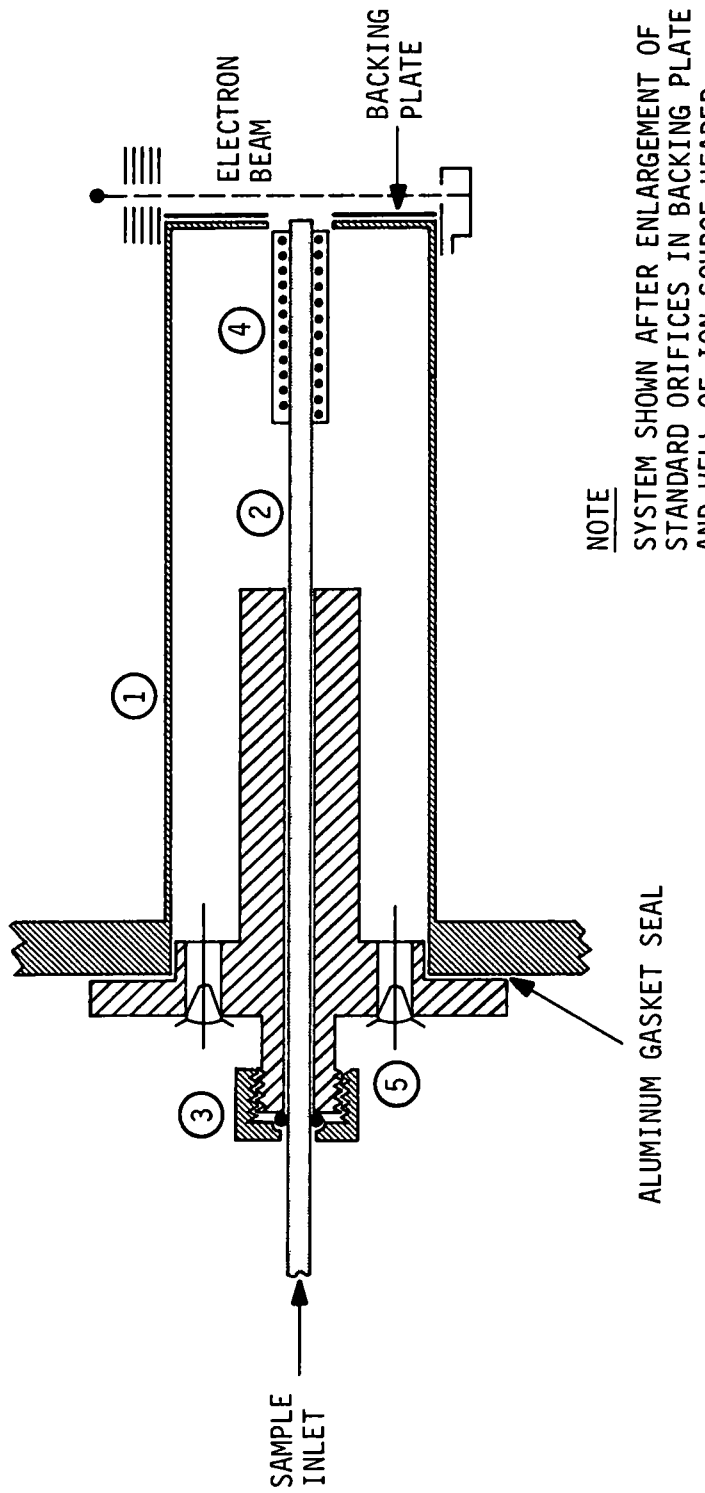


Figure II.13. Coaxial Furnace Inlet System.

The furnace tube (2) was a 1/8 in OD stainless steel tube which could be positioned by sliding through an O-ring sealed quick-disconnect joint (3). The heated region (4), usually 1 in in length, was wound with nichrome wire imbedded in Sauereisen Insa-Lute Adhesive Cement for uniform heating as well as for insulation between the wire and the furnace tube itself. The temperature of the furnace was measured by a chromel-alumel thermocouple which was also imbedded in the Sauereisen. Power and thermocouple leads were introduced through high vacuum electrical feed throughs (5). Furnaces of alumina and quartz (1 in in length and 1 mm ID) were also employed by simply sealing them into the end of the 1/8 in tube. In some instances, the stainless steel furnace was packed with five or six 1 in lengths of monel capillary tubing as a means of increasing the ratio of surface to volume without unduly increasing the contact time.

The sample gas was introduced by means of a Vactronic model VV-50 leak valve connected to a suitable delivery system (usually a lecture bottle filled with the pyrolysis parent gas). The inlet pressure was indicated by either a thermocouple gauge, a Veeco cold cathode discharge gauge, or a Consolidated Electrodynamics Corporation type 41550 micromanometer. The production of the species of interest was maximized by varying pressure, temperature and flow rate.

In initial experiments with this system, the sample gas from the furnace traveled into the ionization region of the mass spectrometer through a 0.032 in orifice in the well of the ion source header and then through a similar orifice in the backing plate (0.015 in thick) of the ion source. To maximize sensitivity, it was later found necessary to enlarge both of these orifices to ¼ in, and, in order to preserve the proper ion optics, to cover the large opening in the backing plate with the same fine mesh that is used on the ion grids. With the backing plate removed, the furnace exit could be positioned directly in the electron beam. However, it was discovered that this caused a lowering of the appearance potential of all species present, including the inert calibrating gas, argon. When the exit was positioned flush with the bottom of the source well, this effect was not noticeable. At first, it was believed that the potential existing on the furnace windings was accelerating the ionizing electrons to an energy a few volts higher than that indicated by the digital voltmeter which was connected to read the

electron energy. These observations were made with furnaces having a single winding of heater wire. Later, when using a furnace with a double winding, the appearance potential lowering was again noted, even though the furnace exit was not advanced into the ionizing region and the grounded end of the windings was located at the furnace exit. The most reasonable explanation of this phenomenon appears to be that the alternating magnetic field from the furnace windings was causing an acceleration of the electron beam, the effect being more noticeable for a furnace with a double winding of heater wire than with a single winding. The furnace inlet system described by Gohlke and which was mounted between the backing plate and the first ion grid, also upset the electron and ion optics in the Bendix source, until DC was used to heat the furnace (II.15).

3. Hot Filament Inlet Systems

The hot filament inlet systems described below were designed for us in pyrolysis experiments at temperatures from about 900° C to the temperature at which the metallic filament collapsed. This upper temperature limit was about 1700° C for platinum, 1100° C for nichrome and about 3000° C for tungsten. Filaments of zirconium, molybdenum, niobium, titanium and tantalum have also been used.

The device shown in Fig. II.14 which fits into the fast reaction well of the S14-107 source was used with gaseous samples. The parent compound was admitted from a gas-handling system through a monel tube (A). This tube ejected gas onto the metallic filament (B), which was formed into a spring-like coil. A portion of the gas rebounding from the filament then passed through a 0.032 in leak (C) into the ionization chamber of the mass spectrometer. The filament was positioned approximately 1/8 in from the electron beam.

The use of a gold foil leak was unnecessary since at the pressures at which the intermediate pumping volume (D) was operated the flow rate into the mass spectrometer was adequately small through a 0.032 in orifice in the fast reaction inlet well. This space was pumped through the line (E) by an auxiliary pumping system. Power was supplied to the filament through two brass support rods (F) which were insulated from the header by high vacuum electrical feed-throughs (G).

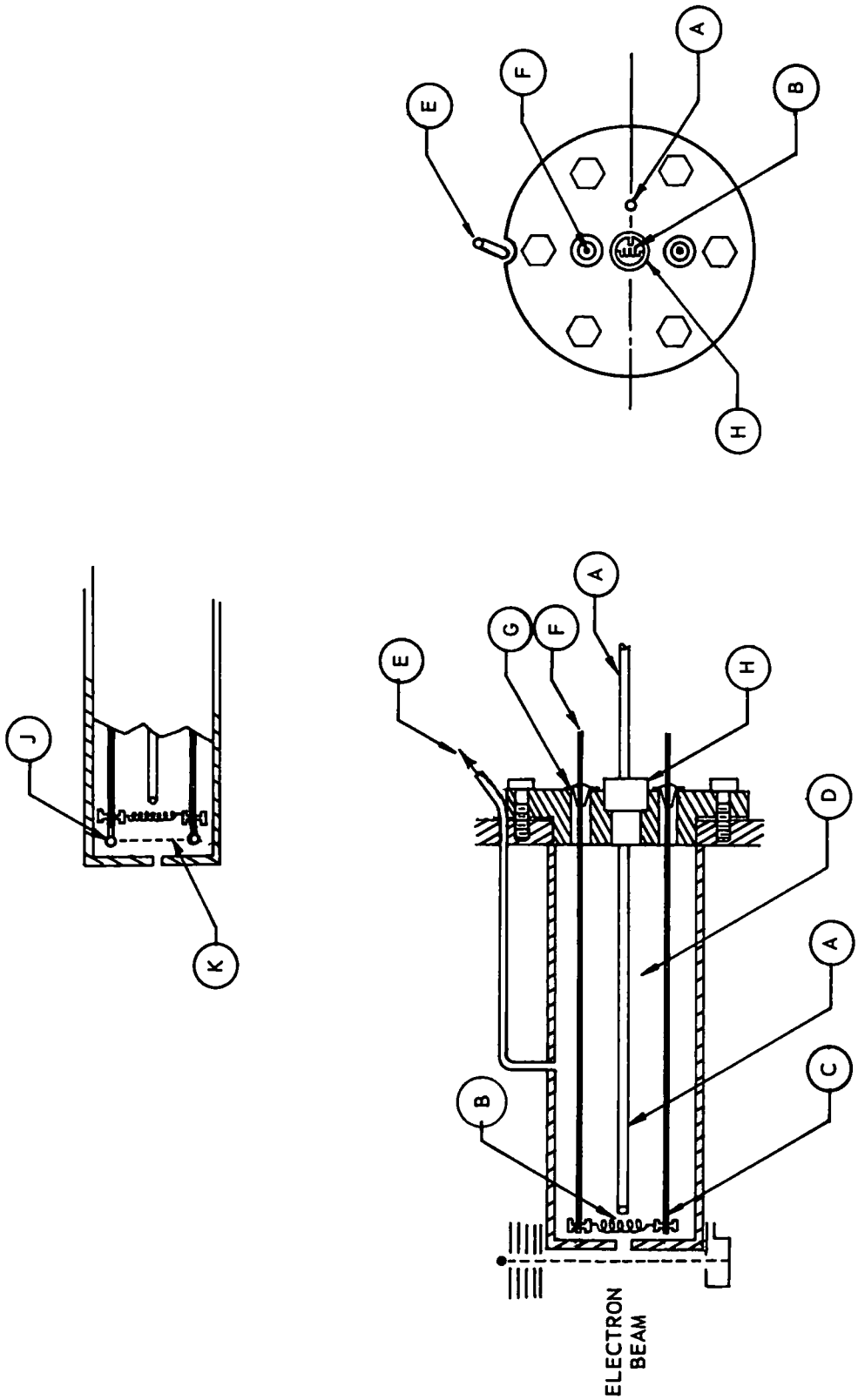


Figure II.14. Hot Filament Inlet System for Gaseous Samples.

The temperature of the filament was measured by a Leeds & Northrup optical pyrometer, Model 8622-C, by sighting through a plexiglass window (H). Because of the small size of the target, the reproducibility of these measurements was only about $\pm$ 10° C, and no corrections were applied. The filament current was supplied from a Sola constant voltage transformer and was regulated by a Powerstat. Fine control was provided by a 110 ohm slidewire resistor, manufactured by James G. Biddle Company in series with the filament.

It was found that the use of a tungsten filament at high temperatures resulted in the production of a considerable number of ions in the inlet system. These ions could have been formed by surface ionization or by the acceleration of electrons between the two filament supports. In order to prevent the passage of these ions into the mass spectrometer and the consequent large increase in the background noise in the spectrum, the retarding grid shown in the insert in Fig. II.14 was installed. Glass rods (J) were attached to the brass filament support rods and very fine stainless steel mesh (K), taken from a discarded ion grid, was stretched across these glass supports. This modification necessitated the movement of the filament to a position approximately 3/8 in from the electron beam. A 6 volt positive bias was applied between this retarding grid and the filament by means of an external battery. The noise due to ions generated outside the electron beam was thereby usually reduced to a level which was difficult to detect. The degree of ionization that occurs on filaments as well as the nature of the entire pyrolysis process itself depends strongly upon the choice of filament. It is evident that the physical arrangement described here lends itself well to the detailed study of surface chemistry.

The similar inlet system shown in Fig. II.15 was constructed for use in experiments involving parent compounds which are solids at room temperature. The filament (A) was held between the leads of the two high vacuum electrical feed-throughs (B) which were mounted on a small header (C). The sample tube (D) passed through the header directly under the filament. This header was mounted on a 1 in tube (E) and positioned so that the filament was within 1/8 in of the leak (F) into the ion source. As in the other inlet systems, an auxiliary diffusion pump system was used to exhaust the intermediate pumping volume (G) through the exit line (H). A window

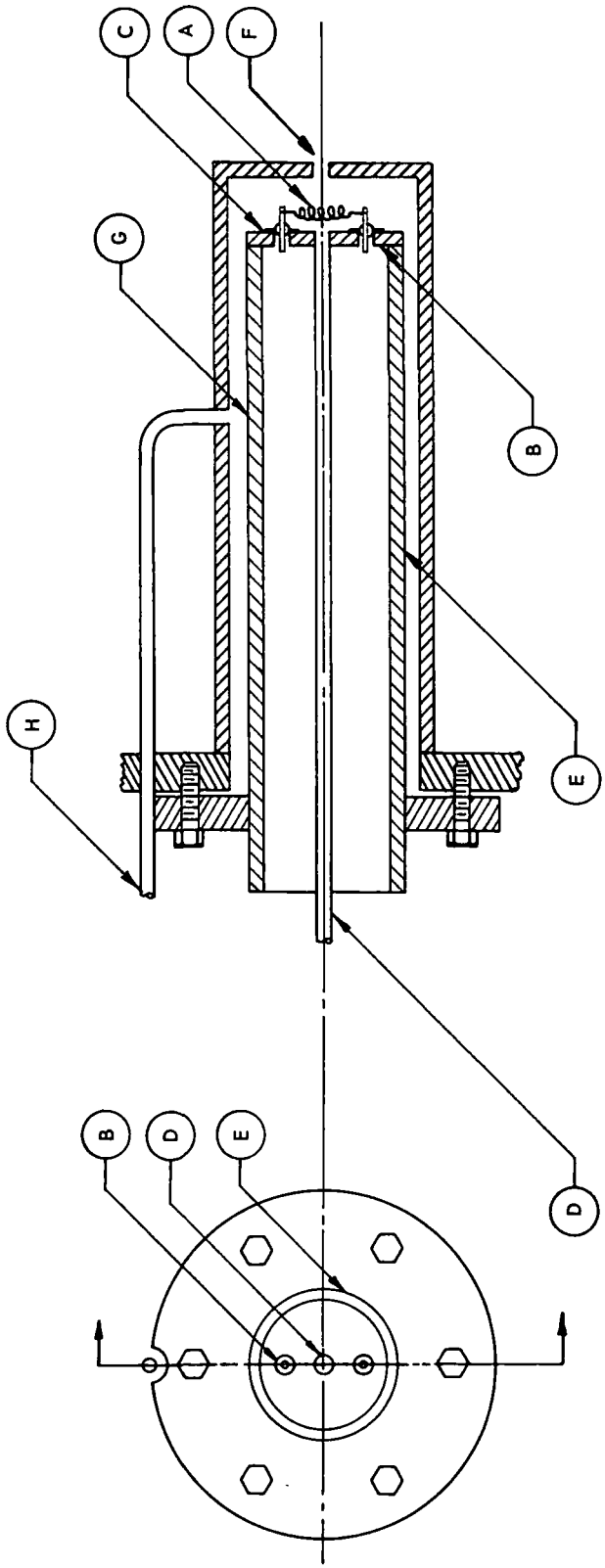


Figure II.15. Hot Filament Inlet System for Use with Solid Parent Compounds.

for observation of the filament was not provided in this inlet system. The temperature was roughly set by noting the adjustments of the Powerstat and slidewire which were required to produce certain temperatures in filaments of a particular resistance but using the hot filament inlet system for gaseous samples. These same settings were used to approximate that same temperature in the solids inlet system.

4. Arrangements for Pyrolysis Studies with Parent Substances Stable only at Very Low Temperatures

Unstable and energy rich molecules of the sort synthesized by cryochemical procedures may be pyrolyzed at still very low temperatures by terrestrial standards. Such pyrolyses in fast flow inlet arrangements are important in the same sense as are similar studies with more ordinary molecules. That is, by subtracting the ionization energy of a fragment produced in such a pyrolysis from the appearance potential of that same fragment without pyrolysis, one obtains the corresponding bond energy. These energetic quantities are particularly interesting for the unusual molecules that are often produced in cryochemical reaction sequences.

To permit furnace pyrolyses of species present in the cryogenic reactor-inlet system shown in Fig. II.1, the copper extension piece (item (16) of Fig. 1) was replaced with a furnace which made it possible to study the initial and perhaps unstable or transitory pyrolysis products of the sample stored in the condensation tube. The furnace attachment (Fig. II:16) consisted of a 3.8 cm long alumina tube (0.103 cm ID) heated over a 2.5 cm region by a tungsten resistance wire (0.0107 cm dia). The alumina tube and heater wire were coated with Sauereisen Insa-Lute Adhesive Cement (No. 1 Paste) to assure uniform heating and were encased in a quartz sleeve to prevent surface ionization on the heater winding itself. The temperature of the furnace was measured by a copper-constantan thermocouple imbedded in the Sauereisen at the center of the heated region. Flow through the furnace was controlled by maintaining the cryogenic inlet arrangement at a temperature such that the condensed species of interest exerted a vapor pressure of approximately 1.0 torr.

Syntheses in the system with the furnace attached were somewhat complicated by the fact that the furnace was very fragile, and the exit port (10) could not be sealed off from the isolation vacuum by use of the teflon block valve as was described earlier. Hence the reactant mixture, or whatever, in

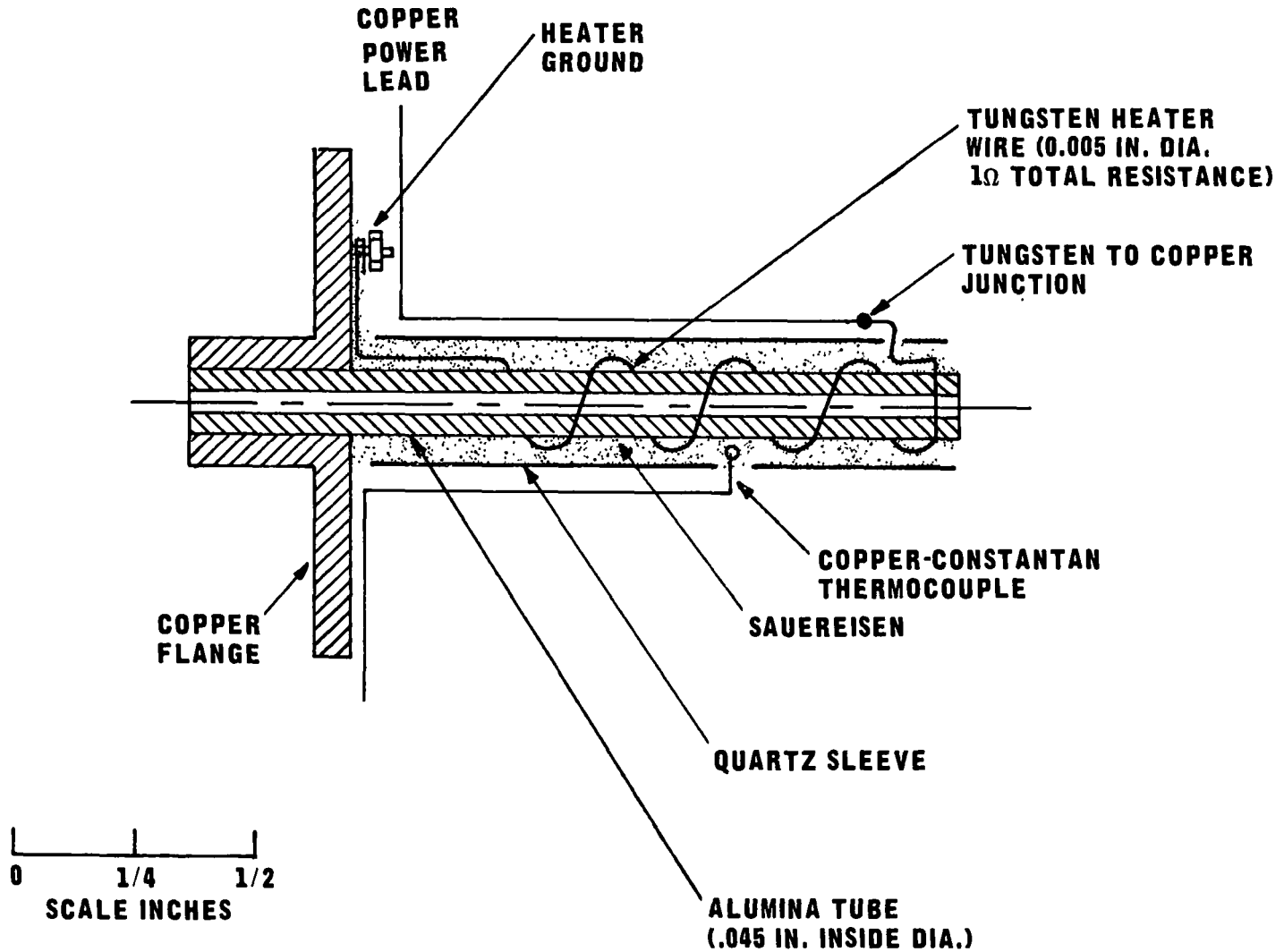


Figure II.16. Schematic Diagram of Furnace Attachment for the Cryogenic Reactor-inlet System.

the system would, of necessity, break the isolation vacuum causing a greatly increased refrigerant load and a corresponding cooling of the entire vacuum lock assembly. It was possible, however, to tolerate this rather poor situation for short periods of time. This arrangement was successfully used in the synthesis of $O_2F_2$ using the concentric electrode reactor (Fig. II.3), with the product then pyrolyzed with the furnace of Fig. II.16 heated to 250° K. For the molecule of interest, $O_2F_2$, this temperature, although still very low relative to room temperature, does indeed constitute a very hot furnace. $O_2F_2$ cracked to give the $O_2F$ free radical, the ionization potential of which was measured to be $12.6 \pm 0.2$ ev (II.8).

It is particularly notable that withdrawing the exit of the furnace less than 6 mm from the edge of the electron beam resulted in such a decrease in the intensity of the $O_2F^+$ radical ion that it was barely detectable.

A second arrangement is shown in Fig. II.17 in which cold reaction products from the reactor-inlet system can be pyrolyzed directly in the electron beam of the spectrometer. A heated coiled wire filament is stretched directly across the exit port of the inlet system. With the extension piece of the inlet system positioned within the ion source as described earlier, the species can be passed directly over the hot filament. This permits detection of pyrolysis products formed by a single collision with the filament and with no subsequent gaseous collisions before analysis. It has been demonstrated that the filament can actually be immersed in the electron beam. This appears to represent the very optimum arrangement for this type of study and apparently has not been attained in any other similar experiments.

Numerous filaments were used in the investigation of the pyrolysis products of $OF_2$ at temperatures of 650°-1000° C. The temperature of the filament was determined by sighting through the observation port (item (13) of Fig. II.1) with a Leeds & Northrup Model 8622-C optical pyrometer. It is interesting to note that these pyrolysis experiments varied markedly with various filaments which suggests that this would be a suitable arrangement for the study of surface chemistry and catalysis. Noise appeared in the spectrum when using these filaments due either to surface ionization or to thermal electrons being accelerated in an oscillatory manner by the 60 cycle

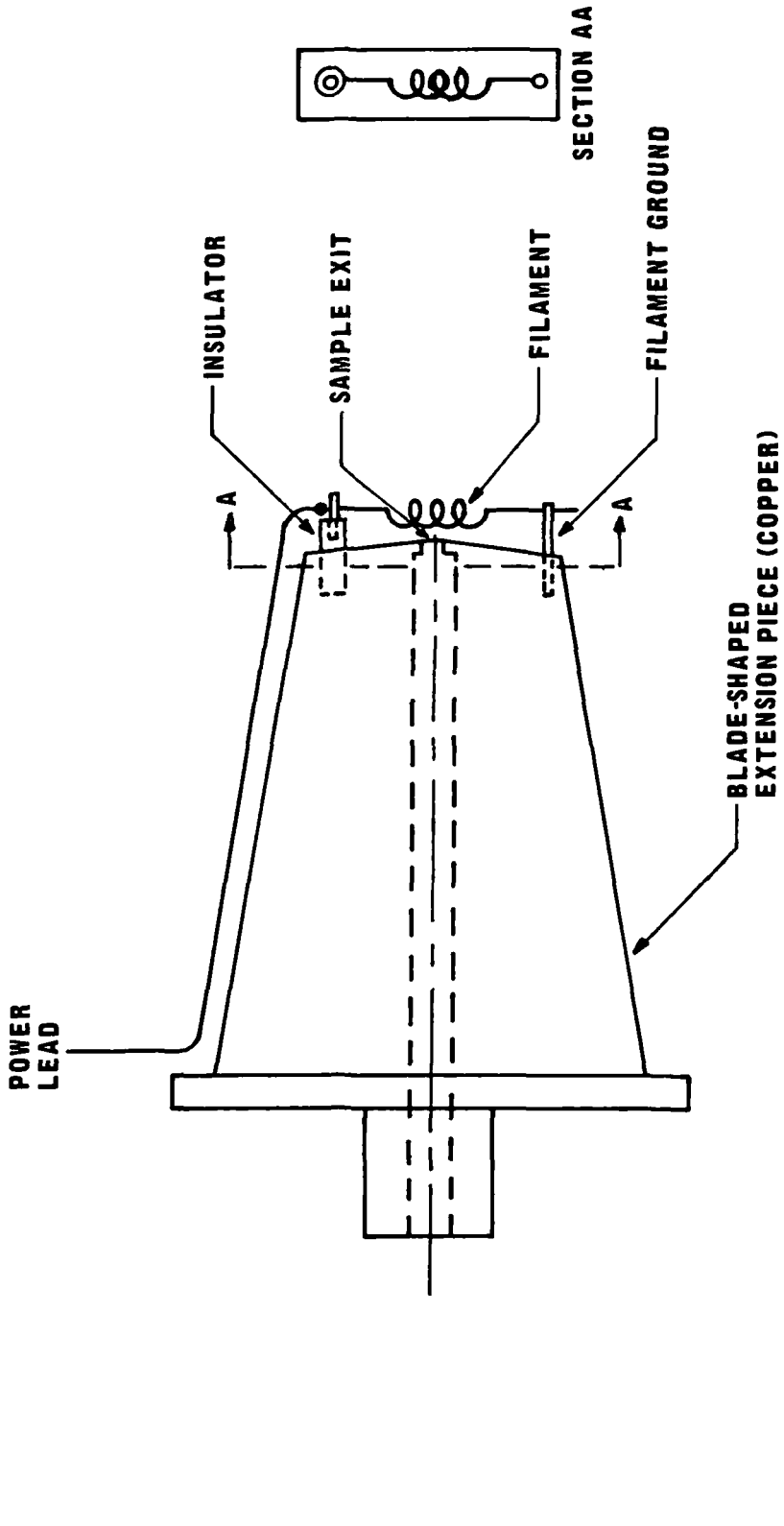


Figure II.17. Schematic Diagram of Hot Filament Arrangement on the Extension Piece of the Cryogenic Reactor-inlet System.

field of the filament. As expected, different metals produce strikingly different amounts of this troublesome noise.

5. Systems for Studying the Effluent from rf Discharge

The experimental arrangement appears in Fig. II.18 which shows a 3/8 in diameter pyrex, quartz, or alumina discharge tube (1) sealed into the fast reaction inlet well (2) of the S14-107 ion source by an O-ring sealed quick disconnect joint (3). A carrier gas, if desired, and the parent gas were admitted through Vactronic Model VV-50 leak valves (4) and (5). The discharge was generated by means of a 50 turn, 2.5 cm diameter coil which was connected through an impedance matching network to an rf power supply as described earlier. A 650 volt potential, supplied by several batteries in series (7), was applied between two parallel metal strips (8) placed on either side of the discharge tube. This was necessary to prevent ions produced by the discharge from entering the ionization region of the mass spectrometer and creating noise. Several turns of aluminum foil (9) situated on either side of the discharge coil restricted the visible glow of the discharge to the region between the foils. Otherwise, the discharge glow would extend over the entire length of tube, heating up the tygon connections to the valves, thereby introducing impurities, and causing noise in the spectrometer. An attempt was made to conduct an in-line discharge, i.e., with the discharge tube coaxial with the drift tube. However, all efforts, whether employing electric fields or magnetic fields or both, to prevent ions from entering the ionization region, failed. It appeared that the nominal 3000 volt drop across the discharge coil was creating highly energetic ions which could not be deflected into the walls in order to allow neutralization by the methods that were used. The $90^{o}$ bend was successful in eliminating the majority of the ions, but the parallel metal strips were necessary for complete elimination.

In operation with argon or hydrogen as a carrier, the discharge and the pressure were adjusted until a fairly intense glow was obtained, the parent gas could then be injected downstream of the coil in an effort to temper the violent action of the discharge itself. In a series of experiments with diborane in which symmetrical cleavage to $BH_3$ was the desired result, such a gentle dissociation was required to be sure, but also the metallic boron deposit that was produced due to complete decomposition masked the

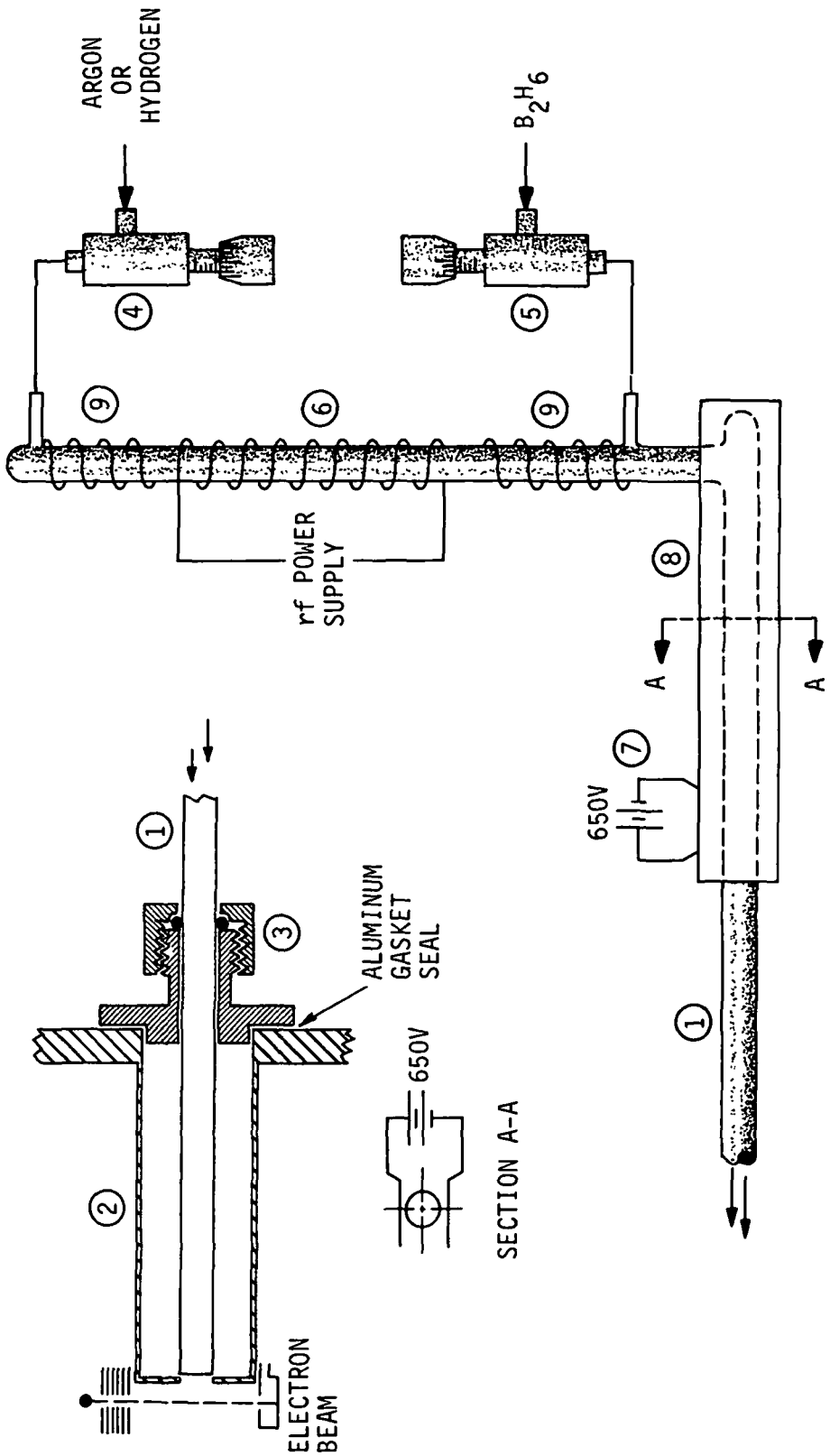


Figure II.18. Radio Frequency Discharge Tube Inlet System.

plasma from the applied rf field.

This discharge system was used to decompose the $OF_2$ molecule in attempts to observe the OF free radical. In these experiments the $OF_2$ gas was injected through a Granville-Phillips variable leak valve into a 0.635 cm ID quartz or alumina discharge tube, with a similar geometry and rf power arrangement as has been described. The gaseous products passed from the discharge region, around a $90^{\circ}$ turn, and directly into the mass spectrometer. The backing plate of the ion source was removed so that the end of the inlet tube could be inserted up to the edge of the electron beam. The total length of the tube from the discharge region to the electron beam was 12.5 cm. The $90^{\circ}$ elbow again proved to be necessary to remove ions formed by the electric discharge, but, alas, no free OF was observed.

## D. TWO MODIFICATIONS FOR INCREASED SENSITIVITY OF THE TOF SPECTROMETER

### 1. Blanking Circuit

The Bendix mass spectrometer has an undesirable feature in that the resistive coated glass electron multiplier plates, which amplify the electron signal produced by the ions arriving at the collector, lose sensitivity quite rapidly, and produce "noise" (diffuse mass peaks appearing at both integral and nonintegral mass numbers) when very large ion currents are present. This situation often exists when one is interested in maximizing a signal that is small relative to other ions that may also be present. In such cases, the noise is a particularly serious problem since one cannot obtain a true reading of the intensity of the ion of interest, and hence appearance potential measurements are impossible.

A blanking circuit, which protects the multiplier glasses by removing the electron signal before it can reach them, and which functions by applying a voltage pulse to the "Z" plate, is available from Bendix but is limited to mass 4, He. A similar and much more useful circuitry has been developed

by Haumann (II.16). A related circuitry was developed during the course of this work, and it is described below.

The main pieces of equipment used for the blanking circuit were a General Radio Company Type 1205-B adjustable regulated power supply and a Rutherford Electronics Company Model B7B pulse generator. The circuit diagram is shown in Fig. II.19. Basically, the circuit provides a square wave, adjustable to a maximum of approximately 340 volts which is applied positively with respect to the normal bias on the plate to the "Z" plate of the multiplier. This plate usually has a bias of -2600 v when operating in the "pulsed positive ions" position. The duration of the pulse is adjustable from 0 to greater than 50 microsec, which is the duty time of the mass spectrometer. In addition, the pulse generator is equipped with a delay circuit so that the beginning of the square wave pulse may be varied from a value of m/e equal to zero to any value of m/e. In this way, if the mass peak of interest lies below the large mass peaks that are creating interference or noise, by proper settings of the delay and pulse duration controls of the pulse generator, the large electron pulses will be prevented from ever reaching the input end of the glasses. Such is also the case when the peak of interest lies above the interfering peaks. This circuit is to be compared to that of Bendix which has no adjustable delay, and to that of Haumann (II.16), which is capable of blanking out interfering mass peaks on both sides of the ion of interest. The Bendix adaptation was designed for use in GLC adaptations in which a large peak due to the carrier (usually helium) is present, and is, of course, quite uninteresting.

2. Modification of the Standard Retarding Potential Difference Circuitry

A disadvantage of the normal RPD arrangement of the grids of the electron gun, as described by Martin (II.17) and shown in Fig. II. 20, is that the maximum attainable trap current (ionizing electron beam) at electron energies normally used for ionization potential measurements (approximate 10-18 volts) had usually been no more than 0.03 microamp. In normal operation, the trap current can be increased to greater than 0.25 microamp. Melton and Hamill (II.18) who modified the Bendix mass spectrometer for the utilization of the RPD technique, attribute the loss of trap current to a defocusing action on the electron beam caused by the deceleration between the control grid

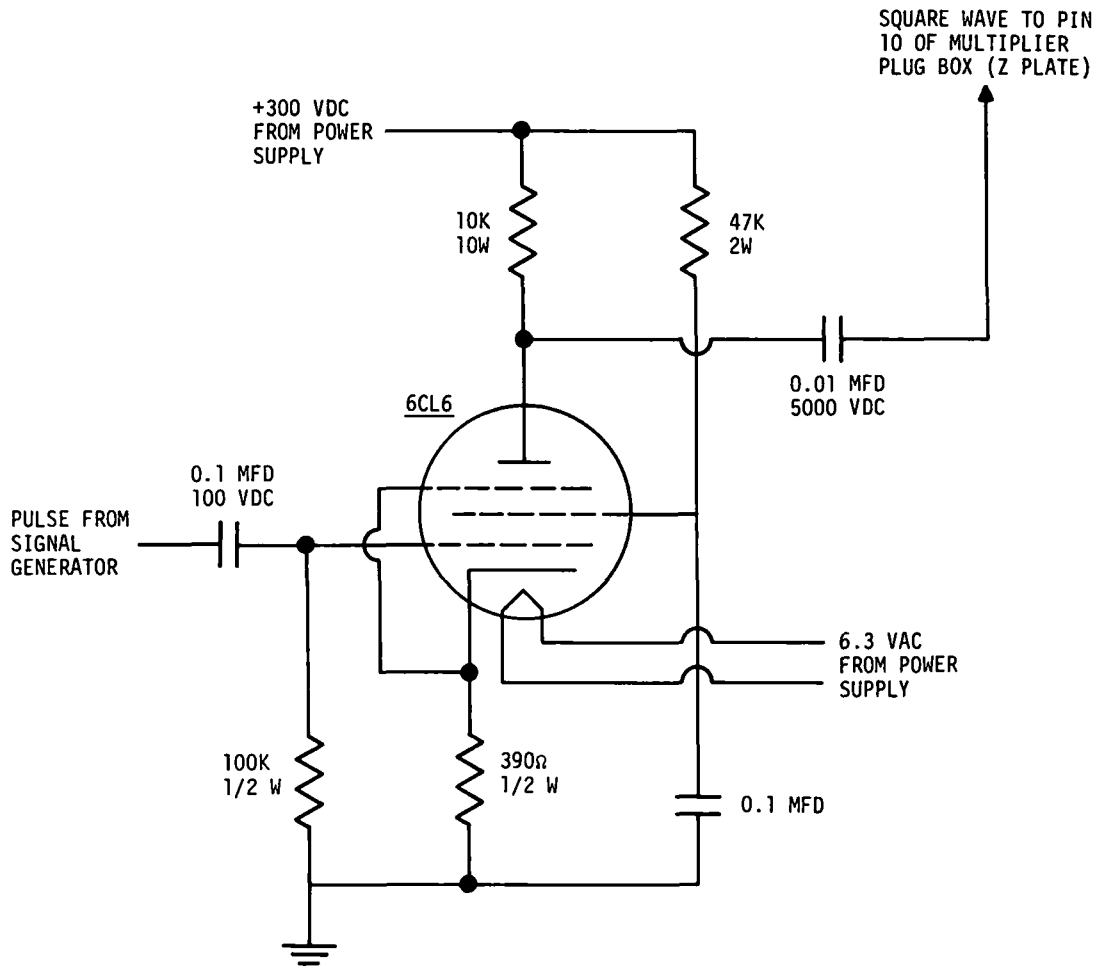


NOTES

1. Signal Generator Triggered by Mass Spectrometer.
2. Standard Jumper Between Pin 10 (Z Plate) and Pin 11 (Grid) of Multiplier Plug Box Removed.
3. 100K, 1/2 W Resistor Installed Between Pin 10 and Pin 11.

Figure II.19. Schematic Diagram of Blanking Circuit.

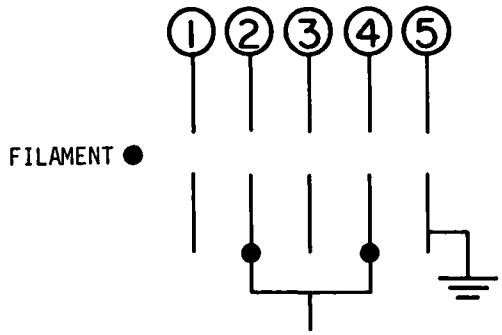


| GRID | | TYPICAL POTENTIAL |
|---|---|---|
| 1. | CONTROL GRID | ∿ 0 WITH 8 VOLT PULSE |
| 2. | RETARD SHIELD | + 2 VOLTS |
| 3. | RETARDING GRID | -0.2 TO -0.4 VOLTS |
| 4. | RETARD SHIELD | + 2 VOLTS |
| 5. | GROUND | + ELECTRON ENERGY |

NOTE

Potentials are with respect to Filament.

Figure II.20. Electron Gun for RPD Studies in Normal Arrangement.

(pulsed approximately +10 volts relative to the filament) and the retarding grid (approximately -0.2 to -0.4 volts relative to the filament). This decrease in trap current and the resulting decrease in sensitivity of the mass spectrometer is then a considerable drawback for ionization potential measurements of species which are present only in very small concentrations.

An interesting observation was made on one occasion after the electron gun grids had been extremely well cleaned, the filament aligned very carefully, and the source magnets positioned for maximum trap current. The maximum trap current reading in the RPD mode of operation was found to be as great as in normal operation. However, the sensitivity of the machine appeared to be less, as was usual, and, in addition, a considerable amount of noise, i.e., diffuse mass peaks appearing at non-integral numbers, was present over the entire range of the mass spectrometer.

During attempts to determine the origin of the noise, the mass spectrometer was switched into the normal pulsed mode of operation with all of the electron grids at ground potential except the control grid which was as shown in Fig. II. 20. Upon lowering the control grid bias to -10 volts w.r.t. the filament while increasing the pulse height, the noise was eliminated. Also, with the mass spectrometer in the pulsed Studier mode of operation, in which ions that are being continuously formed are held in the region of the electron beam before pulsing, the noise was again reduced considerably. These observations led to the conclusion that the noise was being caused by a continuous leakage of the electron beam due to the extremely low bias on the control grid. This would account for the same apparent low sensitivity of the machine even though the trap current had been increased by careful cleaning and alignment of the electron gun. It was further noted that after a period of operation during which the control grid had become dirty, the trap current had dropped to its usual low level in the RPD mode and the noise had simultaneously disappeared.

In order to increase the trap current (without introducing noise) and consequently the sensitivity of the machine in the RPD mode, several different arrangements of the electron gun grids along with the changes in the biases and pulse heights were investigated. The arrangement shown in Fig. II.21 was found to be satisfactory. With a +15 volt bias on the retard shield, a trap current of approximately 0.1 microamp could be obtained, the operating level

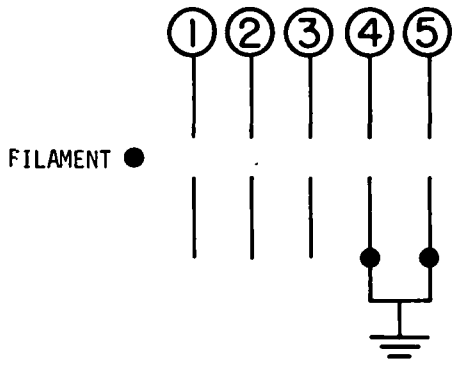


| GRID | TYPICAL POTENTIAL |
|---|---|
| 1. RETARDING GRID | -0.2 TO -0.4 VOLTS |
| 2. RETARD SHIELD | + 15 VOLTS |
| 3. CONTROL GRID | -10 VOLTS WITH 30 VOLT PULSE |
| 4. GROUND | + ELECTRON ENERGY |
| 5. GROUND | + ELECTRON ENERGY |

NOTE

Potentials are with respect to Filament.

Figure II.21. Modified Electron Gun for RPD Studies.

in normal pulsed operating being 0.125 microamp. However, increasing the bias resulted in the onset of noise. Evidently, the additional energy given to the electrons allowed them to overcome the -10 volt bias on the control grid. Of course, the electrons do not possess the 25 ev necessary to overcome this 25 volt barrier, but do so as a result of "peek through" from the grids immediately behind the control grid. Such a phenomenon was responsible for the continuous electron leakage described previously when the grid bias was at a very low value.

It has been mentioned that for ionization and appearance potential measurements the control grid pulse height should be kept at a low value, preferably less than 10 volts. This was certainly not the case here, but no difficulty was experienced in performing energy measurements. This became obvious when values determined by the RPD method were reproduced by the independent semilog matching method. It would appear that any effect that may be introduced by the higher pulse height is compensated for when measurements are performed on the calibrating gas under the identical operating conditions. A similar situation existed when in a pyrolysis experiment it was necessary to calibrate with the furnace on due to the effect of the magnetic field of the furnace windings. This effect was a lowering of the appearance potentials as a result of an added acceleration of the electron beam.

## E. ENERGY MEASUREMENT TECHNIQUES

In a thesis from this laboratory, Martin (II.17) gives a fairly complete discussion of the theory and experimental methods for determining the energetics of molecules and free radicals by mass spectrometric techniques specifically developed for the Bendix instrument and involving principally the RPD technique. However, the semilog matching method of Foner and Hudson (II.19), which was not discussed by Martin, was employed in much of this work. In this technique, the signal from the ion of interest and that of

the standard are adjusted to the same magnitude at an electron energy about three volts above the energy at which the unknown are barely detectable. Intensity vs. electron energy measurements are then made for both the unknown and the standard ion down to the point at which the unknown is again just barely detectable. These data are then plotted on a semilog grid. The shift of the energy scales that is required to superimpose the curves is the experimental difference between the appearance potentials of the unknown and the standard ions.

The energy scale was usually calibrated with argon each time the appearance potential of a particular ion was determined. Since the species of interest was present, in the majority of cases, only as a small fraction of a considerable flow of sample, it was much simpler to adjust the peak height of the ion of interest to match that of argon rather than employing the reverse procedure, which is normally followed. Except for experiences with compounds such as the oxygen fluorides, the calibration of the energy scale essentially did not change even in day to day operation. In fact, the cleaning of the electrons grids and replacement of the filament had practically no effect on calibration. On the basis of this, later appearance potentials measurements were made by making only one calibration when the appearance potentials of up to four different ions were desired. In all pyrolysis experiments, the calibration was conducted with the furnace on in view of the appearance potential lowering effect that had been observed and discussed earlier in this chapter.

# CHAPTER III

## CRYOGENIC REACTIVITY STUDIES

Several chemical reaction systems have been investigated utilizing the apparatus that was described in the previous chapter. These studies were sometimes exercises in chemical synthesis, i.e., the reaction sequence was designed to build molecule A, and sometimes from an interest in conducting reactions between the atoms and several simple molecules of carbon, hydrogen, oxygen, and nitrogen with a view toward relating the chemical behavior at very low temperatures to that at more ordinary temperatures. It was realized that unusual species would likely be synthesized, and this was probably the most interesting aspect of the work. The data are summarized under the several reactions.

### A. REACTION OF ATOMIC OXYGEN WITH ETHANE, ETHYLENE, AND ACETYLENE[f]

These studies were conducted in the reactor arrangements described in Chapter II and involved contacting the hydrocarbon with discharged $O_2$ in a reactor cooled usually to 90° K. The observed products presumably result from the attack of atomic O, but contributions from $O_3$ and excited $O_2$ cannot be definitely ruled out.

#### 1. $O + C_2H_6$

The reaction of O atoms with $C_2H_6$ produced only one product, ethanol, which was detected in the range -60° to -37° C with a maximum rate of evolution at -51° C at which point it exerted a vapor pressure of 0.15 mm Hg. Ozone and $NO_2$ were also present, but these are not termed reaction products since they contain no carbon or hydrogen atoms. This unusual combination of compounds was obtained in studies of the reaction using both TOF mass spectrometer and inlet system and the magnetic spectrometer-reactor configuration.

In addition to the small number of reaction products, the oxygen atom reaction with ethane was also marked by a slow rate of reaction. This

[f] Much of these results have been reported in detail in a Ph.D. thesis by D.B. Bivens, School of Chemical Engineering, Georgia Institute of Technology, May, 1966.

general result was expected since the relative reactivities of saturated and unsaturated hydrocarbons are well known.

Previous studies of the oxygen atom-ethane reaction at or above room temperature have resulted in the detection of carbon dioxide, carbon monoxide, ethanol, formaldehyde, acetaldehyde, and water as reaction products. From a comparison of the reaction conditions and products of the previous studies with that of the present work, some interesting conclusions can be drawn. Evidently the rapid low temperature quenching has eliminated fragmentation and the subsequent further reactions of these fragements of the initial reaction product, ethanol. The quench has also prevented the occurrence of secondary reactions.

This reaction is an example of the isolation and stabilization of an initial reaction product. As discussed in Chapter I, the method of low temperature quenching can give evidence as to the steps involved in the reaction pathway. Accordingly, it can be concluded that ethanol is the primary reaction product, and the products detected by other investigators occur as a result of its fragmentation and/or its further reaction.

Since ethanol alone has been detected, it seems likely that it was formed by an insertion reaction of the O atoms. Both ground state triplet oxygen atoms ($O^3P$) and excited state singlet oxygen atoms ($O^1D$) are to be expected as a result of the highly energetic electrical discharge. Because of the different spin multiplicities, the triplet and singlet atoms should exhibit differences in chemical behavior in their reactions with ethane. A triplet O atom should attack a C-H bond to abstract an hydrogen atom, whereas the singlet O atom should react by direct insertion. The triplet O atom attack should produce several reaction products since the $C_2H_5$ and OH radicals would be present for further reactions with atomic and molecular oxygen and with each other. The singlet O atom attack should initially produce an energetic molecule of ethanol which could then (1) be stabilized by collisional deactivation or by low temperature quenching, or (2) fragment to form simpler compounds, or (3) undergo further oxidation reactions. From these considerations, it would appear that the dominant reaction is that of singlet O atoms with ethane, and the resulting ethanol is stabilized by the low temperature quenching.

These conclusions are supported by previous related work. Wright

(III.1) reacted triplet O atoms with ethane and reported the main reaction products to be formaldehyde, acetaldehyde, and water. Yamazaki and Cvetanovic (III.2) selectively reacted triplet and singlet O atoms with propane and reported that alcohols were formed as a result of reaction with singlet atoms, and abstraction products (2-methylpentane, n-hexane) were formed as a result of reaction with triplet atoms.

Two approaches, the peroxide and the aldehyde theories, have been proposed to explain the mechanism of hydrocarbon oxidation. Since the present low temperature study did not result in the detection of any unstable hydroperoxides ($CH_3OOH$ or $C_2H_5OOH$), and since aldehydes were also absent, it is apparent that the reaction of lowest energy does not proceed by either of the proposed mechanisms. The initial step in both of these molecular oxidation mechanisms is the formation of an alkyl radical, and the presence of ethanol without any accompanying products suggests that no radical was formed. These results also suggest the power of cryochemical techniques in the ellucidation of the reaction mechanism of ordinary and high temperature processes.

The presence of $NO_2$ and $O_3$ was also noted in the quenched reaction mass. The $NO_2$ was probably formed as a result of a small air leak in the ethane valving connections to the reactor. No $NO_2$ was present in either of the feed gases, $He:O_2$ (in 75:25 ratio) and $C_2H_6$, and no $NO_2$ was formed during any of the other O atom reactions.

Following a suggested reaction by Schubert and Pease (III.3), the presence of $O_3$ was originally explained by the reaction

$$C_2H_5O_2\cdot + O_2 \longrightarrow C_2H_5O^{\cdot} + O_3 \qquad (6)$$

However, this possibility must be rejected in view of the observed sole presence of ethanol which indicated the absence of alkyl and alkoxyl radicals.

A more likely proposal for the formation of $O_3$ has been developed, but before it is presented, some additional experimental observations should be mentioned. First, the $O_3$ only appeared during quenching of the ethane reaction at $90^{\circ}$ K, and not during any other O atom reaction. Second, with the experimental apparatus that was used, $O_3$ could not be quenched at $90^{\circ}$ K when only discharged $He:O_2$ was pumped through the reactor, i.e., the

presence of either or both ethane and ethanol were necessary for the condensation of $O_3$. These facts appear reasonable in view of the fact that the reaction of O atoms with ethane was the slowest reaction studied. Hence there should have been a greater number of O atoms present to react according to

$$O + O_2 + M \longrightarrow O_3 + M \qquad (7)$$

where M is the third body necessary to remove the excess energy of reaction. In the other faster reactions most of the oxygen atoms would be removed by reaction with the second reactant (acetylene or ethylene). In the presence of the continuous deposition of ethanol and unreacted ethane, the rate of evaporation of the $O_3$ could be decreased by matrix trapping or by the formation of a solution which would reduce the effective vapor pressure of ozone. Also, ethane and ethanol may well be excellent third bodies for service in Equation (7) above.

2. $O + C_2H_4$

The products obtained from this reaction are listed in Table III.1

Table III.1 PRODUCTS FROM $O + C_2H_4$ REACTION

| Temperature Range, $^{o}$ C | Product Observed |
|---|---|
| -176 to -152 | unreacted $C_2H_4$ |
| -163 to -131 | $CO_2$ |
| -145 to -121 | HCHO |
| -127 to -94 | $CH_3CHO$, $CH_2OCH_2$ |
| -82 to -54 | $CH_3OH$ |
| -65 to -10 | $H_2O$ |
| -60 to -10 | HCOOH |

CO was likely also formed but since it would not condense in the reactor at $90^{o}$ K, it was not detected. Since all of the compounds were well known, they were identified by their mass cracking pattern and from the mechanical characteristic of the reactor-magnetic spectrometer inlet system that maximum gas evolution always occurred at the temperature at which each compound exerted a pressure of approximately 0.1 mm Hg.

All of the compounds listed in Table III.1 are stable at normal temperatures, and it initially appeared that the results obtained from the $O + C_2H_4$ reaction were not very exciting. However, after a comparison with other studies of the O atom-ethylene reaction, some interesting conclusions were drawn.

No attempt was made to determine the product distribution; however, the largest pressure increase occurred during the evolution of the acetaldehyde-ethylene oxide mixture. The vapor pressures of acetaldehyde and ethylene oxide were so similar that no separation of the two compounds occurred during their evolution from the reactor. The relative amounts of acetaldehyde and ethylene oxide were calculated to be 28% and 72%. Though these species are isomers, their mass cracking patterns are sufficiently different to permit identification of both. For acetaldehyde, the ratio of the peak at m/e = 43 to the peak at m/e = 44 (43/44) was 0.78, and for ethylene oxide, the 43/44 ratio was 0.24. These ratios were taken from the American Petroleum Institute tables, and they were confirmed using pure samples of acetaldehyde and ethylene oxide.

The presence of large amounts of ethylene oxide was in direct contrast to the results obtained by Cvetanovic (III.4) and by Avramenko and Kolesnikov (III.5). Cvetanovic reacted oxygen atoms and ethylene and reported that only a trace of ethylene oxide was detected in the reaction products. Studying the same reaction, Avramenko and Kolesnikova did not report the formation of any ethylene oxide.

These different observations may be reconciled by a consideration of the reaction conditions. Both Cvetanovic and Avramenko and Kolesnikov conducted the reactions at or above room temperature, but in the present work the reaction products were immediately quenched to $90^{\circ}$ K. The fast, low temperature quenching evidently stabilized a large amount of the initial product of reaction, ethylene oxide, thereby reducing the amount of subsequent rearrangement (to acetaldehyde) or decomposition and further reaction.

The low temperature stabilization of ethylene oxide lends considerable support to the $O + C_2H_4$ reaction mechanism proposed by Cvetanovic who has suggested that the initial reaction product was an energy-rich ethylene oxide molecule which decomposed to form the final products. Cvetanovic based his proposal on the appearance of a small amount of ethylene oxide and

on the type of the final products which were formed. As noted above, the large amount of ethylene oxide formed in these experiments forms a stronger basis for the Cvetanovic proposal. Evidently in this low temperature isolation and stabilization of ethylene oxide, the initial exothermic reaction product has been trapped and its subsequent decomposition has been partially halted by the low temperature removal of the energy of reaction.

It is instructive to further compare the low temperature data with the data of earlier investigators obtained at more ordinary temperatures. Cvetanovic initially carried out the $O + C_2H_4$ reaction in a molecular oxygen free system. Only when molecular $O_2$ was added did large quantities of formaldehyde, formic acid, alcohols, and water appear. Cvetanovic attributed their formation to the free radical scavenger action of the molecular $O_2$. The same products were detected during the present reaction study, and hence molecular oxygen is evidently present. This is not surprising since the distance from the discharge tube to the reaction was approximately 2 ft and a considerable amount of atom recombination is to be expected. The present study could be more correctly designated as $O + O_2 + C_2H_4$. Excited states of O and $O_2$ are probably also present, particularly would one expect $^1\Delta$ molecular $O_2$, which according to Ogryzlo has a half life of hours (III.6).

The large number of reaction products listed in Table III.1 was a direct indication that the low temperature quenching was not sufficiently efficient to completely arrest the reaction to the point of completely preventing the formation of products observed at more ordinary temperatures. The $CO_2$, HCHO, $CH_3OH$, $H_2O$, and HCOOH were probably formed as a result of several decomposition and radical reaction processes. Some of the possible reactions are:

$$CH_2OCH_2^* \longrightarrow CH_2O + CH_2 \qquad (8)$$

$$CH_3CHO^* \longrightarrow CH_3 + CHO \qquad (9)$$

$$CH_2 + O_2 \longrightarrow CHO + OH + 63\ \text{Kcal} \qquad (10)$$

$$CH_3 + O_2 \longrightarrow CH_2O + OH + 52.7\ \text{Kcal} \qquad (11)$$

$$CH_3 + OH \longrightarrow CH_3OH + 91\ \text{Kcal} \qquad (12)$$

$$CHO + OH \longrightarrow HCOOH + 108\ \text{Kcal} \qquad (13)$$

$$HCOOH^{*} \longrightarrow H_2O + CO \qquad (14)$$

$$HCHO + OH \longrightarrow H_2O + CHO + 27.1\ Kcal \qquad (15)$$

$$CO + OH \longrightarrow CO_2 + H + 25\ Kcal \qquad (16)$$

where the asterisk represents the presence of excess energy. The heat of formation data were taken from compilations in standard reference sources.

Since the U-tube reactor was made of pyrex and was cooled by the use of clear liquid refrigerants, visual observation of the products during reaction and also during the warm-up process was possible. When the $O + C_2H_4$ reaction was carried out, the quenched reaction deposit was yellow. On warming to -110° C, the yellow deposit melted to form a viscous, clear, yellow tinted liquid. This liquid was pumped away leaving behind in the reactor a white solid at -102° C. During further warming, a clear film accompanying the white solid was noted at -80° C. This clear film was probably present at lower temperatures; however, it was not observed until small bubbles began to form at -80° C.

Correlating these observations with the corresponding mass spectral data, the following model may be suggested. The yellow tinted liquid was a low temperature solution of acetaldehyde, ethylene oxide, methanol, water, and formic acid. The acetaldehyde and ethylene oxide were pumped away leaving the white deposit of methanol, water, and formic acid at -102° C. The clear liquid noted at -80° C was methanol (melting point -97° C). The origin of the yellow color was not established; however, it could have been caused by some low temperature molecular interaction (see results from acetylene reaction).

Upon continued study of the reaction at lower flow rates such that all of the ethylene was reacted before it deposited, the entire mass of reaction products condensed to form a yellow tinted glassy appearing solid. On warm-up, carbon dioxide, formaldehyde, and the above mentioned compounds evolved from the yellow-glassy reaction mass. In other experiments with higher ratios of ethylene to oxygen, it was realized that the yellow solid deposit was evidently a mixture of the yellow glass and the unreacted ethylene. The unreacted ethylene formed a white background for the yellow glassy product mass.

The appearance of the yellow glass was an unusual result since all of the compounds will condense separately as white solids at 90° K. As mentioned above, the appearance of the yellow glass was explained in terms of a solid solution which changed to a liquid solution on warming to -110° C. Since the liquid solution disappeared at -102° C when the acetaldehyde and ethylene oxide were pumped away, this seemed to indicate that acetaldehyde and ethylene oxide were the low temperature solvents.

A lower limit on the concentration of oxygen atoms present in the reaction zone was calculated from the flow rates used during the complete reaction of ethylene. Consider an experiment in which the He:$O_2$ flow was 24.0 std. $cm^3$/min and the $C_2H_4$ flow was 0.85 std. $cm^3$/min. Assuming that the oxygen atoms were consumed by the reaction

$$O + C_2H_4 \longrightarrow C_2H_4O \qquad (17)$$

it was calculated that at least 4% of the oxygen molecules must still be dissociated into atoms at the reaction zone after having traveled from the discharge region 2 ft away. As a matter of interest, it was calculated that, at a He:$O_2$ flow rate of 24.0 std. $cm^3$/min and 1.3 mm Hg pressure, it would require 0.3 sec for a molecule (or atom) to travel from the discharge tube to the reaction zone of the U-tube reactor.

3. $O + C_2H_2$

The reaction of O atoms with acetylene occurred with the formation of a blue-green chemiluminescent flame. On being quenched to 90° K, the reaction flame produced a yellow-red deposit of solid products. The product assignments and observations made during the controlled warm-up are summarized in Table III.2.

Table III.2 PRODUCTS FROM $O + C_2H_2$ REACTION

| Temperature Range, °C | Product Observed | Comment |
|---|---|---|
| -163° to -135° | Unreacted $C_2H_2$ | |
| -163° to -135° | $CO_2$ | |
| -135° to -116° | Secondary $C_2H_2$ | red color fading |

| Temperature Range, $^{o}C$ | Product Observed | Comment |
|---|---|---|
| $-103^{o}$ to $-79^{o}$ | $O_2$ | yellow color fading |
| $-82^{o}$ to $-54^{o}$ | $(CHO)_2$ | yellow color fading |
| $-50^{o}$ to $-20^{o}$ | HCOOH | |
| $-79^{o}$ to $-20^{o}$ | $H_2O$ | |
| room temperature | | white, fluffy solid |

It was found experimentally that an excess of acetylene was required to sustain the bright reaction flame and produce the colored reaction products. During warm-up, evolution of acetylene occurred in two separate temperature ranges. The lower temperature evolution was merely unreacted reactant, but during the secondary evolution of acetylene (at $-135^{o}$ to $-116^{o}$ C), the red color began to fade and finally disappeared near $-115^{o}$ C. Since this secondary evolution did not occur when a blank sample of unreacted acetylene was condensed and warmed, the red color and the secondary acetylene evolution are related.

One possible way to account for the acetylene evolution-red color relationship would be in terms of a charge transfer complex. The complex might be formed by the association of $\pi$ electrons from acetylene with formic acid. The red color of the complex would be caused by the transfer of electrons from the acetylene to the formic acid. This electron transfer would be to a lower excited state and cause a shift toward longer wave-lengths of absorption, which is a type of absorption shift that is well known. For an example, when chloranil (yellow) and hexamethylbenzene (colorless) are mixed together, an intensely red solution is formed (III.7), which is due to light absorption by a charge transfer complex of the two compounds. In the present proposal, the acetylene and formic acid would exist only as a low temperature charge transfer complex. On warming, the association would decrease and result in the evolution of acetylene.

In defense of the charge transfer complex proposal, we have also found that benzene will react with oxygen atoms to form red deposits at $90^{o}$ K. No reaction product analysis was made in this instance; however, charge transfer complexes of benzene are well known (III.8), and the red deposit could be another example of such a low temperature complex.

As indicated in Table III.2, both oxygen and glyoxal evolved from the reactor during the fading of the yellow color. Since glyoxal exists as a yellow solid melting at 15° C, the fading color is best explained as due to pumping of the glyoxal from the reactor. Only a slight amount of oxygen evolved from the reactor and its origin and significance were not established.

A white, fluffy solid reaction product remained in the reactor after warming to room temperature. On exposure to the atmosphere, the color of the solid gradually became yellow, and after approximately 48 hours, the color had finally changed to a dark red-brown. The yellow solid resembled hard, amorphous sulfur and the dark red-brown solid appeared as a thick resinous material. The yellow and brown solids were soluble in acetone, slightly soluble in water, and insoluble in carbon disulphide and carbon tetrachloride.

The infrared spectra of the yellow and brown solids were obtained, and although no definite compound assignments can be made solely on the basis of these data, some statements can be made about the types of compounds present. Both unsaturated ester and aldehyde groups appeared to be present. In addition, OH groups were present involved in intermolecular polymeric association. The color and infrared spectra changes seemed to indicate that reactions of oxidation, hydrolysis, and/or decomposition were occurring to increase the concentration of aldehyde groups. The color changes could be explained by an increase in number of =C=O groups or by an increase in system conjugation.

Sensible mechanistic arguments stem from a proposal by Fenimore and Jones (III.9) that the reaction of oxygen atoms with acetylene would proceed with the initial formation of an unstable energy-rich compound according to

$$O + C_2H_2 \longrightarrow C_2H_2O^* \longrightarrow CH_2\text{-}CO \qquad (18)$$

In support of the proposal, Haller and Pimental (III.10) reacted $^3P$ oxygen atoms and acetylene at 20° K in a solid argon matrix and reported the formation of ketene.

The failure to detect ketene in the present work seemed to indicate that the quenching process was not fast enough to stabilize the energy-rich molecule (this reaction would be exothermic by 127 Kcal/mole). When compared

with the O + $C_2H_4$ reaction, in which the initial reaction product, ethylene oxide, has two more bonds than does ketene, which could help absorb the energy of reaction, it is apparent that this could possibly be the reason for the difference in the degree of stabilization that was achieved. Another point which should be considered as regards stabilization of an initial product is the relative effect of reaction with triplet as opposed to singlet oxygen atoms. Haller and Pimentel reacted $^3P$ oxygen atoms with acetylene to form ketene by a process similar to that described by Cvetanovic for the O + $C_2H_4$ reaction. If $^1D$ oxygen atoms (which should be present in the reaction zone) were reacted with acetylene, the electron spins would be lined up such that addition would occur across the carbon atoms, and the initial reaction product would likely have the structure of an oxirene:

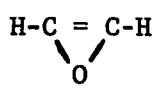

Since $^1D$ oxygen atoms are more energetic than $^3P$ oxygen atoms by 45 Kcal per gm atom, the reaction with $^1D$ atoms would be more exothermic and hence more difficult to stabilize. Also, the oxirene would be more unstable than ketene because of the highly strained ring structure. Earlier attempts to synthesize and observe oxirene (acetylene oxide) have been unsuccessful (III.11, III.12), but experiments such as described here, but with better quenching, may well be successful.

The formation of the several other identified reaction products can be explained in a manner similar to that for the O + $C_2H_4$ reaction. The oxirene and ketene would decompose according to

(19)

or

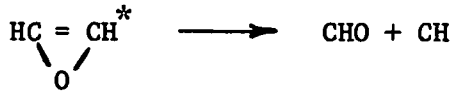

(20)

These radicals could react further with oxygen atoms or oxygen molecules, or they might dimerize, or disproportionate, or abstract, or etc.

## B. REACTION OF ATOMIC OXYGEN WITH AMMONIA[f]

Depending upon the quenching conditions, either of two products which are unstable at room temperature could be produced from the reaction of atomic O with $NH_3$. Diimide, $N_2H_2$, was formed if the reaction was quenched to 90° K, but ammonium ozonide, $NH_4O_3$, appeared upon quenching to 77° K. The ozonide was also formed by the reaction of $NH_3$ with liquid $O_3$ at 77° K.

### 1. Diimide Reaction

The several products that are produced from the quenched atomic O-$NH_3$ flame are summarized in Table III.3.

Table III.3

COMPOUNDS PRODUCED BY THE O + $NH_3$ REACTION QUENCHED TO 90° K

| Temperature Range °C | Compounds Observed |
|---|---|
| -183 to -141 | NO |
| -125 to -110 | $N_2H_2$, $N_2$, $N_2O$, unreacted $NH_3$ |
| -61 to 1 | $H_2O$ |
| -50 to -15 | $N_2H_4$ |
| -1 to 1 | $NH_2OH$ |
| room temperature | $NH_4NO_3$ |

Nitric oxide was identified in the range of -183° to -141° C by its cracking pattern and by measurement of its ionization potential of 9.4 ± 0.2 ev. When the O-$NH_3$ reaction was carried out at room temperature with no low temperature quenching, nitric oxide and nitrous oxide were the main products, but when the reaction vessel was slowly cooled below -115° C, the intensity of the peaks due to nitric oxide and nitrous oxide began to decrease. Either less total reaction was occurring or a portion of those species intermediate to the production of nitric oxide and nitrous oxide were being removed from the reaction zone by the low temperature quenching. Not all of these

intermediate species were removed because NO and $N_2O$ were detected even when the quenching was carried out at 90° K. Therefore, to the extent that the arresting idea is correct, the quenching action was never fast enough to completely stop the formation of the final products. As shown in Table III.3, a number of these intermediate compounds were formed as a result of the low temperature quenching.

The mass of products condensed from the O + $NH_3$ reaction had a bright yellow color similar to that described by Geib and Harteck (III.13) in their early study of this reaction. Geib and Harteck postulated that the yellow compound might be HNO or $NH_3O$. However, this work has shown that the yellow substance was actually the normally unstable compound, diimide. As indicated in Table III.3 and in Fig. III.1, diimide, nitrogen, and nitrous oxide were detected in the temperature range -125° to -110° C with the maximum evolution of each occurring at -115° C. The maximum evolution of unreacted ammonia also occurred at about -115° C. On warming through the temperature range -125° to -110° C, the color of the deposit gradually changed from yellow to white, evidently as a result of the pumping away of the diimide from the reactor. The observations just described agree well with previous observations on diimide (III.14)(III.15). To reiterate, diimide can be condensed as a yellow solid at 90° K, it has a maximum evolution rate at about -113° C, a white deposit remains in the reactor after the diimide vaporizes, and nitrogen evolves at the same time as does the diimide.

To further secure the identification of diimide, its ionization potential was measured and found to be 9.8 $\pm$ 0.2 ev, which is in agreement with the previously reported value of 9.85 $\pm$ 0.1 ev (III.14).

The diimide was probably formed by the combination of two NH radicals on the cold reactor walls,

$$NH + NH + M \longrightarrow N_2H_2 + M \qquad (21)$$

As previously discussed, M is the third body (probably the cold wall) which removes the energy of reaction (about 104 Kcal/mole of $N_2H_2$). The NH radicals could have been formed by the reaction

$$O + NH_3 \longrightarrow NH + H_2O + 74 \text{ Kcal} \qquad (22)$$

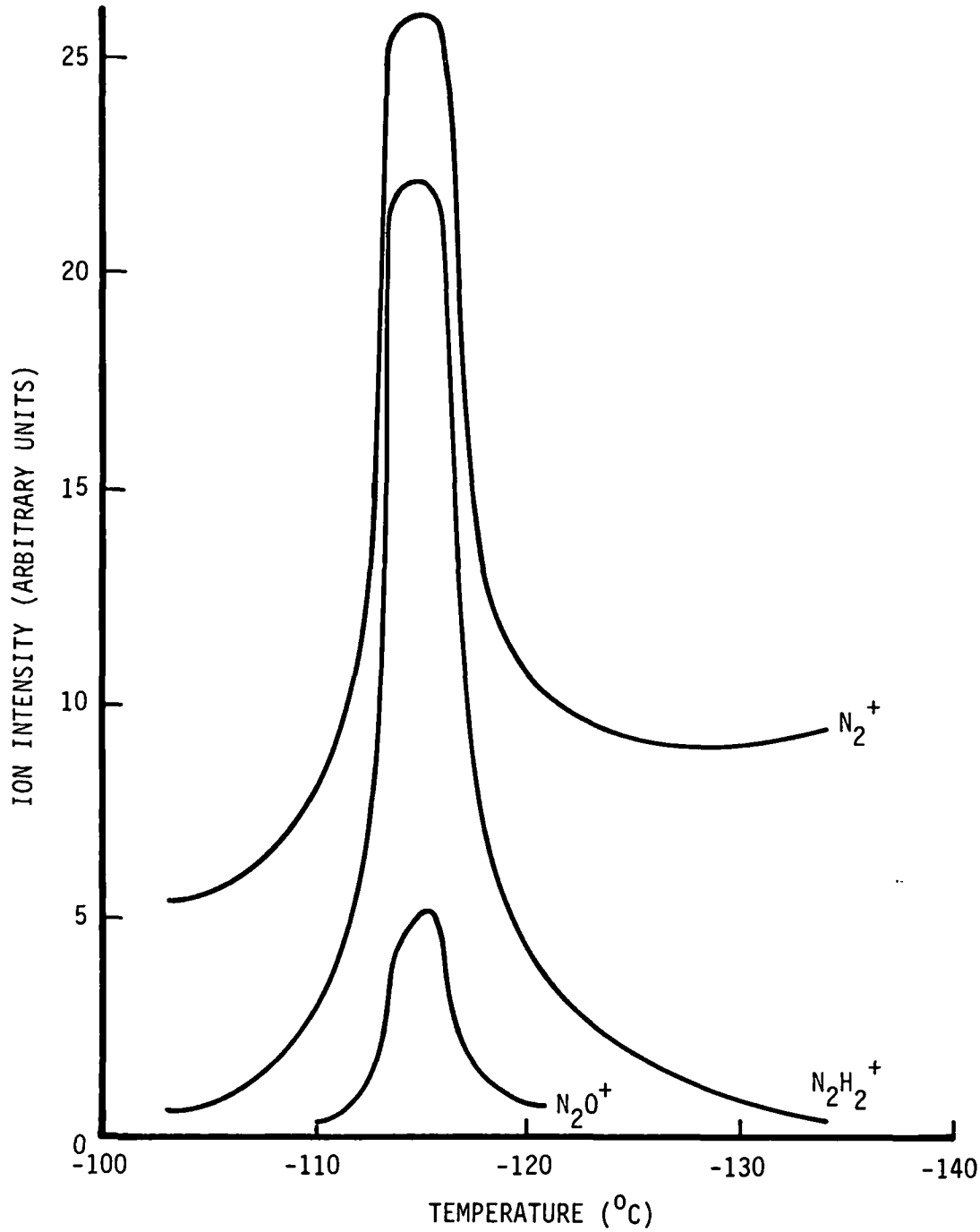


Figure III.1. Variation of Ion Intensities with Temperature of Three Species from the O + $NH_3$ Reaction.

or by the reactions

$$O + NH_3 \longrightarrow NH_3 + OH + 44.5 \text{ Kcal} \quad (23)$$

$$O + NH_2 \longrightarrow NH + OH + 58.5 \text{ Kcal} \quad (24)$$

all of which are obviously to be expected energetically. The $NH_2$, NH, and OH radicals and $H_2O$ have each been previously observed in ammonia-oxygen flames.

Since the present work is the first account of diimide production by the $O + NH_3$ reaction, the percent conversion would be an interesting number. With the feed gas flow rates that were used, the present conversion of ammonia to diimide was approximately 1.3%, as calculated from the relative ion intensities of the major peaks due to ammonia and diimide during their period of evolution from the reactor. It should be recognized that this ratio does not represent the exact percent conversion since (1) the ionization cross section of $N_2H_2$ and $NH_3$ are taken to be the same, and (2) the amount of diimide produced was compared to the amount of unreacted ammonia rather than to the amount of ammonia originally coming into the reactor. However, since the total percent conversion of $NH_3$ to all products was so small, the correction for the amount of reacted ammonia should also be small. The ionization cross section of diimide is unknown, but it should not be different from that of ammonia by a factor of more than 1.5 (see table of typical ionization cross sections listed by Reed (III.16), and hence the percent conversion should be given as $1.3 \pm 0.5\%$.

$N_2O$ was identified from its cracking pattern and by measurement of its ionization potential ($13.3 \pm 0.2$ ev this research, $13.1 \pm 0.05$ literature).

Hydrazine was identified in the range $-50^\circ$ C to $-15^\circ$ C by its cracking pattern. The appearance potential of the $N_2H_2^+$ ion from hydrazine was found to be $11.3 \pm 0.2$ ev, which may be compared to the previous values of $10.98 \pm 0.02$ ev and $11.9 \pm 0.2$ ev reported by Foner and Hudson (III.17) and Dibeler, Franklin, and Reese (III.18) respectively.

The hydrazine could have been formed by the combination of two $NH_2$ radicals

$$NH_2 + NH_2 + M \longrightarrow N_2H_4 + M + 68 \text{ Kcal} \quad (25)$$

and also during the evolution and decomposition of part of the diimide,

$$2\ N_2H_2 \longrightarrow N_2H_4 + N_2 + 86\ \text{Kcal} \qquad (26)$$

This last reaction would also explain the evolution of nitrogen that was observed at -115° C concurrently with the evolution of $N_2H_2$.

The presence of hydroxylamine was detected mass spectrometrically and also from a qualitative chemical analysis. At -1° C, the intensity of the m/e ion current at 33 ($NH_2OH^+$) began to increase. At this temperature the vapor pressure of hydroxylamine is 0.1 torr, which correlates favorably with the vapor pressure vs. sensitivity behavior already noted for other substances. Prior to use of the mass spectrometer, the presence of hydroxylamine was indicated by the addition of Fehling's solution to a water solution of the residue present in the reactor at 0° C. Since hydroxylamine is a reducing agent, its presence was noted when the Fehling's solution was reduced to form a yellow-red precipitate. Hydrazine is also a reducing agent which produces the same colored precipitate when tested with Fehling's solution. However, the hydrazine should have been pumped out of the reactor at temperatures lower than 0° C. In confirmation of this, an additional test solely for the presence of hydrazine gave negative results.

The detection of hydroxylamine was significant since it had previously been proposed to exist as an intermediate in the oxidation of ammonia (III.19), but it had not been definitely established. Hydroxylamine was probably formed by the reaction sequence,

$$O + NH_3 \longrightarrow NH_2 + OH \longrightarrow NH_2OH + 119\ \text{Kcal} \qquad (27)$$

or possibly by a direct insertion.

The presence of ammonium nitrate was apparent from its physical appearance and from qualitative chemical analysis. At room temperature, a white solid remained in the reactor which could not be identified mass spectrometrically since it exhibited insufficient vapor pressure (less than 0.04 torr). Ammonium nitrate is a white solid which melts at 169.6° C. Qualitative tests were made for the ammonium and the nitrate ions, and both tests were positive.

2. Ammonium Ozonide Reaction

While 90° K quenching produced a yellow deposit of reaction products which was described above, in contrast, 77° K quenching produced an orange-red reaction product deposit. It appears that the orange-red deposit at 77° K was produced by the reaction of $O_3$ with $NH_3$ rather than by the reaction of O atoms with $NH_3$. This was demonstrated by condensing a layer of $NH_3$ on top of a layer of $O_3$ which had been pre-cooled to 77° K. A bright yellow colored deposit was produced at 77° K, and as the reactor was slowly warmed, the yellow color began to change to the organge-red color. In another experiment, it was found that the orange-red solid could be formed at 90° K if the O atoms produced by the discharge were forced to strike the liquid oxygen cooled reactor wall before contacting a gaseous stream of $NH_3$. Evidently, $O_3$ formed in the usual way at the cold reactor wall by the reaction

$$O + O_2 + M \longrightarrow O_3 + M \,. \qquad (28)$$

The gaseous $O_3$ then contacted the $NH_3$ and the orange-red deposit was again formed.

During a controlled warm-up with continuous pumping, the orange-red solid disappeared at -70° C, and at room temperature, a white deposit remained in the reactor, which qualitative analysis identified as ammonium nitrate, $NH_4NO_3$.

The gases evolved from the reactor during the warm-up process were identified by use of both the TOF and the magnetic mass spectrometric cryogenic reactor-inlet systems that were discussed in Chapter II, and the results are summarized in Table III.4. Since the vapor pressure of $O_3$ is

Table III.4

OBSERVATIONS UPON WARMING THE PRODUCTS FROM THE $O_3 + NH_3$ REACTION AT VERY LOW TEMPERATURES

| Temperature, ° C | Product |
|---|---|
| -153 | appearance of ozone |
| -136 | maximum evolution of ozone |

| | |
|---|---|
| -126 | disappearance of ozone |
| -112 | maximum evolution of oxygen |
| 0 | water condensed in reactor |
| room temperature | ammonium nitrate |

1 mm Hg at ≒180.4° C, any unreacted $O_3$ present in the reactor would have been noted at temperatures much lower than -153° C. Therefore, the $O_3$ and $O_2$ at the higher temperatures of Table III.4 were apparently products of decomposition. The presence of oxygen, water, and ammonium nitrate, and also the initial orange-red color, suggested that the colored reaction product was $NH_4O_3$, ammonium ozonide.

Solomon and coworkers (III.20) carried out a low temperature ozonization of ammonia and reported the formation of an orange-red solid which was only stable below -126° C. The product decomposed to yield ammonium nitrate, oxygen, and water with a total N/H/O atomic ratio of 1/4.38/3.0. Electron paramagnetic resonance studies indicated the presence of an unpaired electron which was typical of the ozonide ion. The visible absorption spectrum was obtained and compared with that of other known ozonide compounds. All spectra showed absorption in the region of 450 mμ which is also characteristic of the ozonide ion. From these studies, Solomon and coworkers identified the orange-red solid as $NH_4O_3$, and suggested that it would decompose according to

$$2NH_4O_3 \longrightarrow NH_4NO_3 + 1/2\ O_2 + 2H_2O \qquad (29)$$

Herman and Giguere (III.21) also studied the low temperature ozonization of ammonia and reported the formation of an orange-red solid. They studied the infrared spectra of the solid as a function of temperature and assigned bands at 800, 1140, 1260, and 2053 $cm^{-1}$ to the $O_3^-$ ion. The maximum concentration of the ozonide ion was reported to occur upon warming to -115° C.

The results obtained from the present work are in agreement with these few existing literature descriptions and indicate that $NH_4O_3$ has been produced. $NH_4O_3$ is an interesting molecule about which very little is known.

## C. REACTION OF ATOMIC HYDROGEN WITH NITRIC OXIDE[d]

This reaction was chosen for study with the view that the two free radicals might well merely add in a cold environment to give HNO, nitroxyl, as the primary product. The experimental arrangements shown in Figs. II.7 and II.10 were used. Combinations of flow rates and pressures used by previous investigators in purported syntheses of HNO were duplicated. In addition to reacting (or mixing) gaseous NO with discharged hydrogen, various mixtures of hydrogen-argon and hydrogen-helium were discharged and subsequently mixed with NO in the cold reactor. Neither of two reported characteristics of the reaction, (1) red chemi-luminiscent flame or (2) yellow, explosive solid product at 77° K, were ever observed. In addition, no mass spectrometric evidence was obtained which would suggest the presence of HNO; the only products observed during controlled warm-up are presented in Table III.5.

Table III.5

PRODUCTS FROM THE H + NO REACTION

| Temperature, ° C | Product Observed |
|---|---|
| -180 | NO |
| -166 | $N_2O$ |
| -90 | $H_2O$ |

The yellow explosive solid described by Geib and Harteck (III.22) could actually have been impure nitric oxide, since it was found that a yellow compound was condensed in the reactor if either the hydrogen or the nitric oxide were not carefully purified[g]. This yellow compound was likely an

[g] NO from the Matheson Company was 98.5% pure with $NO_2$ as the principal impurity. This was removed by a cold trap maintained at -155° C, the freezing point of 2-methyl-pentane. Electrolytic grade hydrogen was freed of traces of oxygen by passing over palladium asbestos heated to 400° C, or over copper turnings at 800° C. The water was removed by a liquid nitrogen trap.

oxidation product of nitric oxide. It was also found that either pure or contaminated nitric oxide, if condensed at 77° K and allowed to rapidly warm by removing the surrounding dewar of liquid nitrogen, the solid condensed film would crack and produce a click sound which could be taken to be an explosion.

In attempting to detect nitroxyl, the hydrogen peak and also the region at m/e = 31, i.e., due to $HNO^+$, was constantly monitored during the controlled warm-up of the reaction product mass. Also, in the event that nitroxyl did not produce a parent ion ($HNO^+$), the peak at m/e = 30 was studied for any unusual increase in intensity. $NO^+$ from HNO would not be energetically detectable in a background of NO since $I(NO) < A(NO^+)$ from HNO. In no case was there any indication of the presence of stabilized nitroxyl.

Since the early work of Geib and Harteck, there have been three accounts of the trapping of HNO. Brown and Pimentel (III.23) and Robinson and McCarty (III.24) reported the stabilization of HNO in an argon matrix at 20° K and Harvey and Brown (III.25) condensed HNO in an argon matrix at 4° K. No experiments were described in which HNO had been stabilized without the use of a matrix or at a temperature as high as 77° K. From a series of concurrent experiments, Robinson reported in a recent private communication that he and his students had carried out warm-up experiments on HNO stabilized in argon and in krypton matrices. He found that HNO in argon began to disappear, presumably by reaction or dissociation, at about 25° K and HNO in krypton began to disappear at about 36° K. From these observations, Robinson concluded that the quenching and stabilizing of HNO definitely required a rigid, inert matrix. The failure to detect HNO in this work wherein the species must exert a stable vapor pressure of $3 \times 10^{-6}$ torr is then reasonable in view of the much lower temperature loss processes observed by Robinson.

The detection of nitrous oxide and water during the warm-up indicated that the probably short-lived nitroxyl molecule was actually present during the reaction process. Clyne (III.26) had previously reported that the HNO molecule was destroyed by the reactions

$$H + HNO \longrightarrow H_2 + NO \qquad (30)$$

and

$$HNO + HNO \longrightarrow H_2O + N_2O \qquad (31)$$

The relevance of these unsuccessful experiments may be summarized as follows. Only matrix level concentrations of a few tenths of a percent at most of HNO have been observed, and even these are lost at $25^{o}$-$35^{o}$ K. The vapor pressure of NO is 1 mm Hg at $88^{o}$ K, and we would expect the vapor pressure of HNO to be lower. Hence, the likelihood of producing and studying the behavior of "reagent" HNO is poor. Correspondingly, the importance of this species in cometary phenomena would not be great.

## D. REACTION OF ATOMIC HYDROGEN WITH LIQUID OZONE

The possible existence of two hydrogen superperoxides, $H_2O_3$ and $H_2O_4$, has been discussed for many years, and recently a rather convincing array of indirect data have accumulated which, together constitute a rather convincing argument for the existence of these species. However, both compounds have eluded direct observation, and the accumulated evidence is, while convincing, not unequivocal.

The purpose of the present work is to elucidate the question of the possible existence of superperoxides from direct evidence obtained using the mass spectrometer and cryogenic inlet system. Previous experiments in which a clear glassy substance was prepared by reacting H atoms with a film of dark blue liquid $O_3$ at $77^{o}$ K, were repeated. The previously reported existence of two temperature zones during controlled warm-up of the product mass at which $O_2$ evolution occurred, one around $-115^{o}$ C and the other around $-70^{o}$ C, were confirmed.

A cryogenic reactor arrangement for the TOF instrument and very similar to that shown in Fig. II.1, but having only one refrigerant chamber, was used for these studies. The temperature in the reactor was controlled automatically anywhere above $77^{o}$ K by means of the same electric heater,

and refrigerant flow system described earlier. The reactor was lined with pyrex to avoid the catalytic effect of the wall, but this also meant less efficient cooling of the reaction mass could be achieved. (This relatively poor cooling was apparent in the first series of experiments in which an rf discharge in $O_2$ at pressures of about 1 mm Hg failed to yield any $O_3$ when the flowing gas was quenched to 77° K. The geometry of the arrangement was such that the discharge coil was, of necessity, located about 25 in from the cooled reactor.) After the condensation of $O_3$, $H_2$ replaced $O_2$ in the fast-flow discharge system, and atomic H thus produced was pumped over the somewhat supercooled liquid $O_3$ at 77° K. This reaction sequence was identical to that first used by Kobozev, et al. (III.27) in their convincing but not unquestionable, synthesis of $H_2O_4$. However, on controlled warming of such a preparation, not only was no $O_3$ observed but also no hydrogen peroxide was evident, which implied that either the inside walls of the reactor were, in fact, not cold enough to condense the $O_3$ or that the hot incoming hydrogen evaporated the $O_3$ that was condensed. It therefore seemed reasonable to prepare 0.3 to 0.5 ml of liquid $O_3$ externally, transfer it into the reactor and then attempt to effect a reaction with atomic H in the above manner. Clearly this does not completely solve the problem of inefficient cooling, since the hot discharged hydrogen must still be pumped through the reactor. However, reaction was effected in such an arrangement as was evident from the appearance of $H_2O_2$ in the product mass during subsequent controlled warming experiments.

Liquid $O_3$ is very unstable, the expected product, $H_2O_4$, is unstable and hence, not unexpectedly, these experiments were plagued by violent explosions which occurred at various times in the procedure and which usually caused excessive damage to the glass and sometimes even to the metal parts of the system. It has not been possible to relate these explosions to any particularly sensitive step in the procedure. On the contrary, it seems that every step is sensitive. The data do suggest that the explosions are most likely due to the presence of impurities in the system.

All the trouble due to the highly unstable liquid $O_3$ led to the investigation of an alternative system in which H atoms react with molecular $O_2$ to also yield the glassy substance containing the superperoxide, but in smaller concentrations. The discharged hydrogen meets the molecular $O_2$ in a 1 in

tubular reactor, the walls of which are cooled to 77° K, i.e., in the quenched diffusion flame apparatus of Fig. II.7. The condensables at 77° K are collected on the cold surface, and analyzed on slowly raising the temperature.

Although neither of these experiments has yielded positive evidence for the presence of $H_2O_3$ or $H_2O_4$, the results may be summarized as follows: (1) the experiments of Kobozev, et al. (III.27) and others with H atoms and liquid $O_3$ were repeated, and the two zones of $O_2$ release at -115° C and at -70° C were confirmed. Efforts to identify any ions, positive or negative, that might prove the existence of superperoxides, have failed. The only molecules identified were $O_2$, $H_2O$, $H_2O_2$. However, it is believed that part of the ion intensity at m/e = 16 that was found at -115° C, cannot be explained as being just part of the cracking pattern of those molecules known to be present, but rather indicates that O atoms are formed as a result of the decomposition of a presently unidentified species, perhaps the superperoxide. (2) In studies of the $H_2$-$O_2$-Ar system, the same products as mentioned above were obtained. However, between -81° C and -70° C a peak at m/e = 64 appeared which reached a maximum at about -73° C. This peak might be due to $O_4^+$, which in turn might indicate the presence of superperoxide. These experiments, both with liquid $O_3$ and with gaseous $O_2$ are continuing.

## E. REACTION OF DIAZOMETHANE WITH LIQUID KETENE

Ketene was prepared in the usual way by the hot filament pyrolysis of gaseous acetone. A stream of dry $N_2$ bubbled into the acetone boiler acted as a carrier to sweep the acetone over the heated filament and also to carry the products through a trapping and purification train. A trap at -95° to -105° C removed the residual unreacted acetone, a second trap at -196° C condensed the ketene product as well as by-product $CH_4$ and $C_2H_4$.

The former was removed by long term pumping at -196° C and the second by several trap-to-trap distillations between -100° C and -196° C.

Diazomethane was conveniently prepared by the reaction,

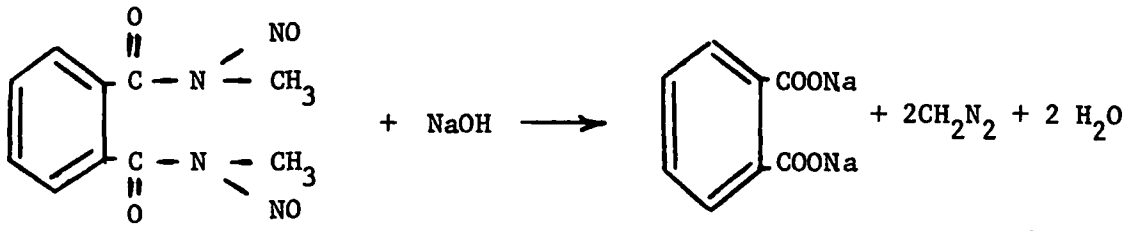


(32)

which was conducted in a solvent mixture of carbitol and diglyme and using a 20 per cent aqueous caustic solution[h]. The solvent and caustic solution was stirred at the ice point and the solid substituted diamide of phthalic acid was added. Upon warming to 20° to 40° C, the yellow diazomethane was evolved, condensed in a water condenser and collected at 90° K. The raw product was purified by trap-to-trap distillation between -90° and -196° C.

The reaction itself was conducted in the following manner. Solid ketene was condensed into the bottom of a trap, and then, by raising the liquid nitrogen refrigerant level, a solid ring of diazomethane was condensed above, but not in contact, with the ketene. The dewar of nitrogen was then quickly replaced with a dewar of 2-methyl-pentane at -145° C whereupon both solids melted. The liquid $CH_2N_2$ slowly ran down onto the liquid $CH_2CO$ causing a vigorous reaction, with the evolution of $N_2$ and the bleaching of the yellow color. The products evolved from this reaction mass were then monitored mass spectrometrically during gentle warming in the usual way of other experiments reported upon herein.

Cyclopropanone has not previously been observed although it is frequently postulated as a transitory reaction intermediate. Its elusive nature results from its formation from ketene and methylene being exothermic by at least 78 Kcal which is 13 Kcal more than the minimum activation energy for

---

[h] We are indebted to Professor L. H. Zalkow of the School of Chemistry at Georgia Tech for this procedure and for providing the diamide reactant.

the opening of the cyclopropane ring. The low temperature formation reported here apparently results from the ability to rapidly remove this energy of reaction. There exists previous tentative evidence for the formation of cyclopropanone in matrix experiments at 20° K by the reaction of photolytically produced $CH_2$ with $CH_2CO$ (III.28). From these new mass spectrometric data, it appears that the earlier ir studies at 20° K which suggested the presence of cyclopropanone were probably correct.

# Appendix A

## AN ANNOTATED PARTIAL BIBLIOGRAPHY ON SOLUBILITY AT CRYOGENIC TEMPERATURES

An area of necessary data for use by the experimentalist in low temperature chemistry is that of solubility. The term is to be interpreted broadly, i.e., we are here interested in the solubilities of gases and solids in cryogens as well as with the mutual solubility or miscibility of the cryogens themselves. It is also important to know the variation of these phenomena with temperature and pressure.

The bibliography presented below, although incomplete, is reasonably inclusive of the sorts of studies that have been made (they are clearly very limited). A comprehensive review of this subject is in progress.

The available cryogens for possible use as solvents in cryogenic reactions or in cryogenic chemical processing is rather larger than one might have expected. A somewhat cursory search of the usual summary sources of vapor pressure and physical constant data revealed about 100 organic substances and about 25 inorganic substances that have melting points below 150° K*. There are, no doubt many more such substances.

---

*Kirk, B. S., Nat. Bur. Stand. Cry. Eng. Lab., proj. 8124, Aug. 1958

---


$O_2$ - $O_3$ System

1. Riesenfeld and Schwab, Naturwissenschaften 10, 470 (1922)
   on solubility

2. Schumacher, Anales asoc. quim. arg. 41, 197 (1953)
   on solubility

3. _____, ibid 41, 203 (1953)
   action of $O_2$ - $O_3$ liquid mixtures on several metals

4. _____, ibid 41, 208 (1953)
   $O_2$ - $O_3$ solubility diagram

5. _____, ibid 41, ? (1953)
   boiling point diagram on page 225

6. _____, ibid 41, 259 (1953)
   propagation of explosions from gas mixtures into liquid mixtures

7. Brown, Hersch and Berger, JCP 23, 103 (1955)
   solubility, compositions at two phase boundary

8. Jenkins and DiPaolo, JCP 25, 296 (1956)
   density of solutions

9. Laine, Comp. rend. 196, 910 (1933)
_____, ibid 198, 918 (1934)
magnetic susceptibility of liquid $O_3$ and $O_3$-$O_2$ liquid mixtures

10. Schumacher, JCP 21, 1610 (1953)
solubility and T-x diagram for $O_2$-$O_3$ liquid mixtures

11. Jenkins and Birdsall, JCP 22, 1779 (1954)
$O_2$-$O_3$ liquid system

12. Brown, Berger and Hersh, JCP, 23, 1340 (1955)
phase diagram for liquid $O_2$-$O_3$ mixtures

13. Hersch, Brabets, Platz, Swehla and Kirsh, ARS Journal 30, 264 (1960)
vapor-liquid equilibria in $O_2$-$O_3$ system

$O_2$

1. Bailey, et al. AD 253231 and AD 253232 (1960 and 61)
soluble impurities in liquid oxygen

2. Stackelberg, Z. physik. Chem. A170, 262 (1934)
solutions of krypton and xenon in liquid $O_2$

3. Inglis, Phil Mag. (6) 11, 656 (1906)
solutions of argon in liquid $O_2$

4. Hunter, J. Phys. Chem. 10, 330 (1906)
solutions of ethane, ethylene and propylene in liquid $O_2$

5. Federova, J. Phys. Chem. USSR 14, 422 (1940)
solutions of $C_2H_2$ and $CO_2$ in liquid $O_2$

6. Ishkin and Burbo, J. Phys. Chem. USSR 13, 1337 (1939)
solutions of $C_2H_2$ and $CO_2$ in liquid $O_2$ and $O_2$-$N_2$ mixtures

7. Tsin, J. Phys. Chem. USSR 14, 418 (1940)
solutions of ethylene and propylene in liquid $O_2$

8. Fastovsky and Krestinsky, J. Phys. Chem. USSR 15, 525 (1941)
solutions of $CH_4$ in liquid $O_2$

9. Burbo and Ishkin, Physica 3, 1067 (1936)
T-x and p-x diagram and data for A-$O_2$ system from $87^{\circ}$-$97^{\circ}$ K

10. Cox and deVries, J. Phys. and Colloid Chem. 54, 665 (1950)
solubility of ethane, ethylene and propylene in liquid $O_2$

11. Karwat, Chem. Eng. Progress 54, 96 (1958)

12. McKinley and Himmelberger, Chem. Eng. Prog. 53, 112 (1957)
solubility of hydrocarbons in liquid $O_2$

13. McKinley and Wang, Ad. Cry. Eng. 4, 11 (1959), Plenum Press, New York
phase equilibria for $CH_4$-$O_2$; $C_2H_6$-$O_2$; $C_2H_4$-$O_2$; $C_3H_8$-$O_2$; $C_3H_6$-$O_2$
systems and solubilities for an additional 14 hydrocarbons in liquid $O_2$

14. Kastovsky and Krestinsky, J. Phys. Chem. USSR 16, 148 (1942)
solubility of solid argon in liquid $O_2$ from 72.8° to 79.09° K

15. Barret, Meyer and Wasserman, JCP 44, 998 (1966)
$O_2$ - A system with emphasis on solid phase diagram

16. Clark, Din and Robb, Proc. Roy. Soc. (London) A221 517 (1954)
$O_2$ - A vapor-liquid equilibria

17. Armstrong, Goldstein and Roberts JRNBS 55, 265 (1955)
vapor-liquid equilibria in $O_2$-$N_2$ system

18. Fastowsky and Petrovsky Zhur. Fiz. Khim. 29, 1311 (1955)
vapor-liquid equilibria for A-$O_2$ system

19. Streng and Kirshenbaum J. Chem. Eng. Data 4, 127 (1959)
mutual solubility of $O_2$-$CH_4$

20. Din and Goldman TFS 55, 239 (1959)
solubility of $N_2O$ and liquid $O_2$

21. Kanarek U.S. 2, 930, 684 March 29, 1960
liquid mixture of $O_2$ and $F_2$ as an oxidizer

22. McKinley, U.S. 2, 939, 778 June 7, 1960
33 mole % $CH_4$ in liquid $O_2$ as an explosive

23. Narinsky Zhur. Fiz. Khim. 34, 1778 (1960)
vapor-liquid equilibria in A-$O_2$ system

## $N_2$

1. Gonikberg and Fastowsky, Acta Physicochem USSR 12, 67 (1940)
solubility of He in liquid $N_2$ from 78°-109° K

2. Ishkin and Burbo, J. Phys. Chem. USSR 13, 1337 (1939)
solubility of solid $C_2H_2$ and $CO_2$ in liquid $N_2$, $O_2$ and $N_2$-$O_2$ mixtures
between 77°-90° K

3. Tsin, J. Phy. Chem. USSR 14, 418 (1940)
solubility of $C_2H_4$ and $C_3H_6$ in liquid $N_2$ and liquid $O_2$

4. Cox and deVries, J. Phy. and Colloid Chem. 54, 665 (1950)
solubility of ethane in liquid $N_2$

5. Fastowsky and Krestinsky, J. Phys. Chem. USSR 15, 525 (1941)
solubility of $CH_4$ in liquid $N_2$

6. Federova, J. Phys. Chem. USSR 14, 422 (1940)
solutions of $C_2H_2$ and $CO_2$ in liquid $N_2$

7. Hunter, J. Phys. Chem. 10, 330 (1906)
solutions of ethylene and propylene in liquid $N_2$

8. Gonikberg, Acta Physicochem USSR 12, 921 (1940)
thermodynamic discussion of the solubility of $H_2$ in liquid $N_2$ at high pressures

9. Ruhemann and Zinn, Phys. Zeit. der Sowjet. 12, 389 (1937)
p-x diagrams for the two binaries $H_2$-CO and $H_2$-$N_2$ at 90°, 83° and 78° K and from 12-50 atm., also the ternary equilibrium in $H_2$-$N_2$-CO. Concerned with washing CO from $H_2$ with liquid $N_2$

10. Bloomer, Institute of Gas Technology, report no. 21
thermodynamic properties of gas-liquid $CH_4$-$N_2$ mixtures

11. Shtekkel and Tsin, J. Chem. Ind. USSR 16, 24 (1939)
$H_2$-$N_2$ phase equilibria and $H_2$-$N_2$-$CH_4$ ternary phase equilibria

12. Rysakov, Teodorovich, Kozyreva and Booll, Bull. State Sci. Res. Inst. of High Press No. 6, 12 (1934)
$CH_4$-$N_2$ phase equilibria

13. Torocheshnikov and Levius, J. Chem. Ind. USSR 16, 19 (1939)
$CH_4$-$N_2$ phase equilibria

14. McTaggart and Edwards, Roy. Soc. Canada 3, 57 (1919)
$CH_4$-$N_2$ phase equilibria

15. Brown and Stutzman, Chem. Eng. Prog. 45, 142 (1949)
vaporization equilibria of 8 light gases in liquid $N_2$, an engineering correlation study.

16. Eakin, Institute Gas Tech. Res. Bull. 26, 40 (1955)
$C_2H_6$-$N_2$ vapor liquid equilibria

17. Schiller and Canjar, Chem. Eng. Prog. Sym. Ser. 49, No. 7
CO -$N_2$ vapor-liquid equilibria

18. Armstrong, Goldstein and Roberts, JRNBS 55, 265 (1955)
vapor-liquid equilibria in $O_2$-$N_2$ system

19. Fastowsky and Petrovsky, Zhur. Fiz. Khim. 30, 76 (1956)
vapor-liquid equilibria in $N_2$-A system.

Light Hydrocarbons


1. Gonikberg, Acta Physicochem USSR 12, 921 (1940)
thermodynamic discussion of solubility of $H_2$ in liquid CO, $CH_4$, $C_2H_4$ and $C_2H_6$. No new data here, but gives sources of data that were used.

2. Ruhemann and Lichter, Phys. Zeit. der Sowjet. 6, 139 (1934)
melting and freezing point curves for $CH_4$-$C_2H_4$ mixture over entire concentration range, eutetic at 84° K and 12.2% (vol) $C_2H_4$, solubility of $C_2H_4$ in $CH_4$ is 2.5% (vol)

3. Shtekkel and Tsin, J. Chem. Ind. USSR 16, 24 (1939)
$CH_4$-$H_2$ binary equilibria and $H_2$-$CH_4$-$N_2$ ternary equilibria

4. Brown and Stutzman, Chem. Eng. Prog. 45, 142 (1949)
vaporization equilibria of six light gases with $CH_4$ and 5 light gases with ethane, an engineering correlation study

5. Benedict, Webb, Rubin and Friend, Chem. Eng. Prog. 47, 571 (1951)
eqn. for prediction of vapor-liquid equilibria in light hydrocarbons

6. Mathot, et al., JCP 23 1551 (1955)
properties of CO-$CH_4$ system at 90° K

7. Ellington, Eakin, Parent, Gami and Bloomer, Thermo. and Transport Prop. of Gases, Liquids and Solids, a Symposium, Lafayette, Ind. 1959, pp 180-194
vapor-liquid equilibria in binary systems of light hydrocarbons


Miscellaneous Inorganic


1. Heastie, Nature 176, 747 (1955)
solid-liquid equilibria in A-Kr system

2. Schmidt, Z. physik. Chem. 20, 363 (1959)
vapor-liquid equilibria in A-Kr system

3. Schmeisser, et al., Angewand. Chem. 71, 523 (1959)
solutions of cis and trans $N_2F_2$

4. Schmidt, Z. physik. Chem. (Frankfurt) 24, 265 (1960)
vapor-liquid equilibria in A-Kr system

5. Volk and Halsey, JCP 33, 1132 (1960)
up to 15% $H_2$ or $D_2$ dissolved in liquid A at pressures to 100 atm;

6. Morgan, Schroeder and Thompson, JCP 43, 4494 (1965)
electrical conductivity of concentrated solutions of Li in $NH_3$ from 65°-300° K; solution shows a eutetic at 89.6° K


$CH_4$


1. Gonikberg and Fastowsky, Acta Physicochem USSR 13, 399 (1940)
solubility of He in liquid $CH_4$ from 90°-106° K

2. _____ and _____, ibid 12, 485 (1940)
solubility of $H_2$ in liquid $CH_4$ from 90°-127° K

3. Volova, J. Phys. Chem. USSR 14, 268 (1940)
vapor-liquid equilibria in $CH_4$-$C_2H_4$ system

# BIBLIOGRAPHY


## Chapter I

I.1 Whipple, Astrophys. J. 113, 464 (1951).

I.2 Donn and Urey, Astrophys. J. 123, 339 (1956).

I.3 A summation of experiences in this program, one of the firstpeace-time programs of university research with government agency sponsorship, appears in Science 118, 227 (1953).

I.4 Advances in Cryogenic Engineering, edited by K. D. Timmerhaus, Plenum Press, New York, Vol. 1, 1960 through Vol. 11, 1966.

I.5 Cryogenic Engineering, Scott, D. Van Nostrand Co., Princeton, N.J., 1959.

I.6 Cryobiology, editor-in-chief, T. I. Malinin, published by the Society for Cryobiology.

I.7 Caswell, Trans. Met. Soc. AIME 236, 257 (1966).

I.8 McGee and Martin, Cryogenics 2, 257 (1962).

## Chapter II

II.1 Eltenton, J. Chem. Phys. 15, 455 (1947).

II.2 Lossing, in "Mass Spectrometry," edited by C. A. McDowell, McGraw-Hill, New York, 1963, p. 442.

II.3 Blanchard and LeGoff, Can. J. Chem. 37, 515 (1959).

II.4 "Collected Works of Sir James Dewar," Edited by Lady Dewar, Cambridge University Press, Vol. I and II, 1927.

II.5 Damoth, "Advances in Analytical Chemistry and Instrumentation," Vol. 4, edited by C. N. Reilley, Wiley, New York 1965.

II.6 Clausing, Z. Physik 66, 471 (1930).

II.7 Biemann, "Mass Spectrometry, Organic Chemical Applications," McGraw-Hill, New York, 1962, p. 33.

II.8 Malone and McGee, J. Phys. Chem. 69, 4338 (1965); ibid. 70, 316 (1966).

II.9 Kirshenbaum and Grosse, J. Am. Chem. Soc. 81, 1277 (1959).

II.10 Milligan, et al., J. Chem. Phys. 41, 1199 (1964), and Mitsch, private communication.

II.11 Johnson, J. Franklin Inst. 210, 135 (1930).

II.12 Spealman and Rodebush, J. Am. Chem Soc. 57, 1474 (1935).

II.13 Herron and Dibeler, J. Research Nat. Bur. Standards 65A, 405 (1961).

II.14 See summary article by Lossing in ref. II.2 above.

II.15 McLafferty, private communication.

II.16 J. R. Haumann, Argonne National Laboratory, private communication, October, 1965.

II.17 Martin, Ph.D. Thesis, Georgia Institute of Technology, Atlanta, March, 1965.

II.18 Melton and Hamill, J. Chem. Phys. 41, 546 (1964).

II.19 Foner and Hudson, J. Chem. Phys. 25, 602 (1956).

Chapter III

III.1 Wright, "Tenth Symposium on Combustion," The Combustion Institute, Pittsburgh, 1965, p. 387.

III.2 Yamazaki and Cvetanovic, J. Chem. Phys. 41, 3703 (1964).

III.3 Schubert and Pease, J. Chem. Phys. 24, 919 (1956).

III.4 Cvetanovic, J. Chem. Phys. 23, 1375 (1955).

III.5 Avramenko and Kolesnikova, Zhur. Fiz. Khim. 30, 581 (1956).

III.6 Heicklen, private communication.

III.7 Murrell, Quart. Rev. 15, 191 (1961).

III.8 Hassel, Mol. Phys. 1, 241 (1958).

III.9 Fenimore and Jones, J. Chem. Phys. 39, 1514 (1963).

III.10 Haller and Pimental, J. Am. Chem. Soc. 84, 2855 (1962).

III.11 McDonald and Schwab, J. Am. Chem. Soc. 86, 4866 (1964).

III.12 Stille and Whitehurst, J. Am. Chem. Soc. 86, 4871 (1964).

III.13 Geib and Harteck, Ber. 66B, 1815 (1933).

III.14 Foner and Hudson, J. Chem. Phys. 28, 719 (1958).

III.15 Rosengren and Pimentel, J. Chem. Phys. 43, 507 (1965).

III.16 Reed, "Ion Production by Electron Impact," Academic Press, New York, 1962, p. 63.

III.17 Foner and Hudson, J. Chem. Phys. 28, 719 (1958).

III.18 Dibeler, Franklin and Reese, J. Am. Chem. Soc. 81, 68 (1959).

III.19 Anderson, Biochem. J. 95, 688 (1965).

III.20 Solomon, et al., J. Am. Chem. Soc. 84, 34 (1962).

III.21 Herman and Giguere, Can. J. Chem. 43, 1746 (1965).

III.22 Geib and Harteck, Ber. 66B, 1815 (1933).

III.23 Brown and Pimentel, J. Chem. Phys. 29, 883 (1958).

III.24 Robinson and McCarty, J. Chem. Phys. 28, 349 (1958).

III.25 Harvey and Brown, J. chim. phys. 56, 745 (1959).

III.26 Clyne, Tenth Symposium on Combustion, The Combustion Institute, Pittsburgh, 1965, p. 311.

III.27 Kobozev, et al., Zhur. Fiz. Khim. 30, 2580 (1956), and many succeeding papers.

III.28 DeMore, et al., J. Am. Chem. Soc. 81, 5874 (1959).